CHARACTERIZATION AND ANTIMICROBIAL PROPERTIES OF GOLD NANOPARTICLES SYNTHESIZED BY *STREPTOMYCES*

SUPAVADEE KERDTOOB

A Thesis Submitted in Partial Fulfillment of the Requirements for the

Degree of Doctor of Philosophy in Biomedical Sciences

Suranaree University of Technology

Academic Year 2021

การตรวจสอบคุณลักษณะและประเมินฤทธิ์ของสารต้านจุลินทรีย์ของ
อนุภาคทองนาโนที่สังเคราะห์โดยเชื้อสเตรปโตมัยสีท

นางสาวสุภาวดี เกิดธูป

วิทยานิพนธ์นี้เป็นส่วนหนึ่งของการศึกษาตามหลักสูตรปริญญาวิทยาศาสตรดุษฎีบัณฑิต
สาขาวิชาชีวเวชศาสตร์
มหาวิทยาลัยเทคโนโลยีสุรนารี
ปีการศึกษา 2564

CHARACTERIZATION AND ANTIMICROBIAL PROPERTIES OF GOLD NANOPARTICLES SYNTHESIZED BY *STREPTOMYCES*

Suranaree University of Technology has approved this thesis submitted in partial fulfillment of the requirements for the Degree of Doctor of Philosophy

Thesis Examining Committee

_____

(Dr. Wanwisa Limphirat)

Chairperson

_____

(Asst. Prof. Dr. Nawarat Nantapong)

Member (Thesis Advisor)

_____

(Assoc. Prof. Dr. Nuannoi Chudapongse)

Member

_____

(Asst. Prof. Dr. Oratai Weeranantanapan)

Member

_____

(Asst. Prof. Dr. Piyada Ngernsoungnern)

Member

_____

(Assoc. Prof. Dr. Chatchai Jothityangkoon)

Vice Rector for Academic Affair

and Quality Assurance

_____

(Prof. Dr. Santi Maensiri)

Dean of Institute of Science

สุภาวดี   เกิดธูป : การตรวจสอบคุณลักษณะและประเมินฤทธิ์ของสารต้านจุลินทรีย์ของ อนุภาคทองนาโนที่สังเคราะห์โดยเชื้อสเตรปโตมัยสีท (CHARACTERIZATION AND ANTIMICROBIAL PROPERTIES OF GOLD NANOPARTICLES SYNTHESIZED BY STREPTOMYCES) อาจารย์ที่ปรึกษา : ผู้ช่วยศาสตราจารย์ ดร.นวรัตน์   นันทพงษ์, 92 หน้า

คำสำคัญ: อนุภาคทองนาโน/ฤทธิ์การต้านเชื้อแบคทีเรีย/ชีวสังเคราะห์/เชื้อสเตรปโตมัยสีท

การสังเคราะห์ทางชีวภาพของอนุภาคนาโน ได้ก่อให้เกิดความก้าวหน้าอย่างมาก ในงาน ทางด้านนาโนเทคโนโลยี ส่งผลให้มีกระบวนการที่เป็นมิตรต่อสิ่งแวดล้อม อนุภาคทองนาโน (AuNPs) เป็นอนุภาคโลหะนาโนที่ได้รับความสนใจเนื่องจากคุณลักษณะเฉพาะของโลหะ เช่น ความต้านทาน การเกิดออกซิเดชัน ความเข้ากันได้ทางชีวภาพ ปราศจากความเป็นพิษ และการใช้งานทางด้านชีว การแพทย์ ในการศึกษานี้การสังเคราะห์ทางชีวภาพของอนุภาคทองนาโนได้ดำเนินการโดยใช้ สารละลายส่วนใสที่ได้จากการเลี้ยงเชื้อสเตรปโตมัยสีทสายพันธุ์ MSK03 และ MSK05 ที่แยกได้จาก ดินในจังหวัดนครราชสีมา ประเทศไทย จากการจัดลำดับยีน 16S rRNA ชี้ให้เห็นว่า MSK03 และ MSK05 คือ *Streptomyces monashensis* และ *Streptomyces spectabilis* ตามลำดับ สารละลายที่ได้จากการเลี้ยงเชื้อสเตรปโตมัยสีททำหน้าที่เป็นสารรีดิวซ์กรดไฮโดรเจนเตตระคลอโรออ ริกในการสังเคราะห์ทางชีวภาพของอนุภาคทองนาโน

การศึกษาลักษณะเฉพาะของอนุภาคทองนาโนทำโดยใช้ UV–visible, XRD, EDXRF, TEM, FTIR และ XANES ผลการทดลองแสดงให้เห็นสเปกตรัมการดูดกลืนสำหรับ surface plasmon resonance ของอนุภาคทองนาโนที่ความยาวคลื่น 530 และ 545 นาโนเมตรโดยใช้เครื่อง UV–visible โครงสร้างผลึกของอนุภาคทองนาโนมีลักษณะเป็นผลึกลูกบาศก์แบบกลางหน้าซึ่งได้รับ การยืนยันโดยเครื่อง XRD ผลลัพธ์จากเครื่อง EDXRF แสดงองค์ประกอบของทองในอนุภาคทองนาโน การวิเคราะห์โดยใช้ TEM พบว่าอนุภาคทองนาโนมีรูปร่างทรงกลม รูปร่างหลายเหลี่ยม และมีขนาด อนุภาคเฉลี่ยตั้งแต่ 20 ถึง 23 นาโนเมตร จากการวิเคราะห์ FTIR   ชี้ให้เห็นว่าหมู่ฟังก์ชัน เช่น คาร์โบไฮเดรต เอมีน และเอไมด์ในสารละลายที่ได้จากการเลี้ยงเชื้อสเตรปโตมัยสีทมีหน้าที่เกี่ยวข้อง กับการรีดิวซ์และการรักษาเสถียรภาพของการสังเคราะห์ทางชีวภาพของอนุภาคทองนาโน สเปกตรัม จาก XANES ยืนยันการรีดิวซ์ของ Au^{3+} เป็น Au^0 อนุภาคทองนาโนที่สังเคราะห์โดยใช้เชื้อสเตรปโต- มัยสีทสายพันธุ์ MSK03 และ MSK05 แสดงฤทธิ์ต้านเชื้อแบคทีเรียทั้งแกรมบวกและแกรมลบโดยใช้ วิธี agar well-diffusion ซึ่งอนุภาคทองนาโนที่สังเคราะห์โดยเชื้อสเตรปโตมัยสีทสายพันธุ์ MSK05 แสดงฤทธิ์ต้านเชื้อ *Staphylococcus aureus* TISTR1466, methicillin-resistant *S. aureus*

(MRSA) DMST20651, MRSA DMST20654, *Escherichia coli* TISTR8465, *Pseudomonas aeruginosa* N90Ps, *P. aeruginosa* TISTR781, *P. aeruginosa* TISTR1287, *Acinetobacter baumanii* และ *Serratia marcescense* ในขณะที่อนุภาคทองนาโนที่สังเคราะห์โดยเชื้อสเตรปโต-มัยสีทสายพันธุ์ MSK03 แสดงฤทธิ์ต้านเชื้อ *S. aureus* TISTR1466, *E. coli* TISTR8465, *P. aeruginosa* N90Ps, *P. aeruginosa* TISTR1287, *A. baumanii* และ *S. marcescense* ดังนั้นเชื้อสเตรปโตมัยสีทสายพันธุ์ MSK03 และ MSK05 จึงเป็นแหล่งข้อมูลเพิ่มเติมเพื่อใช้สำหรับการสังเคราะห์ทางชีวภาพของอนุภาคทองนาโน ซึ่งอนุภาคทองนาโนมีศักยภาพสำหรับการใช้งานด้านชีวการแพทย์ เช่น การรักษามะเร็ง ไบโอเซนเซอร์ การนำส่งยา และฤทธิ์การต้านเชื้อแบคทีเรีย
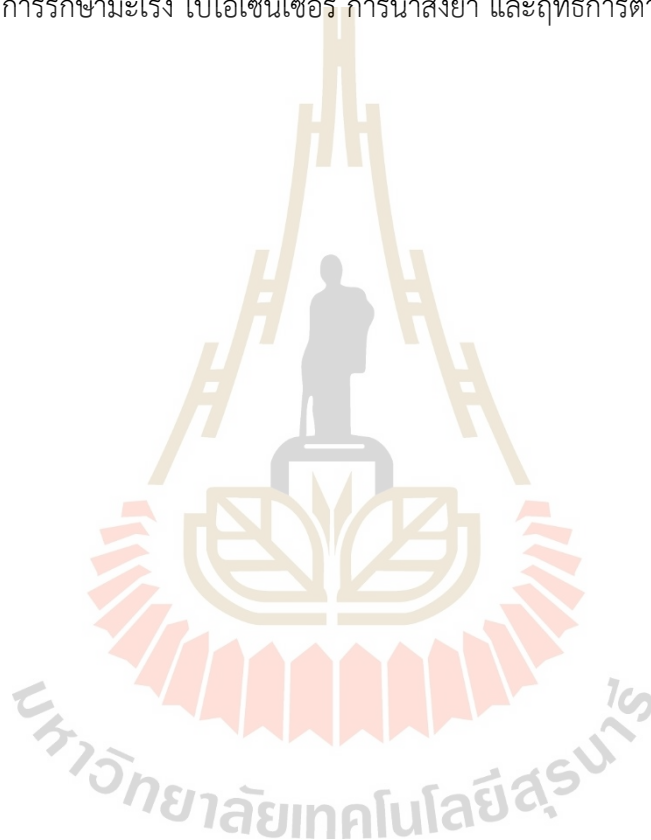
สาขาวิชาปรีคลินิก
ปีการศึกษา 2564

ลายมือชื่อนักศึกษา _สุภาวดี เกิดอู่_
ลายมือชื่ออาจารย์ที่ปรึกษา _____

SUPAVADEE KERDTOOB : CHARACTERIZATION AND ANTIMICROBIAL PROPERTIES OF GOLD NANOPARTICLES SYNTHESIZED BY *STREPTOMYCES*. THESIS ADVISOR : ASST. PROF. NAWARAT NANTAPONG, Ph.D. 92 PP.

Keyword: AuNPs/ANTIMICROBIAL ACTIVITY/BIOSYNTHESIS/*STREPTOMYCES*

Biosynthesis of nanoparticles has produced significant advances in nanotechnology, resulting in an eco-friendly process. Gold nanoparticles (AuNPs) are metal nanoparticles that have gained attention due to its unique features such as oxidation resistance, biocompatibility, lack of toxicity, and biomedical uses. In this research, the AuNPs were synthesized using cultured supernatant of *Streptomyces* strain MSK03 and MSK05 isolated from terrestrial soil in Nakhon Ratchasima, Thailand. The 16S rRNA gene sequence revealed that MSK03 and MSK05 were *Streptomyces monashensis* and *Streptomyces spectabilis*, respectively. The fermented broth of *Streptomyces* sp. was served as the reducing agent of hydrogen tetrachloroauric acid in the biosynthesis of AuNPs.

The biosynthesized AuNPs were characterized using UV–visible, XRD, EDXRF, TEM, FTIR, and XANES spectroscopy. The absorption spectrum for the surface plasmon resonance of AuNPs was observed at 530 nm and 545 nm using UV–visible spectrophotometer. The face-centered cubic (fcc) crystal structure of AuNPs was confirmed using XRD. The EDXRF results of the biosynthesized AuNPs showed the elemental composition of Au elements. TEM analysis revealed that AuNPs were spherical and polygonal in shape, with an average particle size ranging from 20 to 23 nm in diameter. According to FTIR spectroscopy, the functional groups such as carbohydrate, amine, and amide in *Streptomyces* sp. fermented broth were responsible in the reduction and stability of biosynthesized AuNPs. XANES spectra confirmed the reduction of Au^{3+} to Au^{0}. Based on the agar well diffusion assay, the AuNPs synthesized by the strains MSK03 and MSK05 showed strong antibacterial activity against Gram-positive and Gram-negative bacteria. The biosynthesized AuNPs using the strain MSK05 showed antimicrobial activity against *Staphylococcus aureus* TISTR1466, methicillin-resistant *S. aureus* (MRSA) DMST20651, MRSA DMST20654,

Escherichia coli TISTR8465, *Pseudomonas aeruginosa* N90Ps, *P. aeruginosa* TISTR781, *P. aeruginosa* TISTR1287, *Acinetobacter baumanii,* and *Serratia marcescense.* While the biosynthesized AuNPs using the strain MSK03 inhibited *S. aureus* TISTR1466*, E. coli* TISTR8465*, P. aeruginosa* N90Ps*, P. aeruginosa* TISTR1287*, A. baumanii, and S. marcescense*. Thus, *Streptomyces* strains MSK03 and MSK05 provide additional sources for the biosynthesis of AuNPs. The AuNPs have the potential for biomedical applications such as cancer therapy, biosensor, drug delivery, and antimicrobial activity.
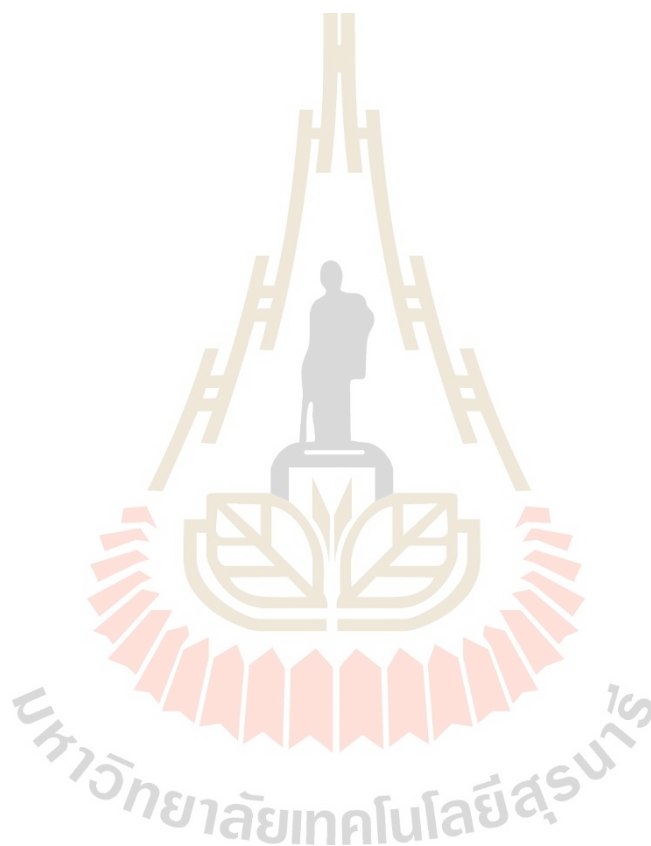
School of Preclinical Sciences   Student's Signature *Supavadee Kerdtoob*

Academic Year 2021   Advisor's Signature

ACKNOWLEDGEMENT

This thesis would not have been possible without the assistance and support. Along the way, I met many wonderful people who never hesitated to support me with their hearts and souls.

First and foremost, I would like to express my sincere gratitude to my advisor, Asst. Prof. Dr. Nawarat Nantapong for the kindness, assistance, advice, and consultation throughout this thesis. My thesis advisor patiently communicated knowledge, concepts, and recommendations while also thoroughly correcting the shortcomings until this thesis was accomplished.

I would like to express my deepest gratitude to Dr. Wanwisa Limphirat, Assoc. Prof. Dr. Nuannoi Chudapongse, Asst. Prof. Dr. Oratai Weeranantanapan, and Asst. Prof. Dr. Piyada Ngernsoungnern, who devoted valuable time to the thesis examination committee. Thank you for your encouragement, sharing ideas, suggestions, and constructive suggestions for improving the thesis.

I appreciate special thanks to the external research fund granter (OROG) for the partial financial support. I would like to offer my sincere thanks to many staffs at the Suranaree University of Technology and the Synchrotron Light Research Institute for their support in the development of this report. I would like to show my thankfulness to all of the lab members for their support and assistance throughout this research.

Finally, I would like to express my deepest gratitude to my parents, relatives, and my friends for always giving me the best support and encouragement in every aspect.

Supavadee Kerdtoob

CONTENTS

CONTENTS (Continued)

LIST OF TABLES

LIST OF FIGURES

LIST OF FIGURES (Continued)

LIST OF ABBREVIATIONS

AuNPs	=	Gold nanoparticles
AIA	=	Actinomycetes isolation agar
°C	=	Degree Celsius
CFU	=	Colony forming unit
cm	=	Centimeter
DLS	=	Dynamic light scattering
DMF	=	Dimethylformamide
DNA	=	Deoxyribonucleic acid
EDXRF	=	Energy dispersive X-ray fluorescence
FT-IR	=	Fourier transform infrared
h	=	Hour
ISP2	=	International *Streptomyces* Project 2
MHA	=	Mueller Hinton agar
mg/g	=	Milligram per gram
mg/mL	=	Milligram per milliliter
mM	=	Millimolar
MRSA	=	Methicillin-resistant *Staphylococcus aureus*
MTT	=	(3-(4,5-Dimethylthiazol-2-yl)-2,5-diphenyltetrazolium bromide
nm	=	Nanometer
PCR	=	Polymerase chain reaction
PDI	=	Polydispersity Index
rpm	=	Round per minute
rRNA	=	Ribosomal ribonucleic acid
SEM	=	Scanning electron microscope
SCB	=	Starch Casein Broth
SPR	=	Surface plasmon resonance
TEM	=	Transmission electron microscope

LIST OF ABBREVIATIONS (Continued)

UV-Vis   = Ultraviolet-Visible

v/v   = Volume by volume

w/v   = Weight by volume

XANES   = X-ray absorption near edge structure

XAS   = X-ray absorption spectroscopy

XRD   = X-ray diffraction

µg/mL   = Microgram per milliliter

µL   = Microliter
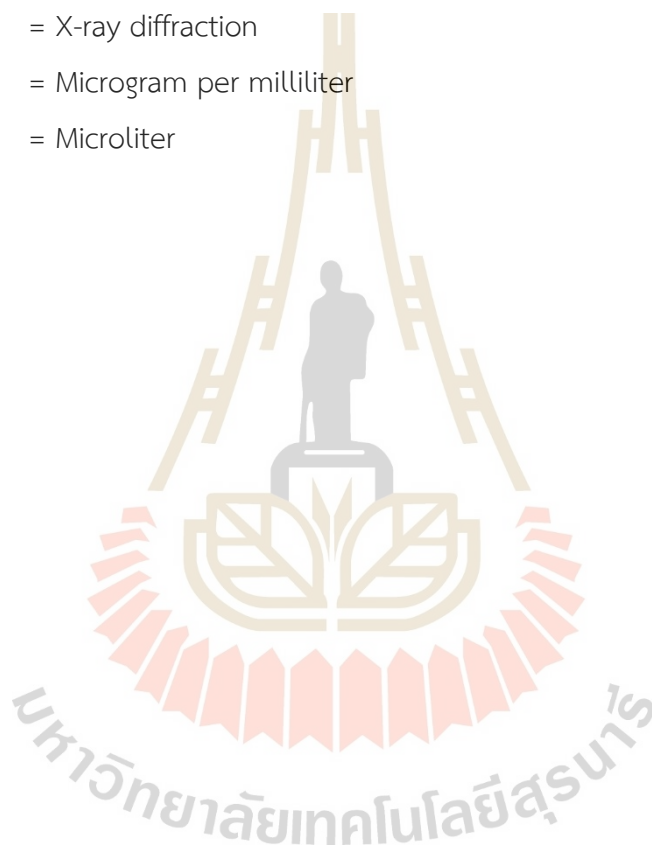
CHAPTER I

INTRODUCTION

1.1 Background/Problem

The research of nanotechnology is one of the most important developing fields of modern study, with applications in technology and science to manufacture new materials at the nanoscale level (Albrecht et al., 2006). Metallic nanoparticle sizes are ranged from 1 to 100 nm (Alanazi et al., 2010). Among all metallic nanoparticles, gold nanoparticles (AuNPs) have stable nature, unique surface morphologies, large surface area, controlled geometry, and high properties of dispersion, catalytic, optical, magnetic, electrical, biocompatibility, and non-toxicity (Yee et al., 2015). Gold nanoparticles have been used in various applications, including optical devices, food, synthetic biology, cellular transportation, and health care (Mohanpuria et al., 2008), biosensor, optical bio-imaging, immune-analysis, detection, drug delivery, and photo-thermolysis of cancer cells and microorganisms (Dykman and Khlebtsov, 2011) and they are applied for treatments, diagnosis, and detection of several diseases (Alvarez et al., 2016; Khan et al., 2014). Besides, the antimicrobial activity of gold nanoparticles has been investigated (Geethalakshmi and Sarada, 2013).

The antibacterial properties of metallic nanoparticles mostly attach to the surface of the microorganism's cell. Thus, the cell has structural changes across the plasma membrane, resulting in distorted membranes (Li et al., 2010). Moreover, metallic nanoparticles also help to enhance in redox processes of the gene expression, depressing the activity of respiratory chain enzymes leading to cell death (Sharma et al., 2009). The major antibacterial activity mechanisms of nanomaterial are described as followed: disruption of energy transduction, inhibition of cell membrane/wall synthesis, production of toxic reactive oxygen species (ROS), enzyme inhibition, photocatalysis, and reduced DNA production (Figure 1.1) (Singh et al., 2014;

Weir et al., 2008). Gold nanoparticles could probably have the antibacterial mechanism, such as accumulation at cell surfaces, heavy electrostatic attraction, and interaction with the cell membrane (Chamundeeswari et al., 2010; Johnston et al., 2010).
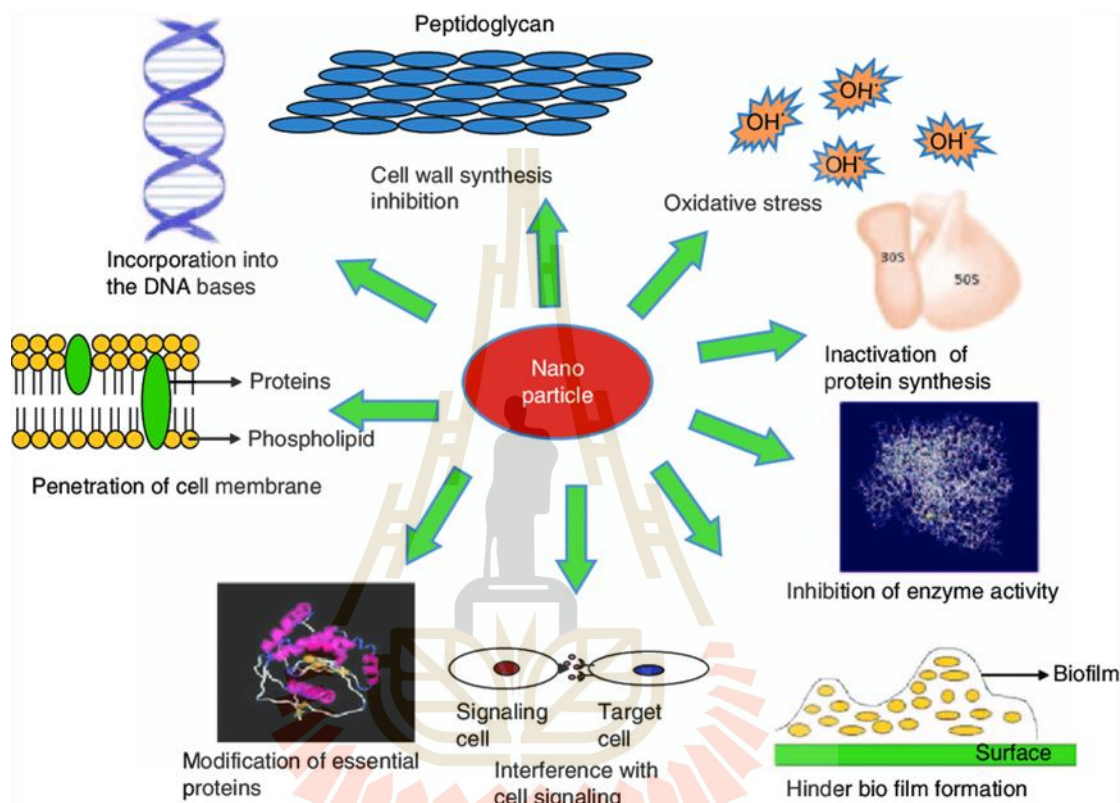
Figure 1.1 Mechanisms for antibacterial activity of nanoparticles (Singh et al., 2014).

Antibacterial activities of gold nanoparticles have been reported against both Gram-positive and Gram-negative bacteria. The most common antibacterial activity against antibiotic-resistant bacteria of gold nanoparticles is *Acinetobacter baumannii*, *Enterrococcus faecium*, *Enterobacter* sp., *Pseudomonas aeruginosa*, *Klebsiella pneumoniae*, and *Staphylococcus aureus* (Rice, 2010). Several gold nanoparticles are synthesized, and their antibacterial activity have been evaluated (Monic et al., 2014). The gold nanomaterial is recognized as a multifunctional material useful for a wide variety of applications. Because of its shape and size, it has a high biological, chemical, and physical value (Dreaden et al., 2012). The development of new

materials or new methodologies for controlling the synthesis of gold nanoparticles is important for several research applications (Grubbs, 2007; Tang et al., 2002; Wong et al., 1998).

Several methods have been used to precisely synthesize nanoparticles in terms of shape, size, and properties such as physical (laser ablation, sonication, and radiation), chemical (sol-gel method, condensation, and lactic acid method), and biosynthesis methods (plant, bacteria, and fungi). However, the synthesis processes in the chemical or physical methods involve the use of stringent synthetic conditions, toxic solvents and chemicals, and non-eco-friendly protocol which was raised toxic chemicals in nature for human consumption and toxic to the environment. In contrast, the biological method of nanoparticles is clean, safe, non-toxic, dynamic and energy-efficient, bio-compatible, economical, and ecofriendly acceptable procedures concerning microorganisms (Khadivi et al., 2012). Moreover, microorganisms can be grown in a low-cost medium, maintaining the safety level by reducing the metal ion into nanoparticles by an enzyme produced by metallic processes (Kumar et al., 2014).

Actinobacteria are Gram-positive, aerobic, non-motile, filamentous bacteria that are commercially interested in their unrivaled ability to produce a wide range of bioactive secondary metabolites and extracellular enzymes with interesting biological activities (Kumar et al., 2014; Zotchev, 2012). Among the Actinobacteria, the *Streptomyces* group is considered the most economically important, because more than 50–55% of bioactive secondary metabolites producing antibiotics of the order Actinomycetales are produced by *Streptomyces* (Chater, 1993; Manivasagan et al., 2014). Only a few *Streptomyces* species have been reported for biosynthesis of AuNPs. The *Streptomyces* isolated from different ecosystems has been accepted as the potential biosynthesis of metal nanoparticles, such as *Streptomyces hygroscopicus* (Sadhasivam et al., 2012), *Streptomyces viridogens* (HM10) (Balagurunathan et al., 2011), *Streptomyces naganishii* (MA7) (Shanmugasundaram et al., 2013), *Streptomyces* spp. (Karthik et al., 2013b) and *Streptomyces avidinii* (Park et al., 2006).

This study was focused on the biosynthesis of the gold nanoparticle using *Streptomyces* sp. The biosynthesized gold nanoparticles were used to investigate antimicrobial activity against Gram-positive and Gram-negative bacteria using the agar well diffusion method. The biosynthesis of gold nanoparticles was characterized using UV–visible spectroscopy, X-ray diffraction (XRD) spectroscopy, Energy-dispersive X-ray spectroscopy (EDX), transmission electron microscopy (TEM) Fourier transform infrared (FTIR) spectroscopy, and X-ray absorption near edge structure (XANES) spectroscopy.

1.2 Research objectives

a) To isolate and identify *Streptomyces* from terrestrial soil
b) To synthesize AuNPs by a green synthesis method using fermented broth of *Streptomyces* sp. MSK03 and MSK05
c) To characterize AuNPs and evaluate their antimicrobial activity against pathogenic microorganisms

1.3 Research hypothesis

The soil-isolated *Streptomyces* sp. MSK03 and MSK05 have the ability to synthesize AuNPs and the biosynthesized AuNPs exhibit antimicrobial activity against tested pathogens.

1.4 Scope and limitation of the study

This work involved the biosynthesis of AuNPs using *Streptomyces* spp. isolated from terrestrial soil in Nakhon Ratchasima province, Thailand. *Streptomyces* sp. (MSK03 and MSK05) was identified based on cultural characteristics and 16S rRNA gene analysis. AuNPs were tested for antimicrobial activity against tested pathogens such as *Bacillus subtilis, Escherichia coli, Pseudomonas aeruginosa, Acinetobacter baumanii, Serratia marcescense, Klebsiella pneumonia, Proteus mirabilis, salmonella typhi, Enterobacter aerogenes, Staphylococcus aureus,* methicillin-resistant *Staphylococcus aureus* (MRSA) and methicillin-resistant *Staphylococcus*

epidermidis (MRSE). The biosynthesized AuNPs was characterized by using UV–visible, XRD, EDX, TEM, FTIR, and XANES spectroscopy.

CHAPTER II

LITERATURE REVIEWS

2.1 Gold nanoparticles

Gold is a bright, too soft, slightly reddish yellow, dense, malleable, solid under standard conditions, transition metal (Depending on the element with which it reacts, it may lose a different number of valence electrons) with the electronic configuration represented by (Xe) $4f^{14}$ $5d^{10}$ $6s^{1}$ and is one of the least reactive chemical elements (Rinehart and Winston, 2005). Since ancient Roman times, gold nanoparticles were used to stain glasses with different colors (Hunt, 1973). In the 1850s, Michael Faraday's investigated the colloidal gold's optical properties (Faraday, 1857). The scattering and absorption of light of the colloidal gold depend on aggregation state, local refractive index, particle size, and shape resulting in different colors (Anderson et al., 1999). Various types of gold nanoparticles has already been used in a variety of applications (Table 2.2) (Link and El-Sayed, 1999). The synthesis and properties of colloidal gold were interesting for scattering and absorption by spherical particles (Sharma et al., 2009; Zeng et al., 2013). Various types of gold nanoparticles are already being used in a variety of applications as shown in Table 2.2. As early as 2500 BC., the ancient Chinese and Egyptians used gold for therapeutic purposes (Daniel and Astruc, 2004).
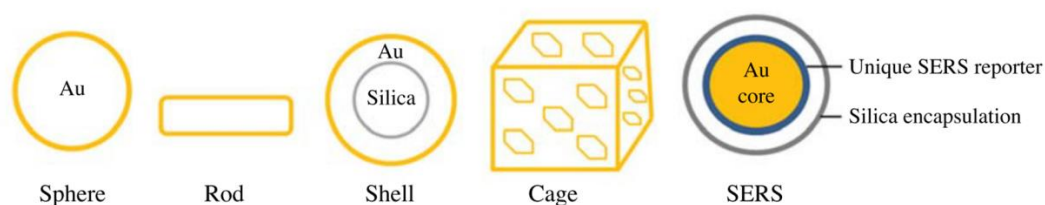
Figure 2.1 Various types of gold nanoparticles (Das et al., 2012).

Gold nanoparticles can easily synthesize in various shapes with sizes ranging from 1 nm to more than 200 nm. The size of gold nanoparticles affects their applications such as the particles size ranging from 2 nm to 15 nm are used in microscopy immunohistochemistry and biomarkers. Chemical sensors, medication delivery, biomarkers, and DNA detection all use particles with sizes ranging from 20 nm to 60 nm. 20 nm to 50 nm particles had the best cellular uptake, whereas 40 to 50 nm particles have the best diffusion into tumor cells. The larger size of gold nanoparticles ranging from 80 to 250 nm is used in optical mammography, electronic devices, forensic science, etc. (El-Sayed et al., 2006).

Table 2.1 The wavelengths of spherical AuNPs depend on size changing (Shah et al., 2014).

Wavelength (nm)	Size of gold nanoparticle (nm)
515	5
520	10
524	20
526	30
530	40
535	50
540	60
553	80
572	100

Gold nanoparticles have the potential for many biomedical applications, due to their large specific surface, high surface activity, good biocompatibility, strong antioxidant property, and suitableness for manipulations at the molecular level (Chithrani et al., 2010; Kong et al., 2017). Gold ionic chemical compounds (gold salts) have been used to relieve TB discomfort and swelling, as well as to halt disease development in people with rheumatoid arthritis, psoriatic arthritis, and bronchial asthma (Rau, 2005; Shaw, 1999). In recent years, colloidal gold nanoparticles are efficient for potential applications depending on their shape and size (Khan et al.,

2014; Mishra et al., 2012; Svedberg and Pedersen, 1940). In general, gold nanoparticles are more recommended than other inorganic nanoparticles for biomedical applications, because of their excellent biological compatibility with human cells (Alanazi et al., 2010; Jain et al., 2006; Shukla et al., 2005), and are easily available for conjugation with various small biomolecules such as amino acids, carboxylic acid, enzymes, proteins (Guglielmo et al., 2010; Wangoo et al., 2008), polyethylene glycol (Khalil et al., 2004), DNA (Kim et al., 2010), RNA (Lee et al., 2009), antibodies (Yang et al., 2009), and peptides (Sun et al., 2008). In addition, these particles can circulate with blood flow and easily reach the targeted site such as the cancer site (Kojima et al., 2010; Ye et al., 2018).

Table 2.2 Shapes of gold nanoparticles and their applications (Khan et al., 2014).

Shape	Size (nm)	Application	Reference
Nanorod	2-5	Photothermal therapy and drug delivery	(Guo et al., 2014)
Hollow particle	25	Photo-electronics, cancer therapy, and catalysis	(Ganeshkumar et al., 2012)
Triangular particle	3.85-7.13	Highly effective against *K. pneumonia* and *E. coli*	(Murawala et al., 2014),
Faceted particle	50-100	Reproducible, Effective, and stable large area substrates for near infra-red surface-enhanced Raman spectroscopy	(Papasani et al., 2012)
Nanocage	50	Effective molecular contrast agent for non-linear endomicroscopy imaging and in vivo medical applications	(Giljohann et al., 2010), (Bisker et al., 2012)
Nanocube	50	Refractive-index sensing and field enhancement applications	(Pissuwan et al., 2011)

The applications in the field of optoelectronics, biological and chemical sensing, biomedical imaging, biological tagging, DNA labeling, photothermal therapy (Alanazi et al., 2010), photoacoustic imaging (Kim and Jon, 2012), catalysis, tracking and drug delivery (Tedesco et al., 2010), cancer antigen and cancer therapy (Guo et al., 2014; Mishra et al., 2012). For medical applications, gold nanoparticles are used for the diagnosis and therapy of cancer cells and microorganisms, and important in HIV therapeutics, and are also being used as target delivery of compounds such as drugs, genes, and proteins (Bowman et al., 2008; Li et al., 2006; Mody et al., 2010).

2.2 Synthesis of gold nanoparticles

Various methods for synthesizing gold nanoparticles have been developed. The general method for synthesizing AuNPs consists of physical, chemical, and biosynthesis methods (Papasani et al., 2012). The methods for producing gold nanoparticles can be classified into two categories, the "top-down" and "bottom-up" techniques (Eustis and el-Sayed, 2006). The top-down technique is a physical method that requires the matter removal from the bulk iron oxide material divided into nanoparticles, such as electron beam lithography and photolithography (Sun et al., 2006). The bottom-up technique is a chemical or an electrochemical that involves the assembly of atoms (produced by ion reduction) into preferred nanomaterials, such as sol-gel processing.(Heidari et al., 2014; Xinghua Sun et al., 2013), photochemical (Jin et al., 2001), nanosphere lithography (Pileni, 1997), templating (Hall et al., 2001), electrochemical, sonochemical (Okitsu et al., 2005), and thermal reduction techniques (Magnusson et al., 1999). The shape and size of gold nanoparticles can be generated using both top-down and bottom-up techniques (Figure 2.2). The morphology of nanoparticles depends on synthesis processes such as the formation of nuclei, growth, aggregation, and absorption of impurities. Whereas the particle size of nanoparticles is influenced by varying factors, such as pH value, temperature, reaction conditions, the reactants concentration, impurities, the nature of the solvent, etc. (Chen et al., 2005; Eustis and el-Sayed, 2006). Compilation of TEM images with various shapes of gold nanostructures synthesized by various methods are shown in Figure 2.3.
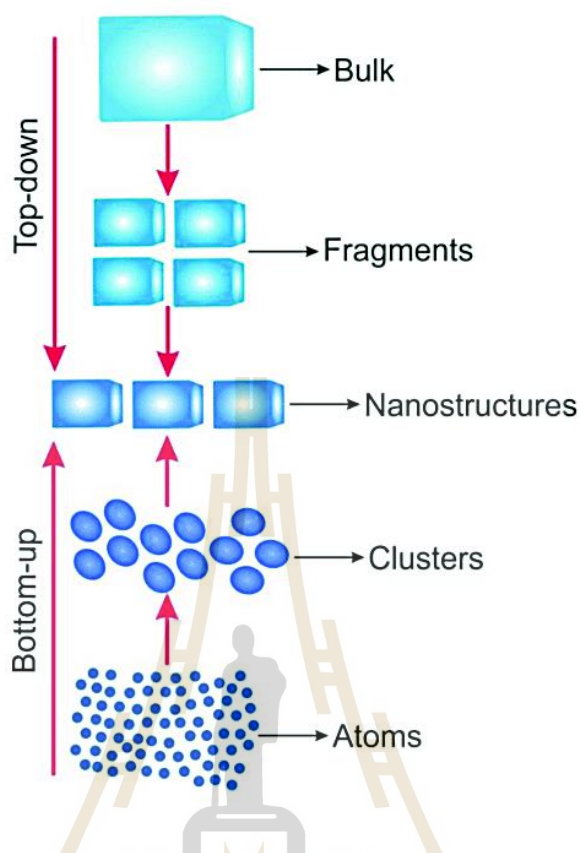
Figure 2.2 The schematic representation of the top-down and bottom-up technique for nanoparticle preparation (Galstyan et al., 2018).

2.3 Biological synthesis of nanoparticles by *Streptomyces*

Streptomyces is the largest genus of Actinobacteria. *Streptomyces* species are capable of producing secondary metabolites such as vitamins, immunosuppressive, and antibiotics. Bacterial interactions with inorganic materials are well known (Bosecker, 1997). Actinobacteria have resistance to harmful heavy metals due to chemical detoxification, which includes the movement of ions via ATPase membrane proteins or chemiosmotic cation or proton anti-transporters, as well as solubility changes (Bruins et al., 2000). In comparison to intracellular production, extracellular production of metallic nanoparticles has many applications in diverse fields such as optoelectronics, sensor technology, electronics, and bio-imaging (Bao et al., 2003; Narayanan and Sakthivel, 2010).
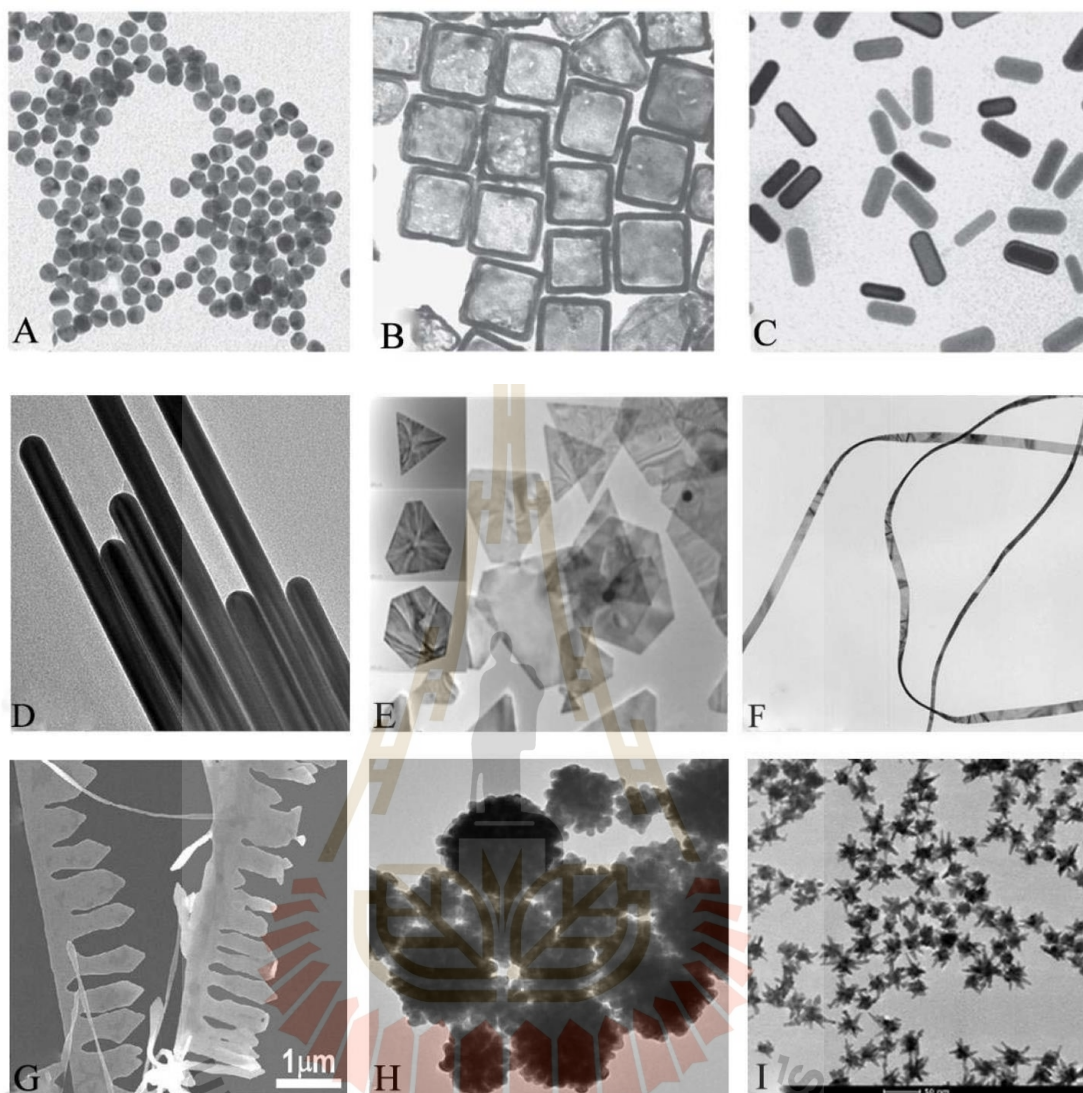
Figure 2.3 Compilation of TEM images with various shapes of gold nanostructures synthesized by various methods. (A-I) Represents the TEM image of the gold nanostructures consisting of (A) gold nanospheres (Cho et al., 2011), (B) gold nanocages (Cho et al., 2011), (C) gold nanorods (Cho et al., 2011), (D) gold nanowires (Kim et al., 2008), (E) gold nanoplates (Liu et al., 2005), (F) gold nanobelts (Zhao et al., 2008), (G) gold nanocombs (Zhao et al., 2008), (H) gold nanoflowers (Li et al., 2010), and (I) gold nanostars (Yuan et al., 2012). (Source: (Shah et al., 2014).

Khadivi et al. (2012) reported the biosynthesized gold nanoparticles using extracellular production of *Streptomyces griseus*. After 48 hours, the XRD and UV-visible spectra of the mixture containing *S. griseus* and 1mM HAuCl$_4$ revealed the formation of gold nanoparticles. The image of TEM revealed spherical gold nanoparticles with an average particle size of 50 nm (Khadivi et al., 2012).

Zonooz et al. (2012) reported biosynthesis of gold nanoparticles by *Streptomyces* sp. The formation of gold nanoparticles was monitored using UV-visible spectroscopy. Moreover, the nanoparticles of gold were characterized using SEM, TEM, and XRD. The result shown shows a spherical shape with the average particle size ranging from 10 to 30 nm (Zonooz et al., 2012).

Sadhasivam et al. (2012) described how *Streptomyces hygroscopicus* assisted in the biosynthesis of multidimensional gold nanoparticles. The control of the key growth parameters, such as reaction time and pH of the solution, resulted in multidimensional gold nanoparticles. The spherical gold nanoparticle has a diameter of 10 to 20 nm (Sadhasivam et al., 2012).

Gopal et al. (2013) reported the actinobacteria-mediated synthesized gold nanoparticles using the *Streptomyces* sp. VITDDK3 cell-free supernatant. The UV-visible spectra (550 nm) were used to characterize the gold nanoparticles. XRD pattern analysis revealed peaks corresponding to Au metal diffraction at (111), (200), (220), and (311). SEM analysis was used to determine the shape of nanoparticles, which had an average size of 90 nm. Moreover, the antifungal activity of these synthesized gold nanoparticles was tested using the agar well diffusion method. The antifungal activity was demonstrated against *Microphyton gypseum* (10 mm) and *Trichophyton rubrum* (13 mm) (Gopal et al., 2013).

Karthik et al. (2013) reported the synthesis of gold nanoparticles via *Streptomyces* stain LK-3. Gold nanoparticles of these methods were found with an average particle size ranging from 5 to 50 nm. Gold nanoparticles were developed by *Plasmodium berghei* (ANKA (PbA)) for the treatment of infected mice. The ANKA (PbA) affected the infected mice, delaying the rise in parasitemia compared with PbA infection for 8 days post-infection and increasing the 85% survivability of the mice. During the gold nanoparticles treatment in PbA infection, the histomorphological

analysis showed no changes in the tissues of the liver and spleen for 8 days post-infection. The result confirmed the down-regulation of TNF-**α** and up-regulation of TGF-**β** in serum and tissue level in ANKA (PbA) compared to PbA infection. Based on the results of the anti-malarial activity, they suggested the synthesized gold nanoparticles using *Streptomyces* sp. LK-3 revealed a potential source for drug development of anti-malarial (Karthik et al., 2013b).

Ibrahim et al. (2016) reported biosynthesized gold nanoparticles using extracellular of *Streptomyces* sp. as a stabilizing /capping/reducing bio-agent and chloroauric acid (HAuCl$_4$) as a precursor. The gold nanoparticles sizes ranged from 4 to 13 nm. They studied UV-blocking for viscose knitted and cotton fabrics surface modification using O$_2$-plasma, followed by treatment with gold nanoparticles and gold nanoparticles combined with ZnONPs or TiO$_2$NPs to provide different functional properties, specifically antibacterial properties (Ibrahim et al., 2016).

2.4 Antibacterial activity of gold nanoparticles

Antibiotics improved medicine by permitting the bacterial infections treatment that were previously thought to be incurable. Unfortunately, many bacteria have developed resistance to the antimicrobial drugs now in use (Shah et al., 2014). Gold nanoparticles are inorganic metals known for potential antimicrobial activity against Gram-negative and Gram-positive bacteria (El-Batal et al., 2013). Green synthesis methods of gold nanoparticles showed antibacterial activities in various fields.

Balagurunathan et al. (2011) used *Streptomyces viridogens* stain HM10 to synthesize gold nanoparticles. The average particle size was between 18 and 20 nm. The antibacterial activities of gold nanoparticles were demonstrated in a well-diffusion method against Gram-negative (E. coli) and Gram-positive (S. aureus) bacteria (Balagurunathan et al., 2011).

Sadhasivam et al. (2012) studied the biogenic synthesis of multidimensional gold nanoparticles using cell-free supernatants of *Streptomyces hygroscopicus.* They have demonstrated the antibacterial properties of metallic gold nanoparticles by using a minimal inhibitory concentration assay. The MTT assay was used to

determine the minimum inhibitory concentrations (MIC) of the biosynthesized gold nanoparticles. Growth inhibition studies were used to test the antibacterial activity of gold nanoparticles against Gram-negative and Gram-positive bacteria such as *Escherichia coli* KACC 10005, *Staphylococcus epidermidis* KACC 13234, *Enterococcus faecalis* KACC 13807, *Salmonella typhimurium* KACC 10763, *Staphylococcus aureus* KACC 13236, *and Bacillus subtilis* KACC 14394 (Sadhasivam et al., 2012).

Ibrahim et al. (2016) used marine *Streptomyces* sp. as reducing agents and chloroauric acid (HAuCl$_4$) as a precursor to biosynthesize gold nanoparticles. According to the results, the addition of gold nanoparticles to activated fabric samples significantly improved antibacterial activity against Gram-negative (*E. coli*) and Gram-positive (*S. aureus*) bacteria (Ibrahim et al., 2016).

CHAPTER III

RESERCH METHODOLOGY

3.1 Isolation and purification of *Streptomyces*

Soil samples were collected from the forest area in Sakaerat Environmental Research Station and Botanical Garden at the Suranaree University of Technology, Nakhon Ratchasima province, Thailand. Soil samples were taken from a depth of 10-15 cm from the upper surface of the soil. The soil samples were collected in sterile polyethylene bags, sealed tightly, immediately taken to the laboratory, and stored at 4°C in a refrigerator until used. For the *Streptomyces* isolation, soil samples were isolated and cultivated on the actinomycete isolation agar (AIA, Himedia) medium using a serial dilution procedure and incubated for 7 days or until the plates were examined for the presence of the colonies at 30-37°C. For purification, isolated colonies were picked up and streaked on International Streptomyces Project 2 (ISP2) agar medium. The purified isolates were cultured in ISP2 broth for 7 days before being added glycerol to make the final concentration 20% and preserved in a freezer at -80°C until required.

3.2 Identification of *Streptomyces* using 16S rRNA gene sequence analysis

A modified approach for fungal DNA extraction was used to extract genomic DNA. The *Streptomyces* strains were grown in 10 mL ISP2 medium for 3-4 days at 30-37°C. Bacterial cells were harvested by centrifugation at 8000 rpm for 10 minutes and the cell pellets were used for DNA extraction. The cell pellet was dispersed in 500 µL of lysis buffer solution and grinded until fine. The cell suspension was transferred to a microcentrifuge tube and mixed with 165 µL of 5M NaCl followed by centrifugation at 4°C, 10,000 rpm for 10 minutes. The supernatant was transferred to a new tube and mixed with 400 µL chloroform and 400 µL isoamyl alcohol by

inverting tube until the solution becomes milky. The sample was then centrifuged at 4°C, 10,000 rpm for 10 minutes. The upper layer was transferred into a new tube. After that, an equal volume of chloroform was added to supernatants. The sample was mixed by inverting the tube and centrifuged at 4°C, 10,000 rpm for 5 minutes. The DNA in an aqueous layer was transferred into a new tube and precipitated with two volumes of 95% (v/v) ethyl alcohol. The sample was mixed by inverting the tube and centrifuged at 4°C, 10,000 rpm for 5 minutes. The precipitated DNA was washed with 300 µL ice-cool 70% (v/v) ethyl alcohol and centrifuged at 4°C, 10,000 rpm for 1 minute. The DNA pellet was dried and resuspended in 50 µL of TE buffer. The quality of extracted DNA was checked using agarose gel electrophoresis.

The genomic DNA of soil isolated was used as a template for polymerase chain reaction (PCR) amplification of the 16S ribosomal RNA (rRNA) gene using universal 16S rRNA primers, 27F 5' AGAGTTTGATCCTGGCTCAG 3' and 1525R 5' AAGGAGGTGWTCCARCC 3' (Lane, 1991). The amplification was performed in a mixed reaction with a final volume of 50 µL containing 10 µL of genomic DNA template, 2 µL of 10 pM 27F primer, 2.0 µL of 10 pM 1525R primer, 25 µL of master mix (EconoTaq® PLUS 2x Master Mix, Lucigen), and 11 µL of nuclease-free water. The amplification was completed using a thermal cycler machine according to the following conditions: initial denaturation at 94°C, 1 cycle for 5 minutes followed by 20 cycles of denaturation at 94°C for 30 seconds, annealing at 55°C for 30 seconds, extension at 72°C for 30 second and a final extension of at 72°C for 7 minutes. Amplified products were electrophoresed at 100 V on a 0.7% (w/v) agarose gel in a TBE buffer. The target band in the gel has been trimmed and purified by using Gel/PCR Purification Mini Kit (Favorgen™). The purified PCR products were submitted for sequencing at Macrogen, Korea.

The sequence of the 16S rRNA gene was compared to the online 16S rRNA database by using the EzBioCloud website (http://www.ezbiocloud.net). After that, CLUSTAL W was used to align the sequences with closely related species. The phylogenetic trees were created by the phylogeny method using MEGA-X (Molecular Evolutionary Genetics Analysis software version X) with a 1000 bootstraps Neighbor-

Joining technique. Finally, Sequence analysis has been done by using the BLAST program (http://www.ncbi.nlm.nih.gov/).

3.3 Preparation of *Streptomyces* for Biosynthesis

Streptomyces sp. was grown in a 500 mL Erlenmeyer flask containing 100 mL of Starch Casein Broth (SCB) and incubated at 37°C under 200 rpm shaking conditions for 5 days. After incubation, the culture was centrifuged at 4°C, 8000 rpm for 5 minutes. The extracellular cell-free supernatant was collected and used in subsequent experiments. On the other hand, the cell pellet of *Streptomyces* sp. was washed using sterile deionized water three times with centrifuged at 4°C, 8000 rpm for 1 minute to remove residues of media. Then, the biomass of *Streptomyces* sp. was resuspended in 100 mL sterile deionized water in an Erlenmeyer flask and cultured for 24 hours in an incubator shaker at 37°C with 200 rpm shaking setting. After incubation, the culture biomass was centrifuged at 4°C, 8000 rpm for 5 minutes. The intracellular cell-free supernatant was collected and used in subsequent experiments.

3.4 Biosynthesis of gold nanoparticles

The extracellular or intracellular cell-free supernatant of *Streptomyces* sp. was added to 1 mM Hydrogen tetrachloroauric acid; $HAuCl_4 \cdot 3H_2O$ (Sigma-Aldrich, USA. ≥99.9%) by using various ratios with a pH of 7. After that, the mixture was incubated at 37°C, 200 rpm for 24-72 h. The biosynthesis of gold nanoparticles was visual identified by observing the color change of the gold aqueous solution. Then, the whole mixture was centrifuged at 4°C, 8000 rpm for 5 minutes. The AuNPs were washed with sterile DI water and collected for further studies. The two controls, a culture supernatant control without $HAuCl_4$ and 1mM $HAuCl_4$ were incubated under the same experimental conditions.

3.5 Characterization of gold nanoparticles

3.5.1 Analysis of gold nanoparticles

The biosynthesized AuNPs were characterized using a UV-visible spectrophotometer to measure the absorbance of colloidal AuNPs solutions (SkanIt Software 5.0 for Microplate Readers RE, ver. 5.0.0.42, Thermo Scientific Multiscan GO, Finland). The absorption spectra of the AuNPs were obtained in approximately wavelength range of 300-800 nm. Zeta potential measurement and particle size distribution from less than a nanometer to several microns of biosynthesis gold nanoparticles were recorded using Zeta-sizer (Malvern Instrument Ltd, USA). An X-ray diffractometer (D8 Advance, Bruker, Germany) was used to investigate the identity and crystallinity of AuNPs. The result of the sample was compared with the reference from Joint Committee on Powder Diffraction Standards (JCPDS). The elemental composition or chemical characterization of gold nanoparticles was notified through EDX spectroscopy analysis (X-ray Fluorescence Energy Dispersive Spectrometer, Model XGT-5200).

3.5.2 Morphological characterization of gold nanoparticles

TEM (FEI/TECNAI G^2 S-Twin, USA) was used to determine the size and morphology of the biosynthesized gold nanoparticles. The morphology and size of the biosynthesized AuNPs were determined by TEM. The morphology of the nanoparticles could be highly variable. Gold nanoparticle formation was confirmed using TEM images. The particle size distribution of biosynthesized AuNPs was measured by dynamic light scattering or zeta-sizer (Malvern Instrument Ltd, USA).

3.5.3 Fourier transform infrared (FTIR) spectroscopy analysis

FTIR spectroscopy can be used to identify potential biomolecules involved in the reduction of Au^{3+} to Au^{0}. Functional groups of organic molecules attached to the surface of AuNPs as well as other surface chemical residues were detected using an FTIR spectrophotometer (FT-IR microscope, Tensor 27, Bruker, Germany). The spectra were scanned in the range of 4000-400 cm^{-1}. The spectral data were compared with the online database to determine the functional group in the sample at https://www.sigmaaldrich.com/TH/en/technical-documents/technical-article/analytical-chemistry/photometry-and-reflectometry/ir-spectrum-table.

3.5.4 X-ray absorption spectroscopy (XAS) analysis

XAS analysis was performed to determine local geometry and structure of gold in the produced AuNPs. The samples were measured by XANES at Synchrotron Light Research Institute (SLRI), Thailand. As a standard, $HAuCl_4$ and gold foil were employed.

3.6 Antimicrobial activity of gold nanoparticles

3.6.1 Antimicrobial activity determination using Agar well diffusion method

The agar well diffusion method is commonly used to assess antimicrobial activity. This method was used to test the ability of the AuNPs to inhibition of the test pathogens including *Bacillus subtilis* TISTR008, *Staphylococcus aureus* TISTR1466*,* methicillin-resistant *Staphylococcus aureus* (MRSA) DMST20651, methicillin-resistant *Staphylococcus aureus* (MRSA) DMST20654, methicillin-resistant *Staphylococcus epidermidis* (MRSE), *Escherichia coli* TISTR8465, *Pseudomonas aeruginosa* N90Ps, *Pseudomonas aeruginosa* TISTR781, *Pseudomonas aeruginosa* TISTR1287, *Acinetobacter baumanii, Serratia marcescense, Klebsiella pneumonia* TISTR1617, *Proteus mirabilis* TISTR100*, Salmonella typhi* TISTR292 and *Enterobacter aerogenes* TISTR1540. The culture supernatant control without $HAuCl_4$ and $HAuCl_4$ was used as the negative control. The Mueller–Hinton agar (Himedia™, India) plate surface was inoculated by spreading on the overnight culture of mid-log phase 5×10^5 CFU/mL test pathogens over the agar surface. Then, a 6 mm diameter hole was punched aseptically with a sterile cork borer. One hundred microliters of the sample as AuNPs solution or the control were transferred into each well and left at room temperature for 1 h to allow the sample to diffuse into the agar. All plates were incubated at 37℃ for 24 h. After the incubation, the plates were observed for inhibition zone formation around the wells. Diameters of the inhibition zone around the well and the diameters of the wells were measured (in mm).

3.6.2 Determination of the minimum inhibitory concentration (MIC)

The minimum inhibitory concentration (MIC) was used to evaluate the antimicrobial activity of the AuNPs against pathogenic organisms. MIC determination of AuNPs against tested pathogens was achieved by using 96-well sterile microplates. Two-fold serial dilutions of AuNPs were inoculated with 50 µL of 5.0×10^{5} CFU/ml of tested pathogen and incubated at 37℃, 100 rpm for 24 h. After incubation, the plates were examined visually for the growth of test organisms. The lowest concentrations of AuNPs that inhibit the growth of tested pathogens were recorded as the MIC value.

CHAPTER IV
RESULTS

4.1 Identification of *Streptomyces* spp.

Streptomyces were isolated from soil samples. The soil samples were collected from Sekaerat Environmental Research Station and Botanical Garden at the Suranaree University of Technology. Several *Streptomyces* spp. were able to isolate from soil samples. The soil isolated strains MSK03 and MSK05 were selected for the synthesis of AuNPs. The *Streptomyces* sp. MSK03 and MSK05 were identified based on cultural, biochemical, physiological, and morphological properties, as shown in Figure 4.1. *Streptomyces* sp. MSK03 was produced leathery growth with white color of aerial mycelium on ISP2 medium. The colony of MSK03 released light yellow pigments that are visible in the form of exudates. The colony morphology of *Streptomyces* sp. MSK05 was rugose, hairy, spiny, brown spores on ISP2 medium. The diffusible black pigment was released from the colony of MSK05 into an agar medium.
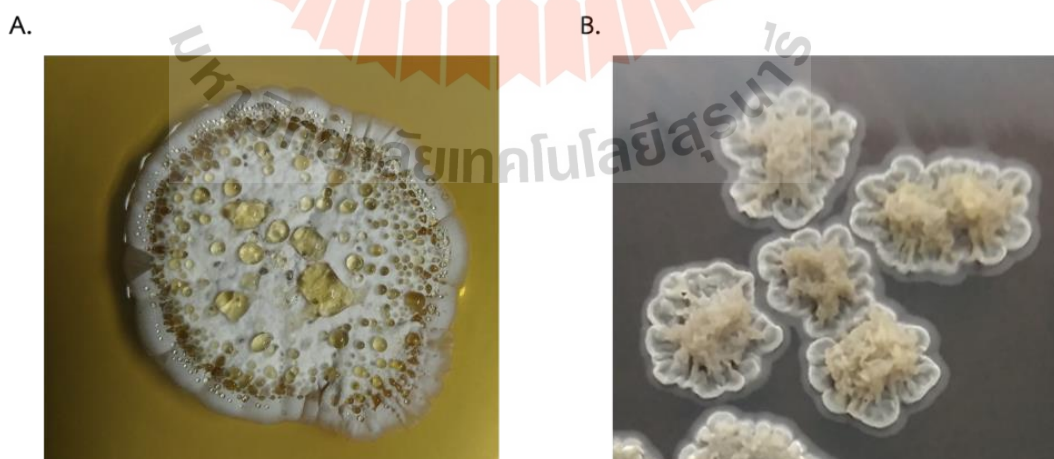
Figure 4.1 Colony morphology of soil isolated *Streptomyces* spp. on ISP2 media after 10 days of incubation. (A) *Streptomyces* sp. MSK03; (B) *Streptomyces* sp. MSK05.

For the molecular identification of *Streptomyces* spp.*,* the 16S rRNA gene sequence of strains MSK03 and MSK05 were amplified using 27F and 1525R primers (Lane, 1991). The 16S rDNA PCR products were submitted to Macrogen (Korea) for sequencing. The GenBank accession numbers of 16S rRNA gene sequence of MSK03 and MSK05 were ON159854 and ON159855, respectively. The 16S rRNA gene sequences of MSK03 and MSK05 were blasted with the 16S rDNA sequence from EzBioCloud database. The 16S rRNA gene of the strain MSK03 showed 99.79% similarity to *Streptomyces monashensis* MUSC 1J^T (accession number; KP998432), while the strain MSK05 showed 99.86% similarity to *Streptomyces spectabilis* NBRC13424^T (accession number; AB184393). The phylogenetic trees of MSK03 and MSK05 were constructed using MEGA software. The 16S rRNA sequence of *Streptomyces* sp. MSK03 and MSK05 were compared to their closest related species to create the phylogenetic tree (Figures 4.2).

4.2 Biosynthesis of gold nanoparticles

The current study used extracellular and intracellular cell-free supernatants of *Streptomyces* sp. (MSK03 or MSK05) as reducing agents to synthesize AuNPs. The AuNPs were synthesized by mixing extracellular or intracellular cell-free supernatant of *Streptomyces* spp. with 1 mM HAuCl$_4$ in the following ratios: 9:1, 8:2, 7:3, 6:4, 5:5, 4:6, 3:7, 2:8, and 1:9. The mixtures were incubated at 37°C, 200 rpm for 24 h. After incubation, the color of a mixture of intracellular cell-free supernatant and HAuCl$_4$ did not change, while the color of a mixture of extracellular cell-free supernatant and HAuCl$_4$ changed from light yellow to purple (Figure 4.3). In addition, fermented broth and HAuCl$_4$ were used as negative controls. The color of negative controls did not change after incubation.
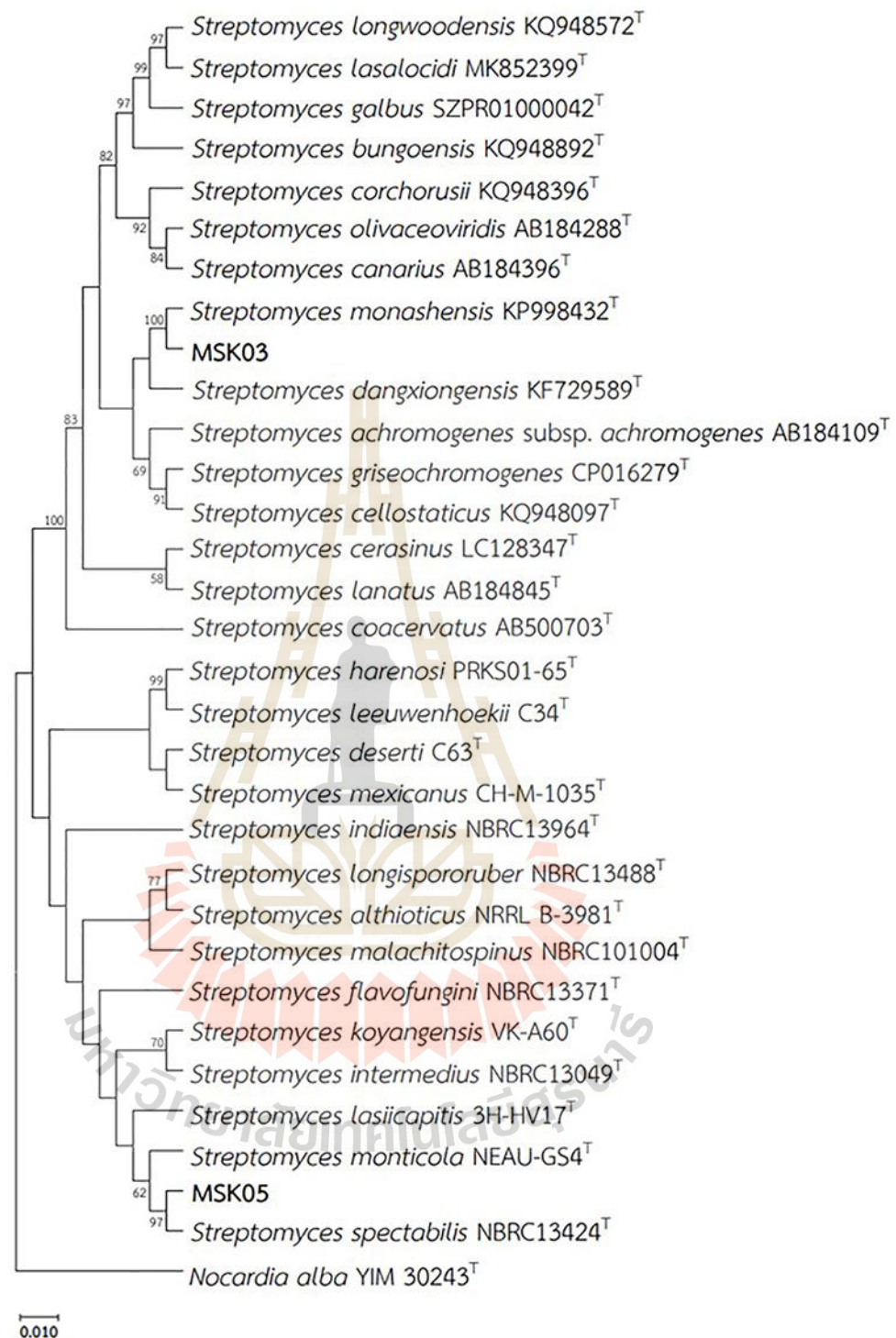
Figure 4.2 Neighbor-joining phylogenetic tree based on 16S rRNA gene indicating the taxonomic position of strain MSK03, MSK05, and related species. Only values greater than 50 of 1,000 replicates bootstrap percentages are shown. A distance of 0.01 substitutions per nucleotide position is indicated by the bar. *Nocardia albayim* 30243[T] was used as an outgroup.

The AuNPs synthesized using extracellular cell-free supernatant of *Streptomyces* sp. MSK03 and MSK05 were designated as MSK03-AuNPs and MSK05-AuNPs, respectively. After incubation, the mixing of extracellular cell-free supernatant and $HAuCl_4$ converted from light yellow to purple. It should be noted that the purple hue represents a surface plasmon resonance (SPR) property of AuNPs. The SPR of AuNPs was detected using UV-Vis spectroscopy. The color of the mixture of extracellular-free supernatant of MSK03 and $HAuCl_4$ changed at the ratios of 5:5, 7:3, and 8:2 (Figure 4.4A). The color of the mixture of extracellular-free supernatant mixture of MSK05 and $HAuCl_4$ changed at the ratios of 3:7, 4:6, 5:5, 6:4, 7:3, and 8:2 (Figure 4.4B).
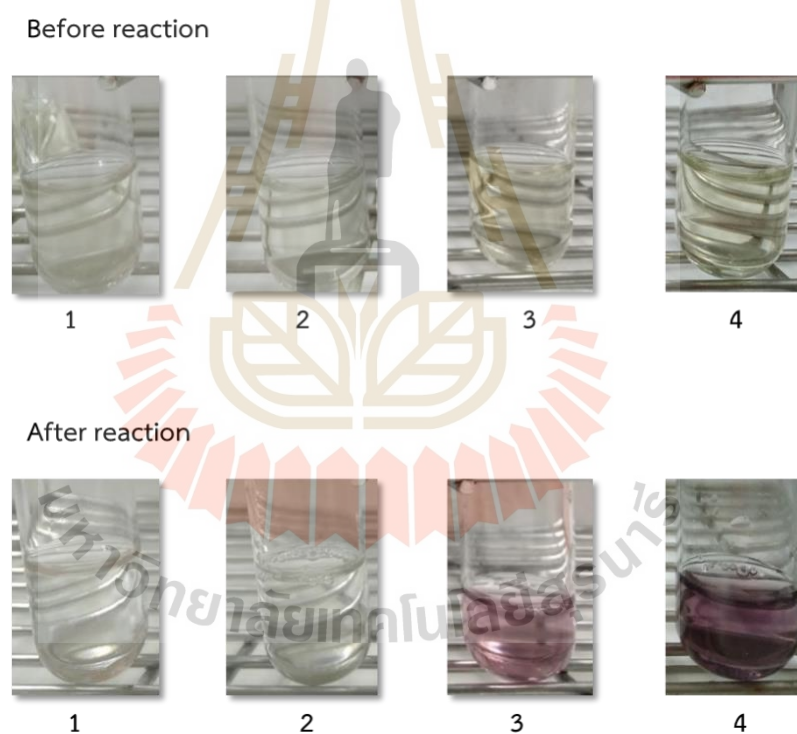
Figure 4.3 Visible observation of the color change of biosynthesis AuNPs by *Streptomyces* sp. (1) 1 mM $HAuCl_4$; (2) Intracellular cell-free supernatant to 1 mM $HAuCl_4$; (3) Extracellular cell-free supernatant of MSK03 to 1mM $HAuCl_4$; (4) Extracellular cell-free supernatant of MSK05 to 1 mM $HAuCl_4$.
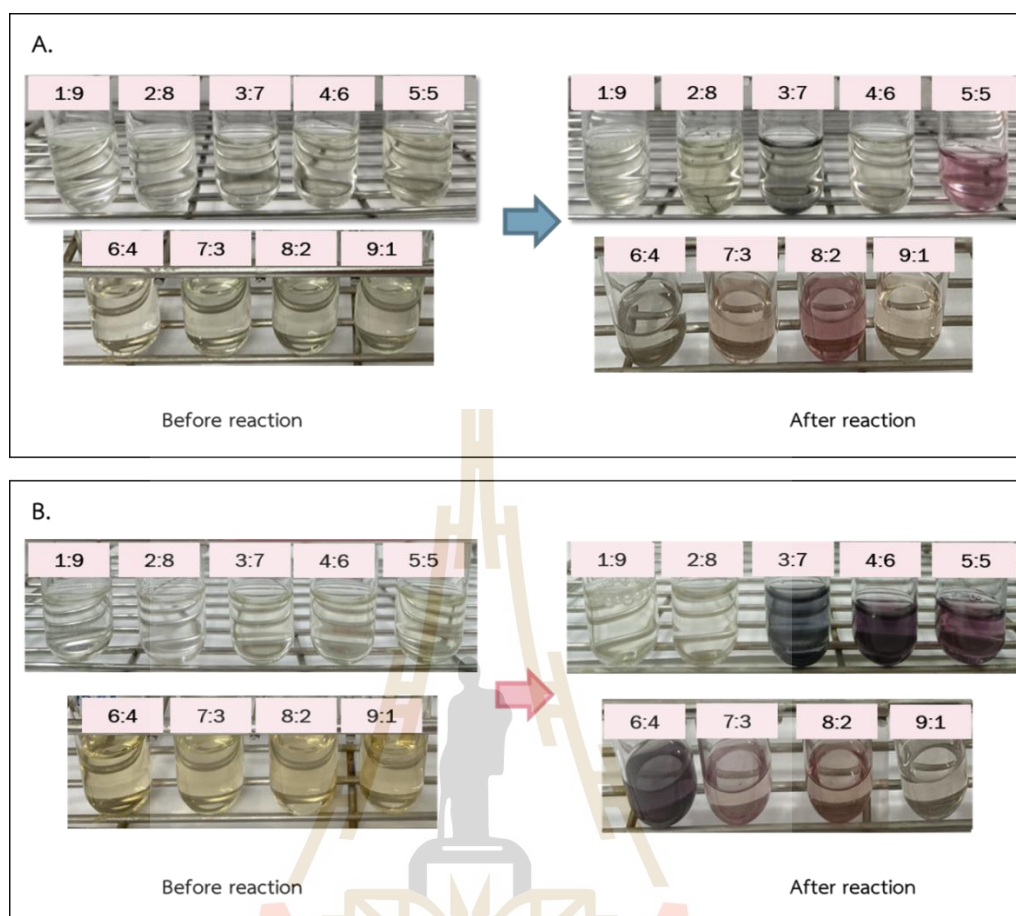
Figure 4.4 Visible observation of the color change of biosynthesis AuNPs obtained by varying the ratio of extracellular cell-free supernatant of *Streptomyces* sp. to 1 mM HAuCl$_4$. (A) Extracellular cell-free supernatant of MSK03 to 1 mM HAuCl$_4$; (B) Extracellular cell-free supernatant of MSK05 to 1 mM HAuCl$_4$.

4.3 Characterization of gold nanoparticles

4.3.1 UV-Vis spectroscopy analysis

UV–Vis absorption spectrophotometry was applied to measure the position of the localized surface plasmon resonance (LSPR) band. A UV-Vis spectroscopy analysis was used to confirm the visual observations of the color change of biosynthesis AuNPs. The absorption spectra of AuNPs were measured from 300–800 nm. MSK03-AuNPs presented the wavelength of maximum absorbance of the LSPR band at 545 nm, while MSK05-AuNPs presented the wavelength of

maximum absorbance of the LSPR band at 530 nm. The absorption spectrum of AuNPs was not observed in the control tests (extracellular cell-free supernatants or HAuCl$_4$), as shown in Figure 4.5. The LSPR band of MSK03-AuNPs was measured at mixing ratios of 5:5, 7:3, and 8:2. The highest absorbance intensity of MSK03-AuNPs was measured at a ratio of 5:5 (Figure 4.6A). The ratio of the mixing of MSK03-AuNPs as 5:5 was collected to study of incubation time of 72 h. The result showed absorption intensity increase with increasing incubation times (Figure 4.6B). The LSPR band of MSK05-AuNPs was measured at mixing ratios of 3:7, 4:6, 6:4, 5:5, 7:3, and 8:2. The highest absorbance intensity of MSK05-AuNPs was measured at the ratio of 5:5 (Figure 4.7A). The ratio of the mixing of MSK05-AuNPs as 5:5 was collected to study of incubation time of 72 h. The result showed absorption intensity increased with increasing incubation times until 24 h. After 24 h, the incubation period was not significant in the SPR band of AuNPs (Figure 4.7B). Therefore, the ratio of the mixing of AuNPs as 5:5 for 72 h was used for further experiments.
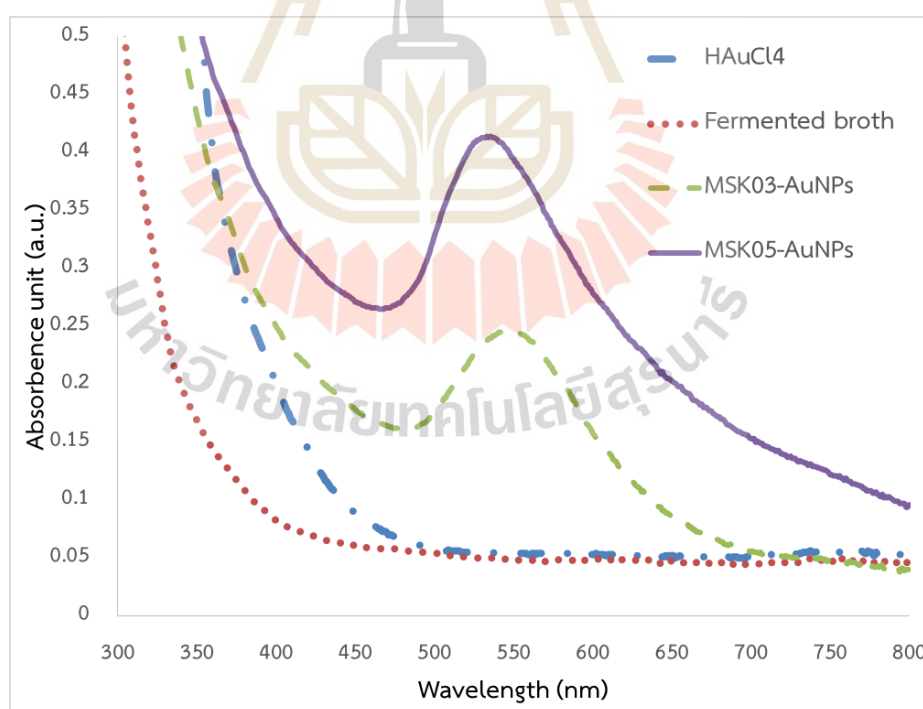
Figure 4.5 UV-Vis spectra of precursor, MSK03-AuNPs, and MSK05-AuNPs incubated at 37°C, 200 rpm for 24h.
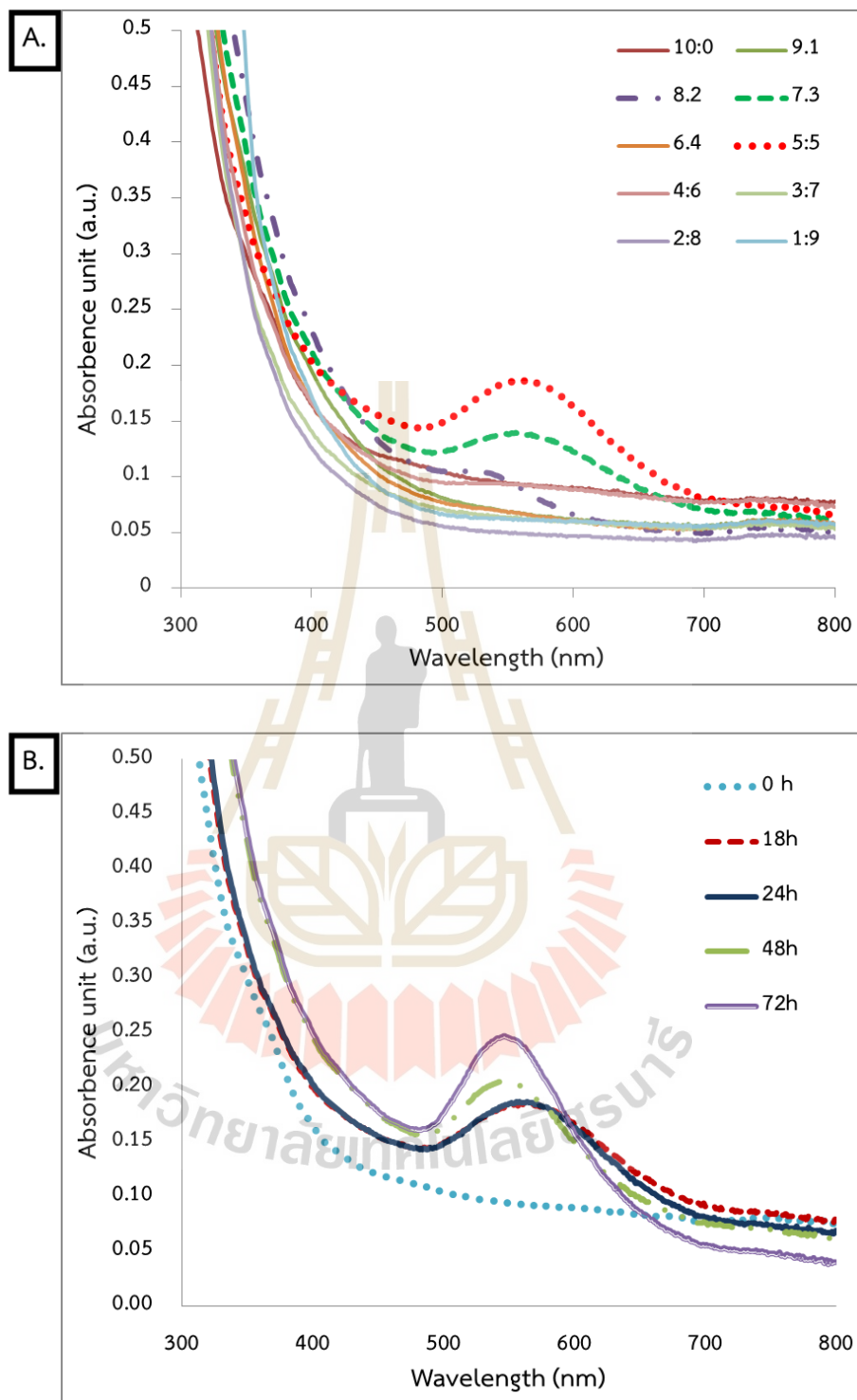
Figure 4.6 UV-Vis spectra of MSK03-AuNPs. (A) UV-Vis spectra of AuNPs in the following ratios: 9:1, 8:2, 7:3, 6:4, 5:5, 4:6, 3:7, 2:8, and 1:9 incubated at 37°C, 200 rpm for 24 h; (B) UV-Vis spectra of AuNPs at the ratio of 5:5 and incubating at 37°C, 200 rpm for 0, 18, 24, 48, and 72 h.

28
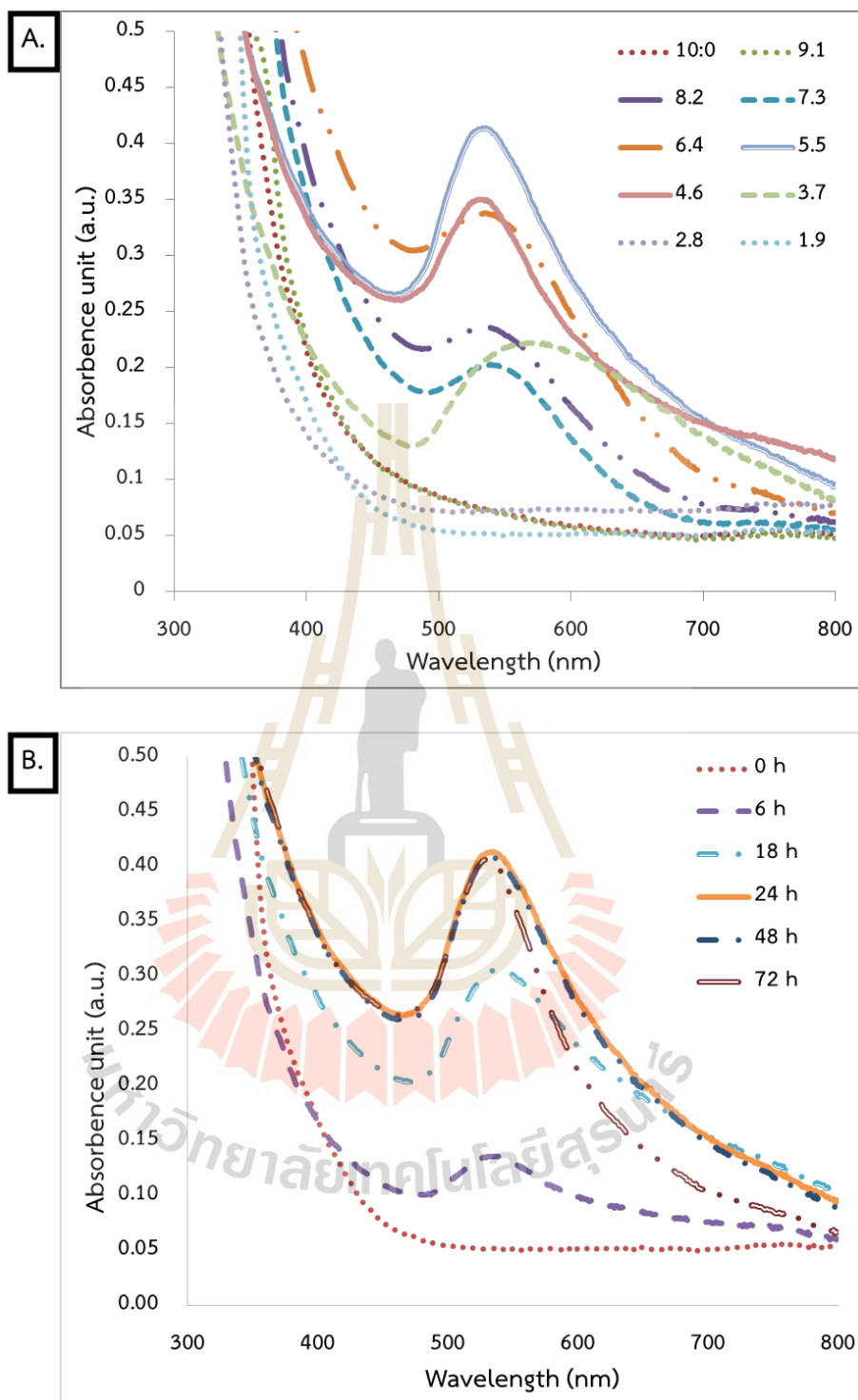
Figure 4.7 UV-Vis spectra of MSK05-AuNPs. (A) UV-Vis spectra of AuNPs in the following ratios: 9:1, 8:2, 7:3, 6:4, 5:5, 4:6, 3:7, 2:8, and 1:9 incubated at 37°C, 200 rpm for 24 h; (B) UV-Vis spectra of AuNPs at the ratio of 5:5 and incubating at 37°C, 200 rpm for 0, 6, 18, 24, 48, and 72 h.

4.3.2 X-ray diffraction (XRD) analysis

A crystalline nanoparticle was confirmed by XRD analysis. The crystal structure of MSK03-AuNPs and MSK05-AuNPs was determined using the XRD pattern, as shown in Figure 4.8. The crystalline of AuNPs was represented by four diffraction peaks. The diffraction peaks of MSK03-AuNPs at 2theta were 38.3, 44.5, 64.9, and 77.8. MSK05-AuNPs had diffraction peaks of 38.5, 44.6, 64.9, and 77.9 at 2theta. The diffraction peaks obtained at different angles were identical to those previously reported for the standard gold metal. Thus, the crystal structure of MSK03-AuNPs and MSK05-AuNPs had the characteristics of cubic lattice surfaces.
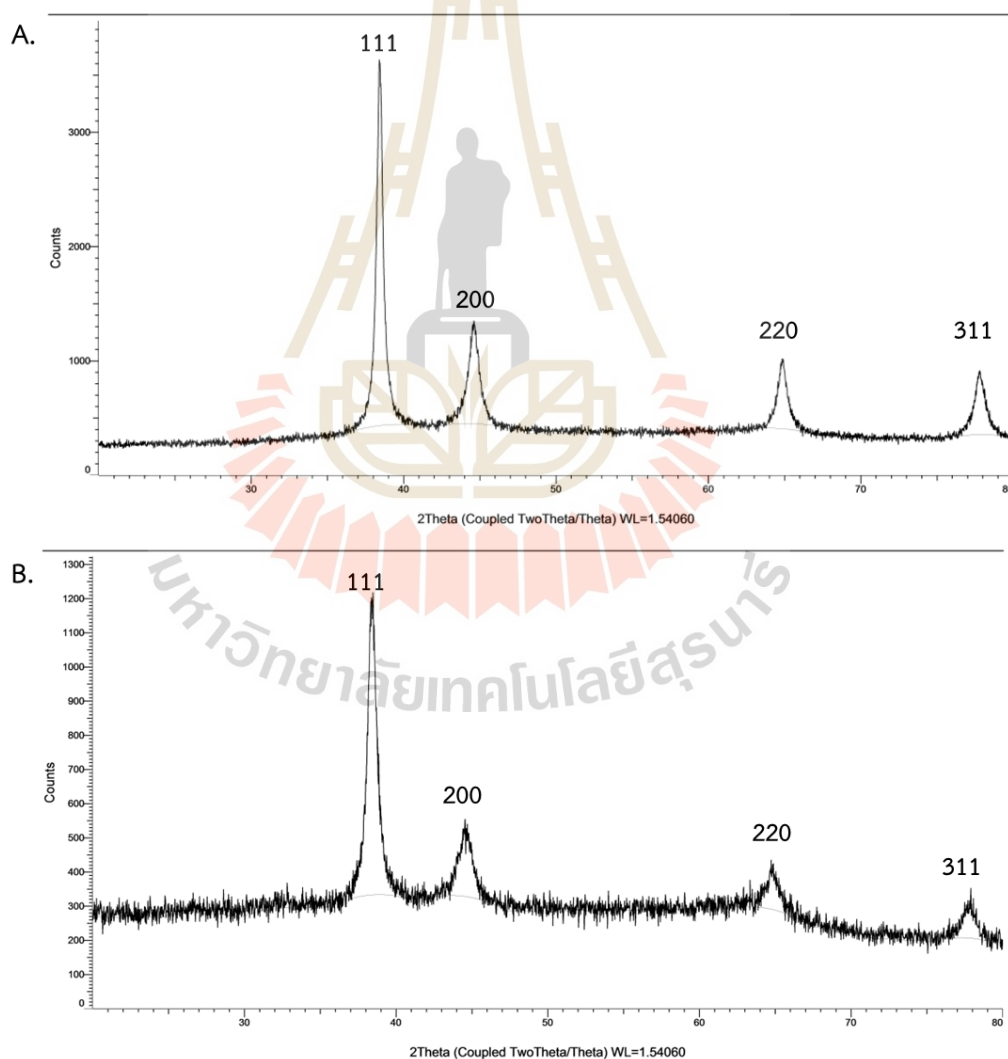
Figure 4.8 The X-ray diffraction pattern of biosynthesized AuNPs. (A) MSK03-AuNPs and (B) MSK05-AuNPs.

4.3.3 Zeta potential measurement and particle size distribution

Dynamic light scattering (DLS or Zeta-sizer) was used to estimate the particle size distribution and potential of AuNPs. The biosynthesized AuNPs were dispersed in a liquid phase. The colloidal AuNPs were prepared by dispersing the AuNPs sample in water. The MSK03-AuNPs had an average size of 46.34 nm with a polydispersity index (PDI) of 0.268, while MSK05-AuNPs had an average size of 23.33 nm with a PDI of 0.465 (Figure 4.9). The stability of the nanoparticles was checked by measuring the adsorption of the dispersion layer around the particle surface by using zeta potential measurements. The results were measured for zeta potential in the range of -150 to +150 mV. The MSK03-AuNPs and MSK05-AuNPs had zeta potential values of -0.53 (±0.14) mV and -0.14 (±0.02) mV, respectively. The results of AuNPs indicated negative repulsion (Figure 4.10).
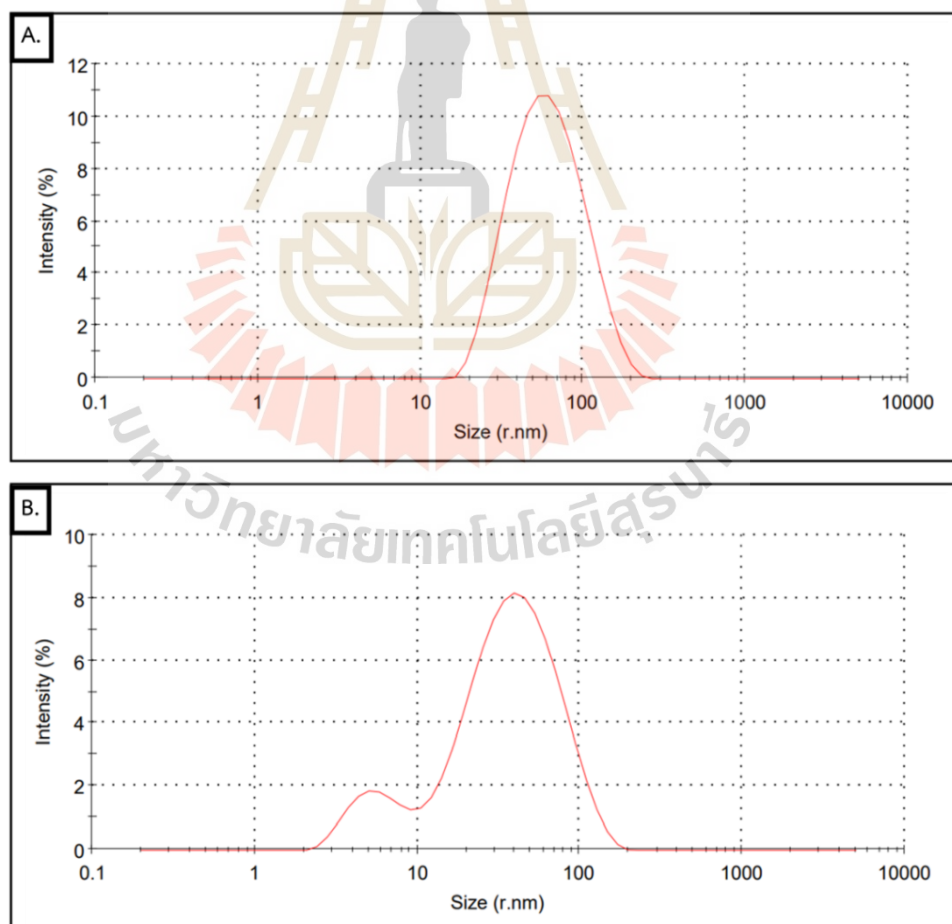
Figure 4.9 The particle size distribution of biosynthesized AuNPs. (A) MSK03-AuNPs and (B) MSK05-AuNPs.
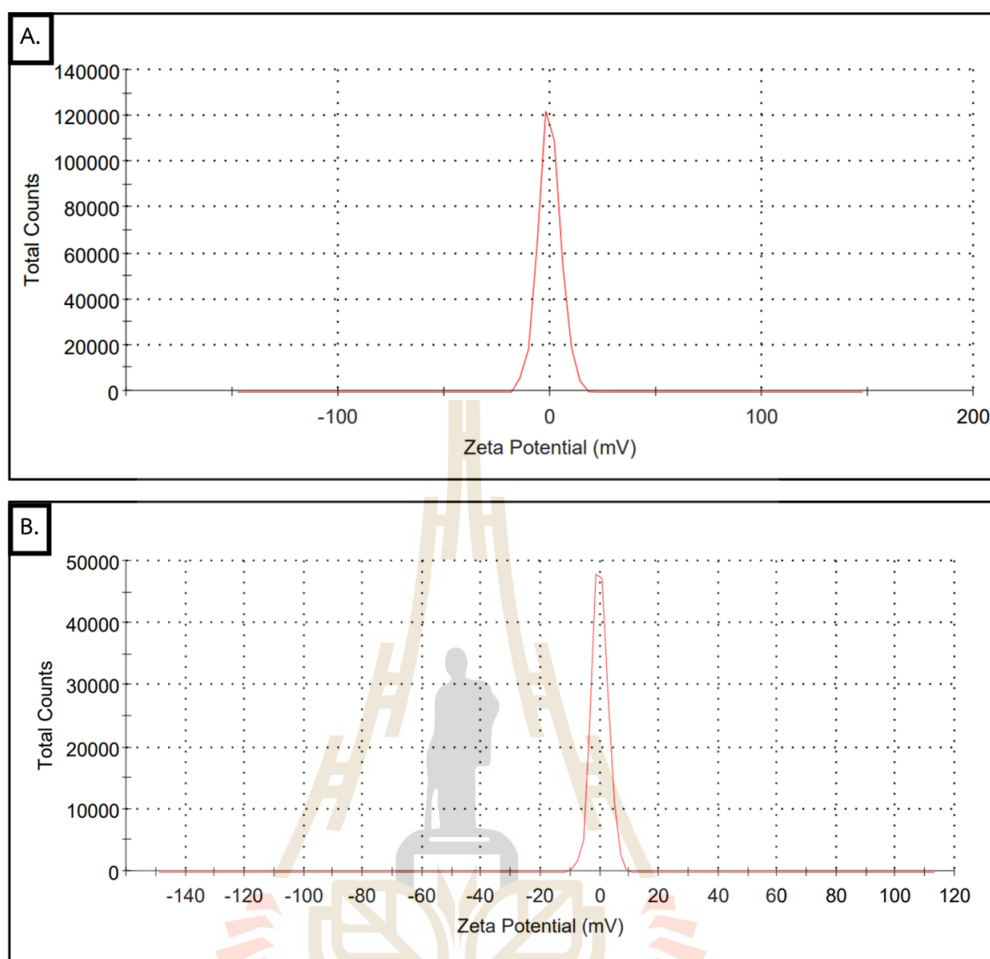
Figure 4.10 Zeta potential of biosynthesized AuNPs. (A) MSK03-AuNPs and (B) MSK05-AuNPs.

4.3.4 Transmission electron microscopy (TEM) analysis

TEM was used to confirm the presence of AuNPs in the samples and to determine the shape and size of biosynthesized AuNPs. The biosynthesized AuNPs using *Streptomyces* sp. MSK03 and MSK05 exhibited mostly spherical and polygonal forms (Figure 4.11A and Figure 4.12A). The average particle sizes of MSK03-AuNPs and MSK05-AuNPs were calculated by measuring the spherical and polygonal AuNPs particle of more than 100 particles from TEM images. The average particle size of MSK03-AuNPs was 23.2 ± 10.7 nm, ranging from 7.1 to 40.0 nm (Figure 4.11B). The average particle size of MSK05-AuNPs was 20.3 ± 9.7 nm, ranging from 3.3 to 40.0 nm (Figure 4.12B).

A.
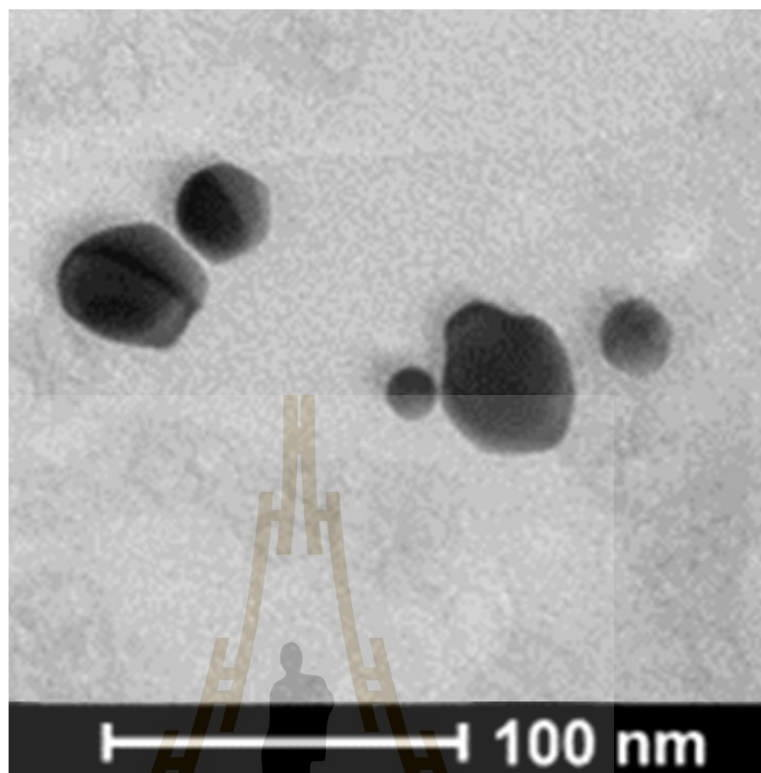
B.
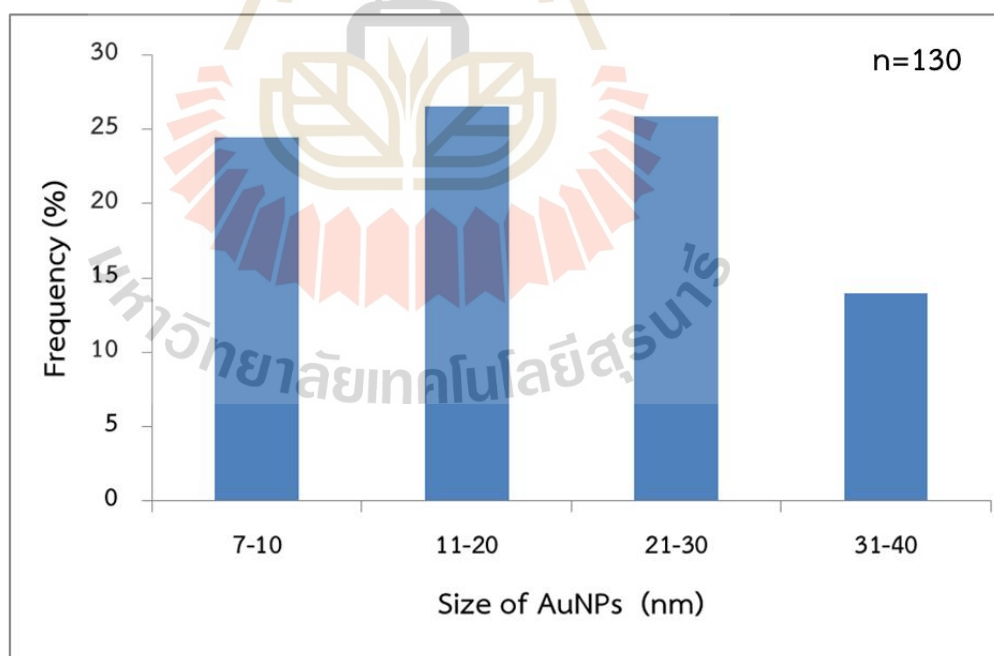
Figure 4.11 TEM image of biosynthesized MSK03-AuNPs. (A) The morphology of MSK03-AuNPs, scale bar=100 nm; (B) The particle size distribution of MSK03-AuNPs, n=130.

A.
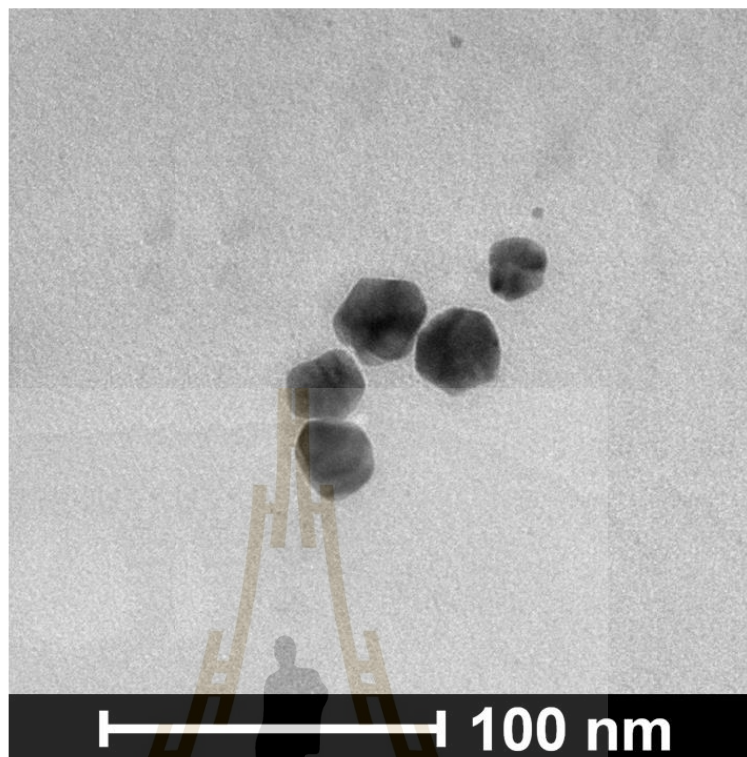
B.
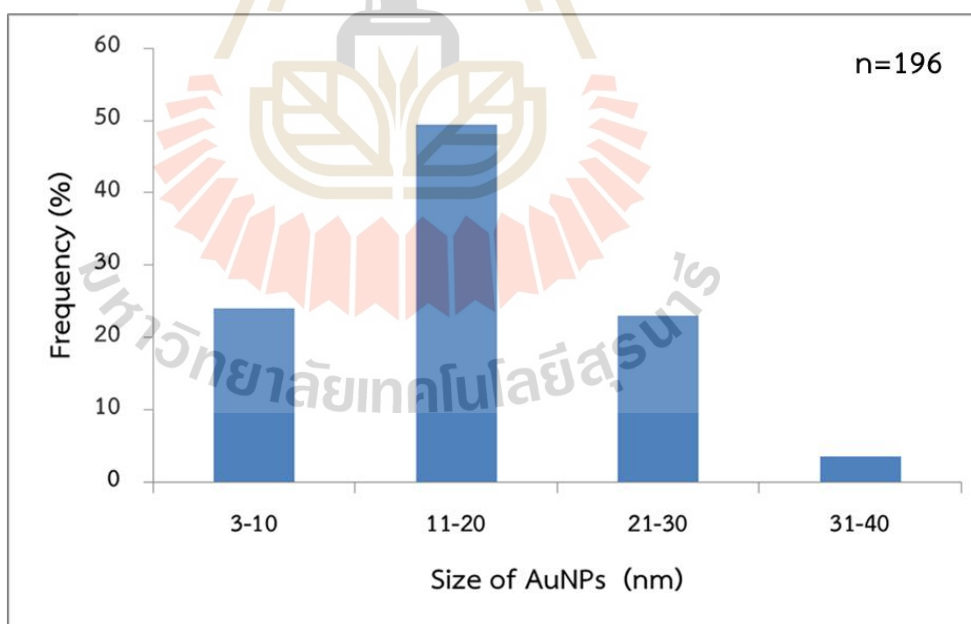
Figure 4.12 A TEM image of biosynthesized MSK05-AuNPs. (A) The morphology of MSK05-AuNPs, scale bar=100 nm; (B) The particle size distribution of MSK05-AuNPs, n=196.

4.3.5 Energy-dispersive X-ray fluorescence (EDXRF) analysis

EDXRF was used to determine the elemental composition of the biosynthesized AuNPs. The EDXRF spectra confirmed that metallic Au was detected in the MSK03-AuNPs and MSK05-AuNPs (Figure 4.13). The EDXRF results indicated that the amount of Au element in the MSK03-AuNPs and MSK05-AuNPs was 8.08% and 7.35%, respectively. Strong optical adsorption peaks of metallic Au were observed at 2.2, 9.7, and 11.5 keV.

4.3.6 Fourier transform infrared (FTIR) analysis

The functional groups involved in the reduction and stabilization of AuNPs were identified using FTIR spectroscopy. FTIR spectra of extracellular cell-free supernatant of *Streptomyces* sp. MSK03 before and after bioreduction of Au^{3+} ions were represented in Figure 4.14. The spectrum showed five major peaks. There was a shift in peak from 3354, 1625, 1364, 1052, and 514 cm^{-1} of the extracellular cell-free supernatant of *Streptomyces* sp. MSK03 to 3270, 1644, 1354, 1017, and 524 cm^{-1} which correspond to N-H or O-H stretching, C=O stretching or N-H bending, C-N stretching or N-H bending, C-H stretching, and C-H bending or metal-ligand stretching, respectively.

FTIR spectra of extracellular cell-free supernatant of *Streptomyces* sp. MSK05 before and after bioreduction of Au^{3+} ions were represented in Figure 4.15. The spectrum was a shift in peak from 3298, 1642, 1356, 1014, and 521 cm^{-1} of the extracellular cell-free supernatant of *Streptomyces* sp. MSK05 to 3270, 1592, 1353, 1019, and 525 cm^{-1} which correspond to N-H or O-H stretching, C=O stretching or N-H bending, C-N stretching or N-H bending, C-H stretching, and C-H bending or metal-ligand stretching, respectively.
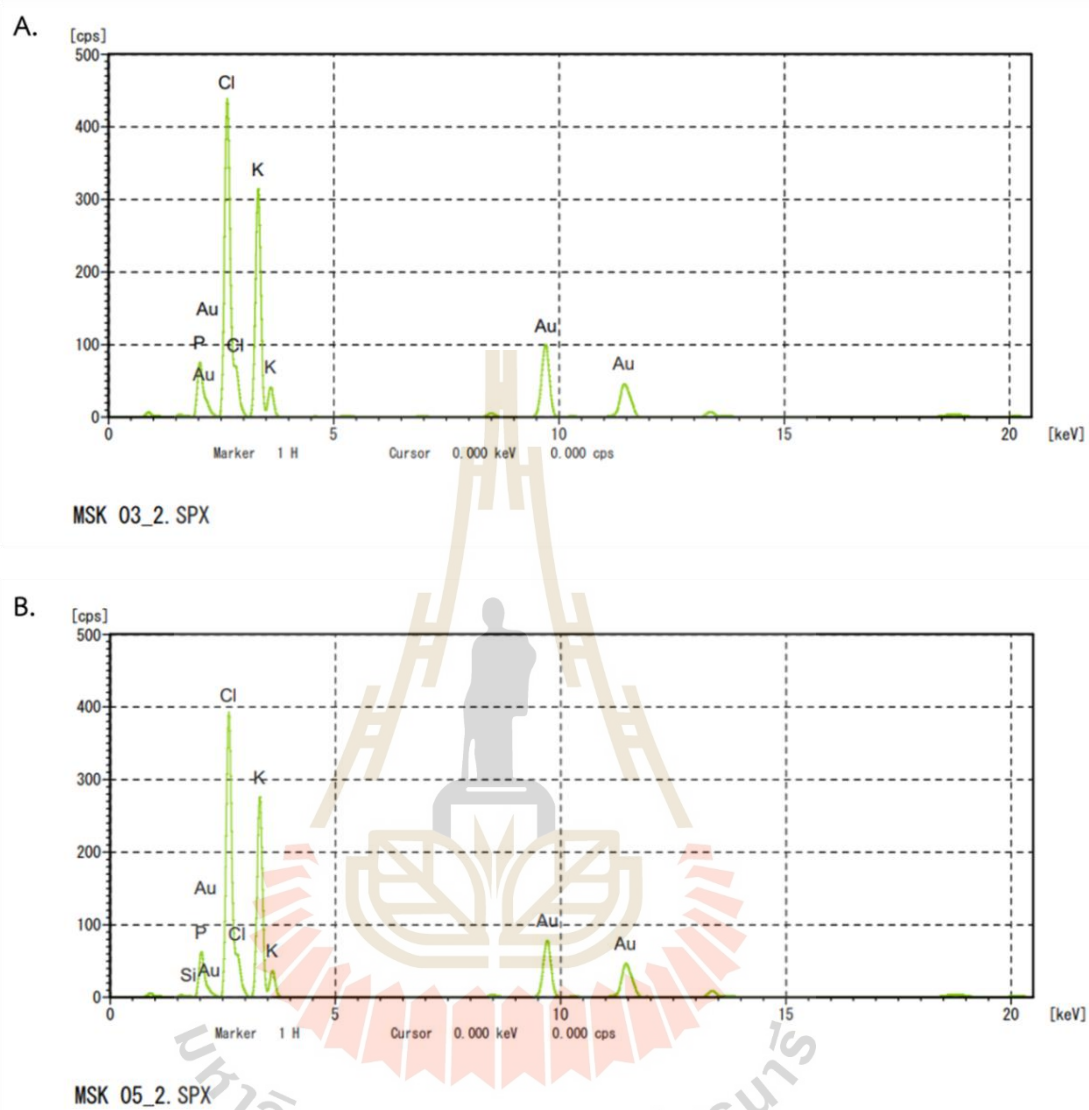
Figure 4.13 Energy dispersive spectra of biosynthesized AuNPs. Gold elements were detected in the spectrum. (A) MSK03-AuNPs and (B) MSK05-AuNPs.
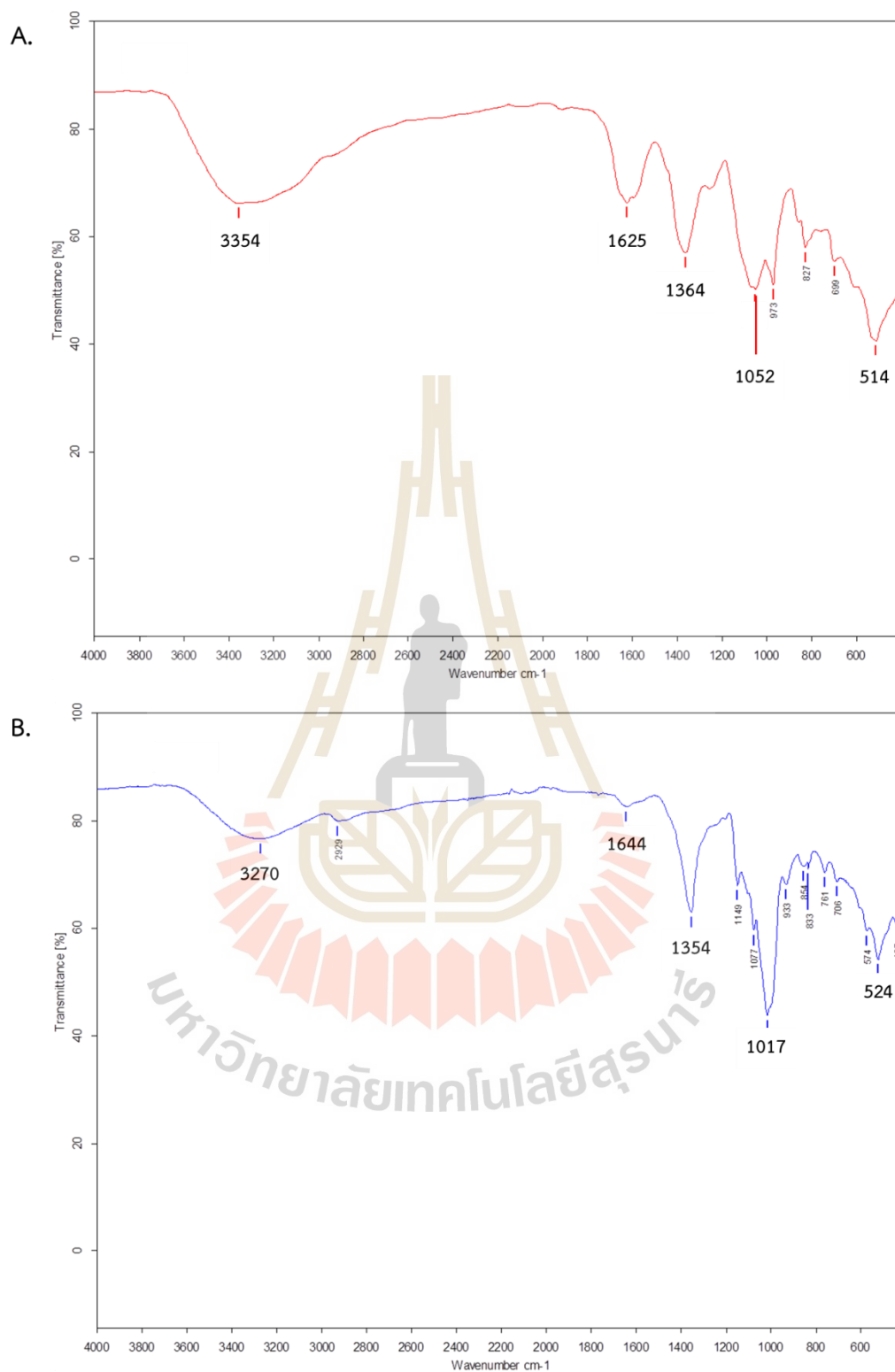
Figure 4.14 FTIR spectra of (A) the extracellular cell-free supernatant of *Streptomyces* sp. MSK03 and (B) the MSK03-AuNPs.
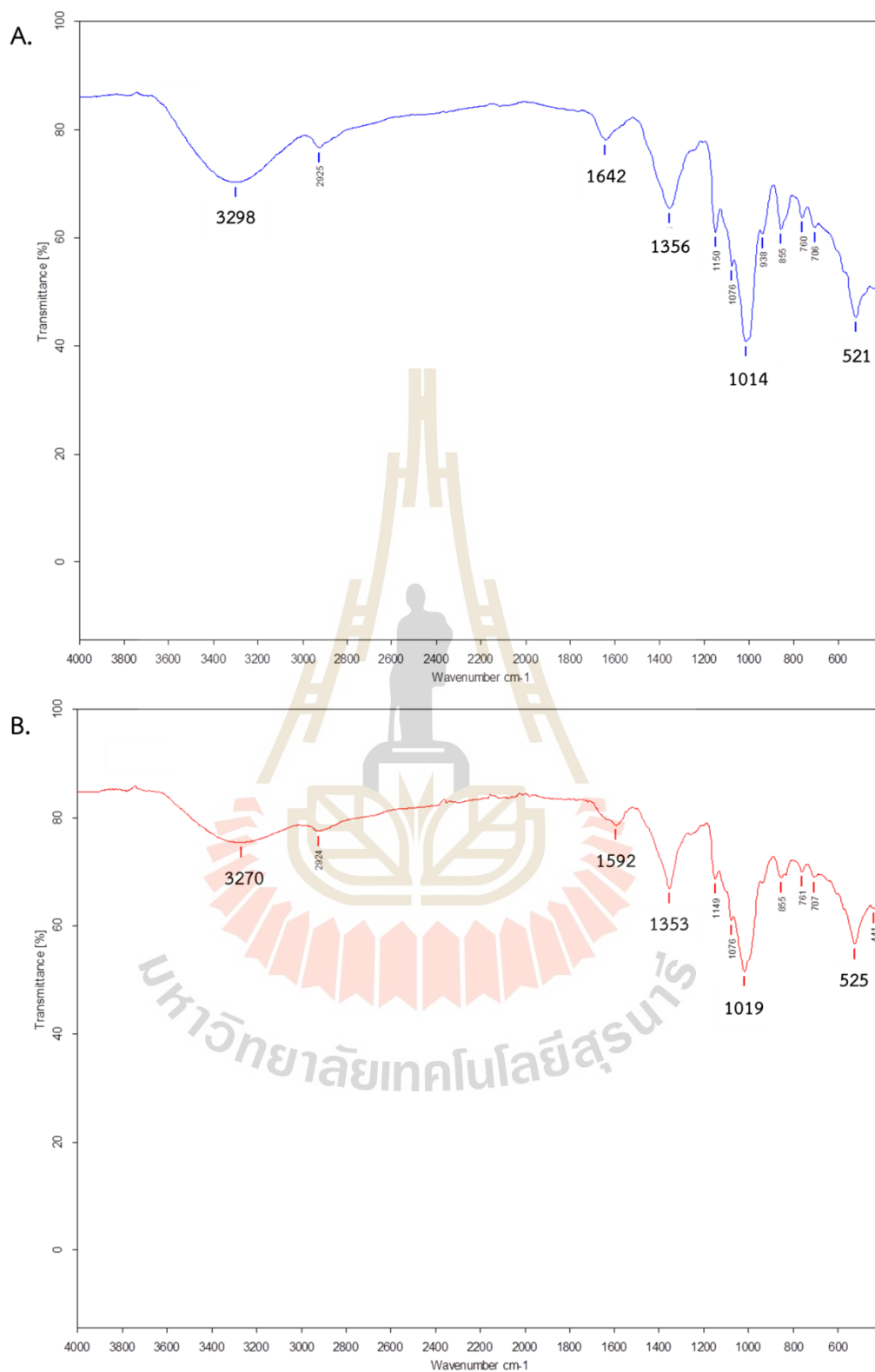
Figure 4.15 FTIR spectra of (A) the extracellular cell-free supernatant of *Streptomyces* sp. MSK05 and (B) the MSK05-AuNPs.

4.3.7 X-ray absorption near edge structure (XANES) analysis

The local geometry and structure of gold in the synthesized AuNPs were determined using XANES analysis. The XANES measurement was carried out in single run at an energy range of 11888.3–11998.4 eV around the Au L3 edge. Pure Au metal foil and $HAuCl_4$ were used as reference materials for Au^0 and Au^{3+}, respectively. The XANES spectra profiles of MSK03-AuNPs and MSK05-AuNPs compared to reference material were shown in Figure 4.16 and Figure 4.17, respectively. The spectra of MSK03-AuNPs and MSK05-AuNPs showed a profile of energy similar to Au metal foil and $HAuCl_4$. Energy profile data indicated a partial reduction of Au^{3+} to Au^0.
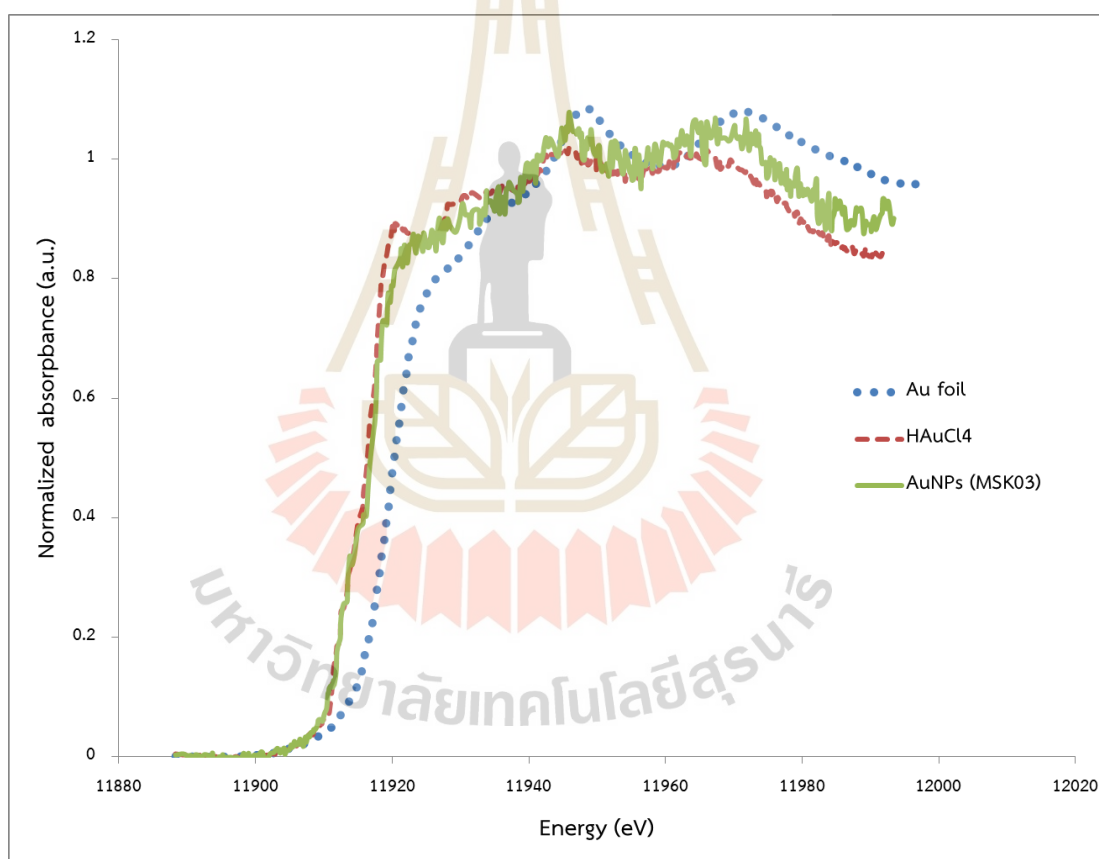
Figure 4.16 XANES spectra of $HAuCl_4$, Au foil and MSK03-AuNPs.
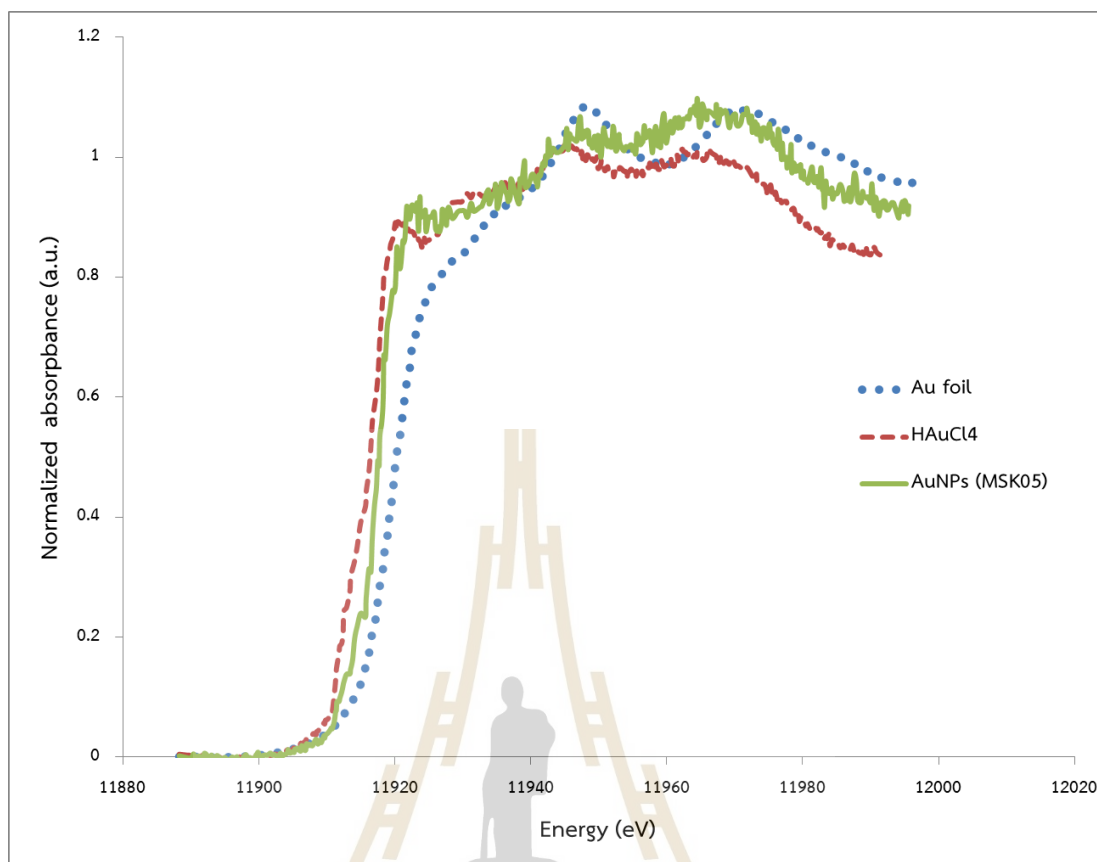
Figure 4.17 XANES spectra of HAuCl$_4$, Au foil and MSK05-AuNPs.

4.4 Antimicrobial activity of gold nanoparticles

Antibacterial activities of AuNPs against pathogens were evaluated by the agar well diffusion method. The fermented broth and HAuCl$_4$ were used as the control. The percentage of Au elemental acquired from EDXRF was used to estimate the amount of AuNPs used for antibacterial testing. Based on EDXRF, the percentages of Au in MSK03-AuNPs and MSK05-AuNPs were 8.08% and 7.35%, respectively. The antibacterial activity of MSK03-AuNPs and MSK05-AuNPs against Gram-negative and Gram-positive bacteria was shown in Table 4.1. MSK03-AuNPs showed antibacterial activity against *S. aureus* TISTR1466, *E. coli* TISTR8465, *P. aeruginosa* N90Ps, *P. aeruginosa* TISTR1287, *A. baumanii,* and *S. marcescense,* while MSK05-AuNPs had antibacterial activity against *S. aureus* TISTR1466, MRSA DMST20651, MRSA DMST20654, *E. coli* TISTR8465, *P. aeruginosa* N90Ps, *P. aeruginosa* TISTR781, *P. aeruginosa* TISTR1287, *A. baumanii,* and *S. marcescense.* The maximum inhibition

zones value of antibacterial activity of MSK03-AuNPs and MSK05-AuNPs was found against *P. aeruginosa* TISTR1287

       The broth microdilution method was used to evaluate the minimum inhibitory concentrations (MIC) of MSK03-AuNPs and MSK05-AuNPs against Gram-positive and Gram-negative bacteria. The reference drugs were vancomycin and tetracycline. The MIC values of MSK03-AuNPs and MSK05-AuNPs were > 141.4 μg/mL against tested pathogens, as show in Table 4.2.

Table 4.1 Antimicrobial activity of MSK03-AuNPs and MSK05-AuNPs (565.6 μg/mL of Au^0).

Tested pathogens	HAuCl$_4$	Inhibition zone (mm)			
		MSK03		MSK05	
		AuNPs	Supernatant	AuNPs	Supernatant
S. aureus TISTR1466	0	12.17±0.76	0	8.33±0.51	0
MRSA DMST20651	0	0	0	10.88±2.17	0
MRSA DMST20654	0	0	0	13.17±0.60	0
E. coli TISTR8465	0	10.61±2.57	0	9.58±2.26	0
P. aeruginosa N90Ps	0	11.20±0.67	0	9.87±1.44	0
P. aeruginosa TISTR781	0	0	0	10.07±0.95	0
P. aeruginosa TISTR1287	0	17.58±0.67	0	22.09±2.27	0
A. baumanii	0	9.44±0.80	0	11.88±3.61	0
S. marcescense	0	8.44±0.23	0	8.19±0.47	0

The values are mean ± standard deviations for triplicate experiments.

Table 4.2 MICs of MSK03-AuNPs and MSK05-AuNPs.

Tested pathogens	MICs (µg/ml)			
	MSK03-AuNPs	MSK05-AuNPs	Vancomycin	Tetracycline
MRSA DMST20654	>141.4	>141.4	8	64
P. aeruginosa TISTR1287	>141.4	>141.4	>128	32
A. baumanii	>141.4	>141.4	>128	>128

CHAPTER V
DISCUSSION AND CONCLUSION

Streptomyces bacteria are the genus of the Actinomycetales order. *Streptomyces* are aerobic, filamentous, Gram-positive bacteria and are commonly found in a variety of environments, especially in soil. *Streptomyces* is a good source of extracellular enzymes and bioactive compounds. *Streptomyces* sp. produces secondary metabolites for clinically important bioactive compounds with antivirals, antitumor, antifungal, antibiotics, and insecticidal properties (Khan et al., 2011; Procópio et al., 2012; Song et al., 2004). The *Streptomyces* has a various colony structure based on spore color, substrate and aerial mycelium development, and diffusible pigment productions (Michael et al., 2012). In this study, *Streptomyces* strain MSK03 and MSK05 were isolated from Sakaerat Environmental Research Station and Botanical Garden at the Suranaree University of Technology, respectively. The phenotypic characteristics, such as colony morphology, sporulation, and pigment, of *Streptomyces* strain MSK03 and MSK05 were identified on ISP2 medium. The identification of bacteria based on phenotypic characteristics was not quite as effective as molecular identification (Zhang et al., 2019).

Thus, the soil isolated MSK03 and MSK05 were identified based on the 16s rRNA gene sequence and phylogenetic connection. The molecular techniques based on 16S rRNA gene sequences were used to confirm the strain of several bacteria (Taylor et al., 2007; Zhang et al., 2019). The 16S rRNA sequencing is widely used for bacteria identification and taxonomic classification. Bacterial identification of the 16S rRNA gene uses approximately 1500 base pair genes located on small subunits in the 30s of prokaryotic ribosomes. The 16S rRNA sequencing has the advantages of speed, cost-effectiveness, and high precision (Case et al., 2007; Kim and Chun, 2014; Reller et al., 2007; Yang et al., 2016). The steps in 16S rRNA sequencing consist of DNA extraction using chemicals, PCR amplification of the target sequence, DNA elution by agarose gel electrophoresis, and follow by target band purification (Antony-Babu et

al., 2017; Takeuchi et al., 1996). For phylogenetic investigations, the 16S rRNA gene is employed to compare different species of bacteria. The comparison of 16S rRNA gene sequences to induce phylogenetic relationships of different bacteria species have been widely used for several decades (Coenye and Vandamme, 2003; Weisburg et al., 1991).

In this research, the 16S rRNA gene of MSK03 shared 99.79% sequence similarity to *S. monashensis* with 100% bootstrap value, while MSK05 shared 99.86% sequence similarity to *S. spectabilis* with 95% bootstrap value. Therefore, soil isolated MSK03 was identified as *S. monashensis,* while MSK05 was identified as *S. spectabilis*. The phylogenetic tree from evolutionary distance data of soil isolates MSK03 and MSK05 was generated by using the neighbor-joining method with 1,000 replications bootstrap analysis. The neighbor-joining method is commonly utilized in the construction of phylogenetic trees because of its excellent accuracy and computational speed in the phylogenetic analysis as demonstrated by computer simulation investigations. The basic idea behind this strategy is to locate pairs of operational taxonomic units (OTUs) that minimize overall branch length at each level of the OTU clustering (Saitou and Nei, 1987).

In recent years, antibiotic-resistant microorganisms have emerged. The development of high-resistance genes has linked to high levels of antibiotic resistance (Hsueh, 2010; Shaikh et al., 2015). Nanotechnology is a rapidly developing field with enormous potential. Nanomedicine offers a good foundation for combating drug resistance (Shaikh et al., 2015). Moreover, nanoparticles are used in a wide range of applications, including agriculture, solar cells, pollution control, waste management, and medicine approaches for anticancer, antitumor, antibacterial activity, and so on (Basu et al., 2015). The particle size of technology at the nanoscale is small particles in nanoscale ranging from 1 to 100 nm (Lee et al., 2020). Nanoparticles are very attractive for a wide variety of biotechnology applications due to their unique chemical and physical properties (Shah et al., 2014). Because of their physical, biological, and chemical characteristics, gold nanoparticles are among the most commonly used metal nanoparticles due to their potential for a wide variety of applications such as water purification, food industry, biological, and medicinal

applications (Menon et al., 2017; Shahzadi et al., 2018; Zhang et al., 2015). Gold metal and gold ionic form have long been recognized to have broad spectrum antibacterial and bactericidal effects (Agnihotri et al., 2013; Zhang et al., 2015; Zhou et al., 2012). The properties of AuNPs depend on morphology and reaction modifications to obtain AuNPs of the desired size, shape, and surface functionality (Shah, Badwaik, and Dakshinamurthy, 2014; Sperling et al., 2008). AuNPs have bio-nanotechnology applications such as sensing for detection and diagnostics, transport of therapeutic agents to the cells, cell imaging, antimicrobial, and so on (Yeh et al., 2012).

Chemical and physical processes, such as chemical, photochemical, and electrochemical reduction, are used to synthesize AuNPs (Kshirsagar et al., 2014; Scaiano et al., 2009; Yang et al., 2011). These methods usually depend on toxic chemicals as reducing or capping agents. The presence of precursor materials may cause the cytotoxicity of healthy cells (Shukla and Iravani, 2018). An environmentally friendly approach to nanoparticle synthesis is expected to overcome the toxicity problem in nanoparticle synthesis. Green synthesis focuses on reducing and eliminating environmentally hazardous processes (Jahangirian et al., 2017; Yang et al., 2011). The green materials, such as biopolymers, enzymes, fungi, bacteria, and plants, were used to synthesize nanoparticles (Lee et al., 2020). Microorganisms are commonly used for the biosynthesis of AuNPs. Actinobacteria isolated from several environments have been identified as potential to synthesize AuNPs. The biosynthesis of AuNPs is available in the intracellular and extracellular of the actinobacteria, including *Streptomyces* (Manivasagan et al., 2016). The biosynthesized AuNPs using intracellular and extracellular *Streptomyces* was illustrated in Table 5.1.

In the synthesis process, the AuNPs exhibit changing colors from light yellow to purple, red, orange, and brown in an aqueous solution. The color change is due to the increase in the size distribution of AuNPs from 1 to 100 nm (Jain et al., 2006). Moreover, the presence of color change is a direct sign of the reduction of Au^{3+} to Au^{0} (Hassanisaadi et al., 2021). Soltani and co-workers reported the color changes from pale yellow to deep red on the AuNPs biosynthesis using *S. fulvissimus* isolate U after incubation at 30°C for 48 h (Soltani et al., 2015). They have also reported a

similar observation of the color changes using *S. microflavus* isolate extracellular after incubation at 28°C for 24 h (Soltani et al., 2016). The color changes from yellow to pinkish purple on the AuNPs biosynthesis using intracellular of *S. viridogens* strain HM10 after incubation at 28°C for 24 h was reported by Balagurunathan et al. (Balagurunathan et al., 2011). In this research, the synthesis of AuNPs used both extracellular and intracellular cell-free supernatants of *Streptomyces* sp. (MSK03 or MSK05) as reducing agents. The color change from light yellow to purple was observed from synthesized AuNPs using extracellular cell-free supernatant of *Streptomyces* spp.

Table 5.1 Biosynthesis of AuNPs using *Streptomyces* spp.

Actinomycete strain	Precursor	Activity	References
S. viridogens HM10	intracellular	antimicrobial	(Balagurunathan et al., 2011)
S. hygroscopicus BDUS 49	extracellular	antimicrobial	(Sadhasivam et al., 2012)
Streptomyces sp.	extracellular	antifungal	(Gopal et al., 2013)
Streptomyces sp LK-3	extracellular	antimalarial	(Karthik et al., 2013a)
Streptomyces sp. NK52	extracellular	anti-lipid peroxidation	(Prakash et al., 2013)
S. fulvissimus isolate U	extracellular	ND	(Soltani et al., 2015)
S. microflavus isolate 5	extracellular	ND	(Soltani et al., 2016)
S. coelicoflavus SRBVIT13	extracellular	anti-hyperglycemic	(Kumar and Rao, 2016)
S. griseoruber	extracellular	catalytic	(Ranjitha and Rai, 2017)
Streptomyces sp. strain NH21	extracellular	antibacterial	(Składanowski et al., 2017)
S. tuirus DBZ39	intracellular	antiviral	(Zainab, 2022)

ND, not determined.

The optical properties of AuNPs are phenomena caused by surface plasmon resonance (SPR). The plasmon band occurs when the frequency of electron oscillations in the conduction band of AuNPs resonates with the frequency of incoming light radiation. The SPR in AuNPs requires a specific frequency range of light radiation, which is commonly observed in the visible regions (Mie, 1908; Shankar et al., 2004). UV–Vis absorption spectrophotometry was used to determine the position of localized surface resonance plasma resonance (LSPR) bands to confirm the color change of the synthesized AuNPs (Sharma et al., 2016). The specific frequency of the surface plasmon resonance peak depends on the shape and size of AuNPs (Huang and El-Sayed, 2010; Link and El-Sayed, 1999). In general, spherical AuNPs have been shown a single plasmon band ranging from 500 to 580 nm (Hu et al., 2020; Kim et al., 2016; Poinern, 2014). Sathish Kumar and Bhaskara Rao (2016) reported the maximum absorbance peak at 540 nm to confirm the presence of biosynthesized AuNPs using *S. coelicoflavus* SRBVIT13. Soltani et al. (2015) reported a strong peak with a maximum absorbance of synthesized AuNPs using *S. fulvissimus* isolate U at 550 nm. In this study, the biosynthesized AuNPs using *Streptomyces* sp. MSK03 and MSK05 showed the highest intensity of the LSPR band for AuNPs at 545 and 530 nm, respectively. The results confirmed the presence of AuNPs synthesized by *Streptomyces* sp. MSK03 and MSK05.

In addition, the increase in the particle size of AuNPs affects the change of the maximum absorption that shows a red shift of wavelength (wavelength increasing). The increase in absorbance wavelength is caused by higher electromagnetic retardation. The intensity of the absorbance peak also demonstrates the higher number of AuNPs. The increase in AuNPs concentration led to an increase in the absorbance intensity (Cui et al., 2012; Link and El-Sayed, 1999; Menon et al., 2017; Shukla and Iravani, 2017; Zhou et al., 2012). In this study, UV-Vis absorbance was used to observe the AuNPs synthesis process. The different incubation times of the AuNPs synthesis process depend on reducing agents. This evidence pointed to the reduction of Au^{3+} to Au^{0} by reducing agents found in extracellular cell-free supernatant of *Streptomyces* sp. MSK03 and MSK05. The AuNPs were synthesized using extracellular cell-free supernatant of *S. monashensis* MSK03 and *S. spectabilis*

MSK05 at 37°C for 72 h. The incubation process takes shorter than the biosynthesis of AuNPs using other reducing agents such as extracellular cell-free supernatant of *S. hygroscopicus* BDUS 49, which has been taken 120 h for the incubation process (Sadhasivam et al., 2012). The biosynthesis of AuNPs using *S. viridogens* HM10 as reducing agents has been taken 120 to 168 h for incubation process (Balagurunathan et al., 2011). The detailed mechanism of the reduction process of Au^{3+} to Au^{0} remains unclear. Several researchers have been proposed the reducing agents of biosynthesized AuNPs such as components like lipids, carbohydrates, nucleic acids, or proteins (Shah et al., 2014). While the reducing agents of biosynthesized AuNPs using *Streptomyces* spp. have been proposed as cell wall reductive enzymes and enzymes on the cytoplasmic membrane (Ahmad et al., 2003; Manivasagan et al., 2016)

The probable organic functional groups of capping, stabilizing, and reducing agents for the synthesized AuNPs can be identified using FTIR analysis. The functional groups of biomolecules that are attached to the surface of AuNPs have the potential to involve the reduction of Au^{3+} to Au^{0} (Dahoumane et al., 2016; Elavazhagan and Arunachalam, 2011; Chithrani et al., 2006; Manivasagan et al., 2016). Sathish Kumar and Bhaskara Rao (2016) reported that the functional groups of proteins such as amide, carboxyl, and hydroxyl groups from *S. coelicoflavus* SRBVIT13 are attached to the AuNPs surface as stabilizing agents. Soltani Nejad et al. (2016) reported the presence of hydroxyl groups, carboxyl groups, and N–H stretching of amine groups in biomass of *S. microflavus* isolate No. 5 that are involved in the AuNPs reduction. The presence of a different functional group corresponding to N-H or O-H, C-H, C=O, C-O, and the metal-ligand stretching frequency from the FTIR spectra of the synthesized AuNPs using *S. griseoruber* was reported by Ranjitha and Rai (2017). It has been suggested the possible compounds with N–H or O–H functional groups for the AuNPs stabilization (Dhas et al., 2014). In this study, FT-IR spectra of the biosynthesized AuNPs using extracellular cell-free supernatant of *Streptomyces* sp. MSK03 and MSK05 showed similar regions of five major peaks: N-H or O-H stretching, C=O stretching or N-H bending, C-N stretching or N-H bending, C-H stretching, and C-H bending or metal-ligand stretching. The FT-IR spectra were identified using the FTIR

database. The absorption peaks of O-H, N-H, and C=O stretching correspond to the functional groups of carbohydrate, amine, and amide, respectively. The other regions of N-H bending, C-H stretching, and C-H bending correspond to the amine functional groups of the protein. These results indicated the probable functional groups of *Streptomyces* sp. MSK03 and MSK05 might be associated with the reduction of Au^{3+} and stabilization of AuNPs. The change in peak intensity or shift in the wavenumber of functional groups from the extracellular-free supernatant to AuNPs describes the class of functional groups involved in the interaction of AuNPs and biomolecules (Wan et al., 2020).

The surface charge or zeta potential of colloidal AuNPs solutions was determined using DLS (Jiang et al., 2009). Zeta potential results describe the surface charge, stability, and aggregation condition of colloidal particles of biosynthesized AuNPs (Graily-Moradi et al., 2020; Mittal et al., 2013; Muthuvel et al., 2014). Typical zeta potential values of surface charge of nanoparticles in colloidal solution range from +100 to -100 mV (Shnoudeh et al., 2019). A large positive or negative zeta potential value indicates that the nanoparticle dispersion is physically stable due to the electrostatic repulsion of individual particles. The zeta potential of the nanoparticles with values less than -25 mV or more than +25 mV usually have high degree of stability. While a low zeta potential value of nanoparticle dispersion will lead to coagulation, flocculation, or aggregation due to Van der Waals interaction, resulting in poor physical stability (Brock, 2004; Clogston and Patri, 2011a; Clogston and Patri, 2011b; Horie and Fujita, 2011; Sapsford et al., 2011; Shnoudeh et al., 2019). Karthik et al. (2013a) reported the zeta potential as 28.6 mV, indicating the stability of biosynthesis of AuNPs using marine actinobacterial in remaining distinct in each liquid. Składanowski et al. reported the zeta potential of -14.5 mV of biosynthesized AuNPs using *Streptomyces* sp. strain NH21, indicating moderate stability of nanoparticles (Składanowski et al., 2017). In this research, the value of zeta potential of MSK03-AuNPs and MSK05-AuNPs was -0.53 mV and -0.14 mV, respectively. The MSK03-AuNPs and MSK05-AuNPs had low zeta potential values, resulting in poor physical stability due to coagulation, flocculation, or aggregation of nanoparticles dispersion.

EDXRF technique was used to confirm the chemical or elemental composition of metal nanoparticles (Shah et al., 2015; Strasser et al., 2010). The electron beam hits the inner electrons shell of the atom, knocking out the inner electrons and resulting in a positively charged electron hole. After that, the electron hole in the vacant position is replaced by another electron from the outer shell. The standard two-dimensional graph of the EDX spectrum represents the ionization energy, while the ordinate represents the counts. It has been reported the optical absorption peak of surface plasmon resonance adsorption in gold nanocrystal at around 2.30 keV (Arunachalam et al., 2013). Sathish Kumar and Bhaskara Rao reported the EDX profile of the biosynthesized AuNPs using marine *S. coelicoflavus* SRBVIT13. The EDX pattern of the sample exhibits signals for O, C, and Au atoms, confirming biomolecular capping on AuNPs surfaces. The EDX profile of the biosynthesized AuNPs using *S. coelicoflavus* SRBVIT13 showed the gold signals at around 2.20, 9.70, and 11.42 keV (Kumar and Rao, 2016). Soltani et al. reported the EDX profile of the biosynthesized AuNPs using *S. fulvissimus* isolate U, which represents the number of AuNPs in the biomass. The EDX profile of the biosynthesized AuNPs using *S. fulvissimus* showed strong signals for AuNPs at different places at 2.20, 9.70, and 11.5 keV (Soltani et al., 2015). In addition, it has been reported the EDX profile of the biosynthesized AuNPs using *S. microflavus* isolate 5 that showed strong signals of AuNPs at 2.20, 9.70, and 11.5 keV (Soltani et al., 2016). In this study, the EDX results confirmed the presence of gold elemental in synthesized AuNPs. The presence of a gold pattern in the MSK03-AuNPs is similar to MSK05-AuNPs (Figure 4.13). The EDX spectra of Au elements were observed at approximately 2.2, 9.7, and 11.5 keV. The other elements, including chloride (Cl), potassium (K), and phosphorus (P), were detected in the colloidal AuNPs due to traces of the cell-free supernatant and the gold salt.

The TEM provides information on the morphology, shapes, and size of nanoparticles (Montes et al., 2011; Schaffer et al., 2009). In this study, The TEM images of MSK03-AuNPs and MSK05-AuNPs were spherical and polygonal. The spherical shape is a general morphology of biosynthesized AuNPs using *Streptomyces* sp. (Manivasagan et al., 2016). For example, biosynthesized AuNPs using *S. viridogens*,

S. griseus, *S. hygroscopicus*, *Streptomyces* sp. ERI-3, *S. microflavus*, and *S. tuirus* DBZ39 had spherical morphology (Balagurunathan et al., 2011; Khadivi et al., 2012; Sadhasivam et al., 2012; Soltani et al., 2016; Zainab, 2022; Zonooz et al., 2012). Menon's review study shown that the size of biosynthesized AuNPs with spherical shape ranges from 1 to 200 nm (Menon et al., 2017). While the size of spherical biosynthesized AuNPs produced by *Streptomyces* sp. has been recorded to range between 5 to 50 nm (Manivasagan et al., 2016; Menon et al., 2017). In this study, the TEM result of MSK03-AuNPs represents the spherical shape with an average size of 23.2 ± 10.7 nm, ranging from 7.1 to 40.0 nm. MSK05-AuNPs represent the spherical shape with an average size of 20.3 ± 9.7 nm, ranging from 3.3 to 40.0 nm. In addition, DLS was used to estimate the particle size distribution of biosynthesized AuNPs using a liquid solution (Mittal et al., 2013; Muthuvel et al., 2014; Wu et al., 2018). In this study, MSK03-AuNPs had an average particle size of 46.34 nm in the hydrodynamic diameter range, with a PDI of 0.268. MSK05-AuNPs have an average size of 23.33 nm and a PDI of 0.465. The PDI of more than 0.1 indicates the polydisperse particle size distributions of MSK03-AuNPs and MSK05-AuNPs (Raval et al., 2019). It has been reported that the particle size observed in the TEM image is smaller than that measured by the DLS analyzer (Muthuvel et al., 2014; Ranjitha and Rai, 2017). Muthuvel et al. reported that the DLS result for AuNPs had an average particle size of around 50 nm, while the TEM image showed the size distribution of AuNPs ranging from 5 to 35 nm with an average size of 32 ± 6 nm (Muthuvel et al., 2014). Ranjitha and Rai reported that the DLS result for AuNPs using *S. griseoruber* to have an average particle size of around 80.9 nm, while the TEM image showed the size distribution of AuNPs range from 5 to 50 nm (Ranjitha and Rai, 2017). They have been proposed that the TEM image measures the particle size of the dried sample, while DLS measures the particle size distribution of the hydrodynamic particle diameter with a dynamic light scattering of AuNPs dispersed in a liquid phase (Muthuvel et al., 2014; Ranjitha and Rai, 2017).

XRD is a common technique for determining the diffraction pattern of compounds. XRD analysis is a widely used to determine the crystal structure of AuNPs (Bennur et al., 2016; Jeffery, 1971; Manivasagan et al., 2016). The diffraction

peaks of MSK03-AuNPs and MSK05-AuNPs were compared to an XRD standard for AuNPs structure Joint Committee on Powder Diffraction Standards reference no. 04-0784 in a database of XRD patterns maintained by the International Center for Diffraction Data. The diffraction peaks of AuNPs were located at approximately 2theta of 38°, 45°, 65°, and 78° (Figure 4.8) which correspond to (111), (200), (220), and (311) reflections of the face-centered cubic (fcc) structure of the standard gold metal (Au^{0}), respectively (Balagurunathan et al., 2011; Cheng et al., 2015; Prakash et al., 2013; Ranjitha and Rai, 2017; Ren et al., 2015; Kumar and Rao, 2016; Soltani et al., 2015). Khadivi Derakhshan et al. reported XRD spectra of the biosynthesis of AuNPs by *S. griseus* and $HAuCl_{4}$ to represent the AuNPs formation after 48 h. The XRD spectrum of biosynthesized AuNPs using *S. griseus* revealed five intense peaks, 38.27, 44.60, 64.68, 77.55, and 82.35, which correspond to fcc structure of AuNPs (Khadivi et al., 2012). The XRD pattern analysis revealed peaks on the biosynthesized AuNPs using the cell-free supernatant of *Streptomyces sp.* VITDDK3 at 38.10 (111), 44.28 (200), 64.42 (220), and 77.37 (311), corresponding to the diffraction plane of Au^{0} was previously reported by Gopal et al. (Gopal et al., 2013). Sathish Kumar and Bhaskara Rao reported the XRD pattern of biosynthesized AuNPs using *S. coelicoflavus* SRBVIT13. The results of biosynthesized AuNPs using *S. coelicoflavus* SRBVIT13 showed the crystalline nature of AuNPs at 2theta of 38.28, 44.27, 64.65, and 77.66, corresponding to the reflection planes of the fcc phase of AuNPs (Kumar and Rao, 2016).

XANES is an absorption spectroscopy technique that used to describe the local electronic structure of an atom. The use of synchrotron radiation in XANES spectroscopy is an authorized technique for determining the electronic, magnetic, and structural properties of matter. Photon absorption in XANES stimulates an electron from a core state to an empty state. To excite an electron at the core level, the photon energy must be equal to or higher than the binding energy of that level. When the photon energy is scanned, a new absorption channel is opened. XANES is an element-selective technology because absorption edge energy corresponds to core-level energy that is unique to each element. XANES is a powerful technique for studying mineral surfaces and adsorbents on mineral surfaces and characterizing bulk

minerals. The element specificity of XANES spectroscopy and the ability to access comprehensive data in the absence of long-range order are two of its unique features. In many cases, the density of unoccupied electronic states in a process is demonstrated to be closely related to the X-ray absorption spectra. XANES can provide a detailed picture of local electrical structure of an element (Bianconi, 1980; Henderson et al., 2014). X-ray absorption fine structure spectroscopy at the Au L3 and L2 edges indicated the formation of AuNPs *in situ*. The electronic and dispersion characteristics of AuNPs during their growth were analyzed using a series of X-ray absorption near-edge structure spectra at both edges (Ohyama et al., 2011). Konishi et al. reported the different profile energy of XANES spectra between Au^0 (Au foil), Au^{3+} ($HAuCl_4$), and synthesized AuNPs using the bacterium *Shewanella algae*. XANES spectra showed the oxidation state of synthesized AuNPs using *S. algae* to be Au^0, confirming that *S. algae* can reduce Au^{3+} to Au^0 (Konishi et al., 2007). In this study, MSK03-AuNPs and MSK05-AuNPs were investigated at the Au L3 edge using XANES. As a result, XANES spectra of AuNPs were compared with Au^0 and Au^{3+}. XANES spectra of MSK03-AuNPs and MSK05-AuNPs represent the region between Au^0 and Au^{3+}. So, it can be concluded that *S. monashensis* MSK03 and *S. spectabilis* MSK05 cell-free supernatants can reduce $AuCl_4^-$ ions into Au elements.

Medicinal applications of AuNPs depend on the shape, size, and nanoparticle compositions (Hu et al., 2020). The applications of spherical AuNPs of different sizes were shown in Table 5.2. AuNPs are useful for antibacterial effects and attacking intracellular microorganisms due to their small dimensions. It has been reported that the small size of AuNPs demonstrated high antimicrobial activities (Lai et al., 2015; Slavin et al., 2017; Wang et al., 2017). Moreover, the surface chemistry of the synthesized AuNPs is one of the important factors in the properties and functionality of AuNPs. It has been reported the conjugate status of AuNPs for therapeutic and cellular applications. Surface chemistry can be categorized based on the type of surface functionalization, which includes amine, citrate, nucleic acid, lipid, peptide, and antibody ligands. The surface functionalization of amine have been reported an effect on the application of drug delivery, gene transfection, oligonucleotide transfection, and antiviral activity (Giljohann et al., 2010). Several studies have been

reported the characteristic of biosynthesized AuNPs that had chemical stability, well-developed surface chemistry, and appropriate small size easier to interact with bacteria. Antibacterial activity of the biosynthesized AuNPs has been reported against both Gram-negative and Gram-positive bacteria such as *Entercoccus faecium*, *K. pneumoniae*, *A. baumannii*, *P. aeruginosa*, *E. coli*, *E. aerogenes*, and *S. aureus.* Moreover, AuNPs can potentially operate as antibiotic transporters or delivery vehicles, increasing the bactericidal activity of antibiotics. AuNPs had the potential to be utilized as antibiotic transporters or delivery vehicles, hence boosting bactericidal action (Bindhu and Umadevi, 2014; Rice, 2010; Shah et al., 2014; Zhang et al., 2015). The possible antimicrobial mechanism of AuNPs has been suggested, such as cell membrane interaction, accumulation on the cell surfaces, and heavy electrostatic attraction (Chamundeeswari et al., 2010; Johnston et al., 2010).

Table 5.2 Medicinal applications of AuNPs with different sizes.

Morphology	Size (nm)	Application/activity	References
Nanosphere	2	Drug delivery	(Peng et al., 2019)
Nanosphere	2-10	Antioxidant	(Tahir et al., 2015)
Nanosphere	4-10	Antimicrobial	(Ahmad et al., 2013)
Nanosphere	5-10	Drug delivery, Bioactivity	(Rossi et al., 2016)
Nanosphere	10-20	Antimicrobial	(Sadhasivam et al., 2012)
Nanosphere	15-20	Antiviral	(Zainab, 2022)
Nanosphere	20-37	Anticancer, Antimicrobial	(Ramalingam et al., 2017)
Nanosphere	100	Therapeutics (PTT and RT)	(Hu et al., 2017)

RT, Radiation therapy; PTT, Photothermal therapy

For the antimicrobial activity of AuNPs that were synthesized using *Streptomyces* sp. Balagurunathan et al. reported antimicrobial activity of biosynthesized AuNPs using *S. viridogens* strain HM10. Spherical AuNPs (18-20 nm particle size) derived from *S. viridogens* HM10 inhibited *S. aureus* and *E. coli* with

inhibition zones of 14 and 20 mm, respectively (Balagurunathan et al., 2011). In this study, the antimicrobial activity against several pathogenic bacteria was measured using the agar well diffusion method. The synthesized AuNPs appear to inhibit the growth of test pathogenies effectively. The inhibition zone of MSK03-AuNPs and MSK05-AuNPs was observed against *S. aureus* TISTR1466*, E. coli* TISTR8465*, P. aeruginosa* N90Ps*, P. aeruginosa* TISTR1287*, A. baumanii, and S. marcescense*. In addition, MSK05-AuNPs also observed inhibition zones against MRSA DMST20651, MRSA DMST20654, and *P. aeruginosa* TISTR781 (Table 4.1).

In most cases, AuNPs have previously been shown ineffective at killing pathogenic bacteria. It has been reported that the bactericidal of biosynthesized AuNPs is very weak at high concentrations (Zhang et al., 2015). The antimicrobial activity of biosynthesized AuNPs using *S. hygroscopicus* BDUS 49 was previously reported by Sadhasivam et al. (2012) Spherical of biosynthesized AuNPs using *S. hygroscopicus* with an average size of 10 to 20 nm inhibited *S. aureus, E. coli*, and *S. typhimurium* with a MIC value of 32 µg/mL. While, AuNPs had MICs of 64, 128, and 256 g/ml against *B. subtilis, S. epidermidis*, and *E. faecalis*, respectively (Sadhasivam et al., 2012). Składanowski et al. (2017) reported antimicrobial activity of biosynthesized AuNPs using the supernatant of *Streptomyces sp.* strain NH21. The AuNPs of *Streptomyces* sp. NH21 showed spherical shape with a small size of 10±14 nm. They have been studied the MIC value at various concentrations (1.25–200 µg/mL) of biosynthesized AuNPs using *Streptomyces* sp. NH21 against *Bacillus subtilis, E. coli, S. aureus, K. pneumoniae*, and *P. aeruginosa* (Składanowski et al., 2017). In this study, the MIC profile of MSK03-AuNPs and MSK05-AuNPs showed MIC values of more than 141.4 µg/mL against tested pathogens.

In conclusion, the *Streptomyces* sp. strains MSK03 and MSK05 were isolated from soil samples. Based on 16S rDNA sequence, the strains MSK03 and MSK05 were identified as *S. monashensis* and *S. spectabilis*, respectively. The extracellular cell-free supernatants of *Streptomyces* sp. MSK03 and MSK05 can be used to synthesize AuNPs. The biosynthesized AuNPs is considered the simple and an eco-friendly process. The biosynthesized AuNPs (MSK03-AuNPs and MSK05-AuNPs) showed spherical shape with particle size ranging from 3.3 to 40 nm. The UV-Vis spectra

confirmed the LSPR band of the biosynthesized AuNPs at 530 and 545 nm. The use of *Streptomyces* sp. for the synthesized AuNPs in the large-scale manufacturing processes has higher growth rates and easier and cheaper cultivation requirements (Gopal et al., 2013; Soltani et al., 2015). Thus, *Streptomyces* sp. MSK03 and MSK05 were found to be a candidate for the AuNPs production.
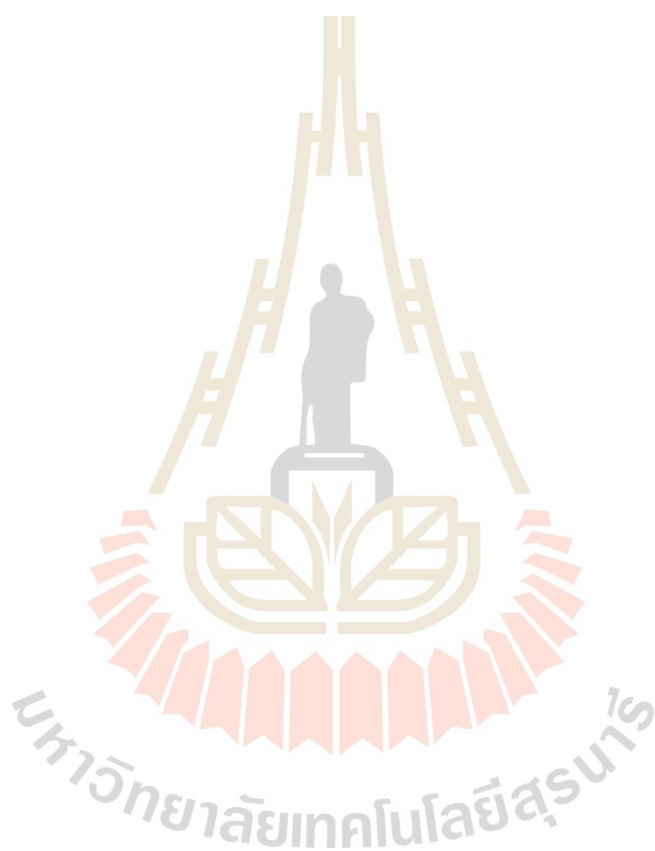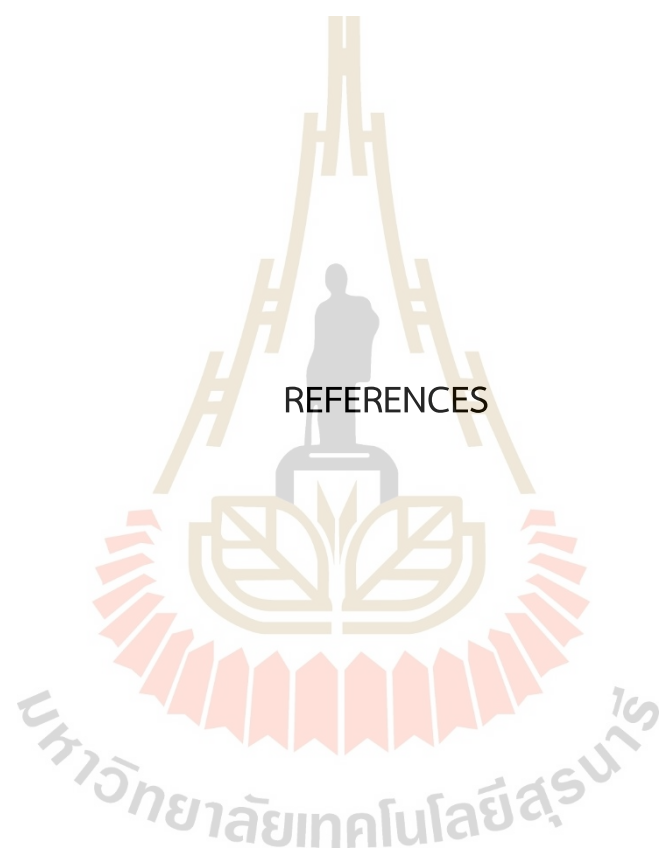
REFERENCES

REFERENCES

Agnihotri, S., Mukherji, S., and Mukherji, S. (2013). Immobilized silver nanoparticles enhance contact killing and show highest efficacy: elucidation of the mechanism of bactericidal action of silver. *Nanoscale, 5*(16), 7328-7340.

Ahmad, A., Senapati, S., Khan, M. I., Kumar, R., Ramani, R., Srinivas, V., and Sastry, M. (2003). Intracellular synthesis of gold nanoparticles by a novel alkalotolerant actinomycete, Rhodococcus species. *Nanotechnology, 14*(7), 824.

Ahmad, T., Wani, I. A., Manzoor, N., Ahmed, J., and Asiri, A. M. (2013). Biosynthesis, structural characterization and antimicrobial activity of gold and silver nanoparticles. *Colloids and Surfaces B: Biointerfaces, 107*, 227-234.

Alanazi, F. K., Radwan, A. A., and Alsarra, I. A. (2010). Biopharmaceutical applications of nanogold. *Saudi Pharmaceutical Journal, 18*(4), 179-193.

Albrecht, M. A., Evans, C. W., and Raston, C. L. (2006). Green chemistry and the health implications of nanoparticles. *Green chemistry, 8*(5), 417-432.

Alvarez, R. A., Cortez-Valadez, M., Bueno, L. O. N., Hurtado, R. B., Rocha-Rocha, O., Delgado-Beleño, Y., . . . Flores-Acosta, M. (2016). Vibrational properties of gold nanoparticles obtained by green synthesis. *Physica E: Low-dimensional Systems and Nanostructures, 84*, 191-195.

Anderson, M. L., Morris, C. A., Stroud, R. M., Merzbacher, C. I., and Rolison, D. R. (1999). Colloidal gold aerogels: Preparation, properties, and characterization. *Langmuir, 15*(3), 674-681.

Antony-Babu, S., Stien, D., Eparvier, V., Parrot, D., Tomasi, S., and Suzuki, M. T. (2017). Multiple Streptomyces species with distinct secondary metabolomes have identical 16S rRNA gene sequences. *Scientific Reports, 7*(1), 11089.

Arunachalam, K. D., Annamalai, S. K., and Hari, S. (2013). One-step green synthesis and characterization of leaf extract-mediated biocompatible silver and gold nanoparticles from Memecylon umbellatum. *International journal of nanomedicine, 8*, 1307-1315.

Balagurunathan, R., Radhakrishnan, M., Rajendran, R. B., and Velmurugan, D. (2011). Biosynthesis of gold nanoparticles by actinomycete Streptomyces viridogens strain HM10. *Indian Journal of Biochemistry & Biophysics, 48*, 331-335.

Bao, C., Jin, M., Lu, R., Zhang, T., and Zhao, Y. Y. (2003). Preparation of Au nanoparticles in the presence of low generational poly (amidoamine) dendrimer with surface hydroxyl groups. *Materials chemistry and physics, 81*(1), 160-165.

Basu, S., Maji, P., and Ganguly, J. (2015). Biosynthesis, characterisation and antimicrobial activity of silver and gold nanoparticles byDolichos biflorusLinn seed extract. *Journal of Experimental Nanoscience, 11*(8), 660-668.

Bennur, T., Khan, Z., Kshirsagar, R., Javdekar, V., and Zinjarde, S. (2016). Biogenic gold nanoparticles from the Actinomycete Gordonia amarae: application in rapid sensing of copper ions. *Sensors and Actuators B: Chemical, 233*, 684-690.

Bianconi, A. (1980). Surface X-ray absorption spectroscopy: Surface EXAFS and surface XANES. *Applications of Surface Science, 6*(3), 392-418.

Bindhu, M., and Umadevi, M. (2014). Antibacterial activities of green synthesized gold nanoparticles. *Materials Letters, 120*, 122-125.

Bisker, G., Yeheskely-Hayon, D., Minai, L., and Yelin, D. (2012). Controlled release of Rituximab from gold nanoparticles for phototherapy of malignant cells. *J Control Release, 162*(2), 303-309.

Bosecker, K. (1997). Bioleaching: metal solubilization by microorganisms. *FEMS Microbiology reviews, 20*(3-4), 591-604.

Bowman, M.-C., Ballard, T. E., Ackerson, C. J., Feldheim, D. L., Margolis, D. M., and Melander, C. (2008). Inhibition of HIV fusion with multivalent gold nanoparticles. *Journal of the American Chemical Society, 130*(22), 6896-6897.

Brock, S. L. (2004). Nanostructures and Nanomaterials: Synthesis, Properties and Applications By Guozhang Cao (University of Washington). Imperial College Press (distributed by World Scientific): London. 2004. xiv+ 434 pp. $78.00. ISBN 1-86094-415-9. In: ACS Publications.

Bruins, M. R., Kapil, S., and Oehme, F. W. (2000). Microbial Resistance to Metals in the Environment. *Ecotoxicology and Environmental Safety, 45*(3), 198-207.

Case, R. J., Boucher, Y., Dahllöf, I., Holmström, C., Doolittle, W. F., and Kjelleberg, S. (2007). Use of 16S rRNA and rpoB genes as molecular markers for microbial ecology studies. *Appl Environ Microbiol, 73*(1), 278-288. doi:10.1128/aem.01177-06.

Chamundeeswari, M., Sobhana, S. S., Jacob, J. P., Kumar, M. G., Devi, M. P., Sastry, T. P., and Mandal, A. B. (2010). Preparation, characterization and evaluation of a biopolymeric gold nanocomposite with antimicrobial activity. *Biotechnol Appl Biochem, 55*(1), 29-35.

Chater, K. F. (1993). Genetics of differentiation in Streptomyces. *Annual review of microbiology, 47*(1), 685-711.

Chen, Y., Gu, X., Nie, C. G., Jiang, Z. Y., Xie, Z. X., and Lin, C. J. (2005). Shape controlled growth of gold nanoparticles by a solution synthesis. *Chem Commun (Camb)*(33), 4181-4183.

Cheng, L., Li, X., and Dong, J. (2015). Size-controlled preparation of gold nanoparticles with novel pH responsive gemini amphiphiles. *Journal of Materials Chemistry C, 3*(24), 6334-6340.

Chithrani, B. D., Ghazani, A. A., and Chan, W. C. (2006). Determining the size and shape dependence of gold nanoparticle uptake into mammalian cells. *Nano letters, 6*(4), 662-668.

Chithrani, D. B., Dunne, M., Stewart, J., Allen, C., and Jaffray, D. A. (2010). Cellular uptake and transport of gold nanoparticles incorporated in a liposomal carrier. *Nanomedicine: Nanotechnology, Biology and Medicine, 6*(1), 161-169.

Cho, E. C., Zhang, Q., and Xia, Y. (2011). The effect of sedimentation and diffusion on cellular uptake of gold nanoparticles. *Nature nanotechnology, 6*(6), 385-391.

Clogston, J. D., and Patri, A. K. (2011a). Zeta potential measurement. In *Characterization of nanoparticles intended for drug delivery* (pp. 63-70): Springer.

Clogston, J. D., and Patri, A. K. (2011b). Zeta potential measurement. *Methods Mol Biol, 697*, 63-70.

Coenye, T., and Vandamme, P. (2003). Intragenomic heterogeneity between multiple 16S ribosomal RNA operons in sequenced bacterial genomes. *FEMS Microbiology Letters, 228*(1), 45-49.

Cui, X., Liu, M., and Li, B. (2012). Homogeneous fluorescence-based immunoassay via inner filter effect of gold nanoparticles on fluorescence of CdTe quantum dots. *The Analyst, 137*, 3293-3299.

Dahoumane, S. A., Wujcik, E. K., and Jeffryes, C. (2016). Noble metal, oxide and chalcogenide-based nanomaterials from scalable phototrophic culture systems. *Enzyme and Microbial Technology, 95*, 13-27.

Daniel, M.-C., and Astruc, D. (2004). Gold nanoparticles: assembly, supramolecular chemistry, quantum-size-related properties, and applications toward biology, catalysis, and nanotechnology. *Chemical reviews, 104*(1), 293-346.

Das, M., Shim, K. H., An, S. S. A., and Yi, D. K. (2012). Review on gold nanoparticles and their applications. *Toxicology and Environmental Health Sciences, 3*(4), 193-205.

Dhas, T. S., Kumar, V. G., Karthick, V., Govindaraju, K., and Narayana, T. S. (2014). Biosynthesis of gold nanoparticles using Sargassum swartzii and its cytotoxicity effect on HeLa cells. *Spectrochimica Acta Part A: Molecular and Biomolecular Spectroscopy, 133*, 102-106.

Di Guglielmo, C., López, D. R., De Lapuente, J., Mallafre, J. M. L., and Suàrez, M. B. (2010). Embryotoxicity of cobalt ferrite and gold nanoparticles: a first in vitro approach. *Reproductive Toxicology, 30*(2), 271-276.

Dreaden, E. C., Alkilany, A. M., Huang, X., Murphy, C. J., and El-Sayed, M. A. (2012). The golden age: gold nanoparticles for biomedicine. *Chemical Society Reviews, 41*(7), 2740-2779.

Dykman, L., and Khlebtsov, N. (2011). Gold nanoparticles in biology and medicine: recent advances and prospects. *Acta Naturae 3*(2 (9)), 34-55.

El-Batal, A. I., Hashem, A.-A. M., and Abdelbaky, N. M. (2013). Gamma radiation mediated green synthesis of gold nanoparticles using fermented soybean-garlic aqueous extract and their antimicrobial activity. *SpringerPlus, 2*(1), 1-10.

El-Sayed, I. H., Huang, X., and El-Sayed, M. A. (2006). Selective laser photo-thermal therapy of epithelial carcinoma using anti-EGFR antibody conjugated gold nanoparticles. *Cancer letters, 239*(1), 129-135.

Elavazhagan, T., and Arunachalam, K. D. (2011). Memecylon edule leaf extract mediated green synthesis of silver and gold nanoparticles. *International journal of nanomedicine, 6*, 1265.

Eustis, S., and el-Sayed, M. A. (2006). Why gold nanoparticles are more precious than pretty gold: noble metal surface plasmon resonance and its enhancement of the radiative and nonradiative properties of nanocrystals of different shapes. *Chem Soc Rev, 35*(3), 209-217.

Faraday, M. (1857). X. The Bakerian Lecture.—Experimental relations of gold (and other metals) to light. *Philosophical Transactions of the Royal Society of London*(147), 145-181.

Galstyan, V., Bhandari, M. P., Sberveglieri, V., Sberveglieri, G., and Comini, E. (2018). Metal oxide nanostructures in food applications: Quality control and packaging. *Chemosensors, 6*(2), 16.

Ganeshkumar, M., Sastry, T. P., Sathish Kumar, M., Dinesh, M. G., Kannappan, S., and Suguna, L. (2012). Sun light mediated synthesis of gold nanoparticles as carrier for 6-mercaptopurine: Preparation, characterization and toxicity studies in zebrafish embryo model. *Materials Research Bulletin, 47*(9), 2113-2119.

Geethalakshmi, R., and Sarada, D. (2013). Characterization and antimicrobial activity of gold and silver nanoparticles synthesized using saponin isolated from Trianthema decandra L. *Industrial Crops and Products, 51*, 107-115.

Giljohann, D. A., Seferos, D. S., Daniel, W. L., Massich, M. D., Patel, P. C., and Mirkin, C. A. (2010). Gold Nanoparticles for Biology and Medicine. *Angewandte Chemie International Edition, 49*(19), 3280-3294.

Gopal, J. V., Thenmozhi, M., Kannabiran, K., Rajakumar, G., Velayutham, K., and Rahuman, A. A. (2013). Actinobacteria mediated synthesis of gold nanoparticles using Streptomyces sp. VITDDK3 and its antifungal activity. *Materials Letters, 93*, 360-362.

Graily-Moradi, F., Maadani Mallak, A., and Ghorbanpour, M. (2020). Biogenic synthesis of gold nanoparticles and their potential application in agriculture. In *Biogenic Nano-Particles and their Use in Agro-ecosystems* (pp. 187-204): Springer.

Grubbs, R. B. (2007). Solvent-tuned structures. *Nature Materials, 6*(8), 553-555.

Guo, Q., Guo, Q., Yuan, J., and Zeng, J. (2014). Biosynthesis of gold nanoparticles using a kind of flavonol: Dihydromyricetin. *Colloids and Surfaces A: Physicochemical and Engineering Aspects, 441*, 127-132.

Hall, S. R., Shenton, W., Engelhardt, H., and Mann, S. (2001). Site‐specific organization of gold nanoparticles by biomolecular templating. *ChemPhysChem, 2*(3), 184-186.

Hassanisaadi, M., Bonjar, G. H. S., Rahdar, A., Pandey, S., Hosseinipour, A., and Abdolshahi, R. (2021). Environmentally Safe Biosynthesis of Gold Nanoparticles Using Plant Water Extracts. *Nanomaterials, 11*(8), 2033.

Heidari, Z., Sariri, R., and Salouti, M. (2014). Gold nanorods-bombesin conjugate as a potential targeted imaging agent for detection of breast cancer. *Journal of Photochemistry and Photobiology B: Biology, 130*, 40-46.

Henderson, G. S., De Groot, F. M., and Moulton, B. J. (2014). X-ray absorption near-edge structure (XANES) spectroscopy. *Reviews in Mineralogy and Geochemistry, 78*, 75-138.

Horie, M., and Fujita, K. (2011). Toxicity of metal oxides nanoparticles. In *Advances in molecular toxicology* (Vol. 5, pp. 145-178): Elsevier.

Hsueh, P.-R. (2010). New Delhi Metallo-β-lactamase-1 (NDM-1): An Emerging Threat Among Enterobacteriaceae. *Journal of the Formosan Medical Association, 109*(10), 685-687.

Hu, R., Zheng, M., Wu, J., Li, C., Shen, D., Yang, D., . . . Dong, W. (2017). Core-shell magnetic gold nanoparticles for magnetic field-enhanced radio-photothermal therapy in cervical cancer. *Nanomaterials, 7*(5), 111.

Hu, X., Zhang, Y., Ding, T., Liu, J., and Zhao, H. (2020). Multifunctional Gold Nanoparticles: A Novel Nanomaterial for Various Medical Applications and Biological Activities. *Frontiers in Bioengineering and Biotechnology, 8*.

Huang, X., and El-Sayed, M. A. (2010). Gold nanoparticles: Optical properties and implementations in cancer diagnosis and photothermal therapy. *Journal of Advanced Research, 1*(1), 13-28.

Hunt, L. (1973). The early history of gold plating. *Gold Bulletin, 6*(1), 16-27.

Ibrahim, N. A., Eid, B. M., and Abdel-Aziz, M. S. (2016). Green synthesis of AuNPs for eco-friendly functionalization of cellulosic substrates. *Applied Surface Science, 389*, 118-125.

Jahangirian, H., Lemraski, E. G., Webster, T. J., Rafiee-Moghaddam, R., and Abdollahi, Y. (2017). A review of drug delivery systems based on nanotechnology and green chemistry: green nanomedicine. *International journal of nanomedicine, 12*, 2957.

Jain, P. K., Lee, K. S., El-Sayed, I. H., and El-Sayed, M. A. (2006). Calculated absorption and scattering properties of gold nanoparticles of different size, shape, and composition: applications in biological imaging and biomedicine. *The journal of physical chemistry B, 110*(14), 7238-7248.

Jeffery, J. W. (1971). Methods in X-ray Crystallography.

Jiang, J., Oberdörster, G., and Biswas, P. (2009). Characterization of size, surface charge, and agglomeration state of nanoparticle dispersions for toxicological studies. *Journal of Nanoparticle Research, 11*(1), 77-89.

Jin, R., Cao, Y., Mirkin, C. A., Kelly, K. L., Schatz, G. C., and Zheng, J. G. (2001). Photoinduced conversion of silver nanospheres to nanoprisms. *Science, 294*(5548), 1901-1903.

Johnston, H. J., Hutchison, G., Christensen, F. M., Peters, S., Hankin, S., and Stone, V. (2010). A review of the in vivo and in vitro toxicity of silver and gold particulates: particle attributes and biological mechanisms responsible for the observed toxicity. *Crit Rev Toxicol, 40*(4), 328-346.

Karthik, L., Kumar, G., Keswani, T., Bhattacharyya, A., Reddy, B. P., and Rao, K. V. (2013a). Marine actinobacterial mediated gold nanoparticles synthesis and their antimalarial activity. *Nanomedicine, 9*(7), 951-960.

Karthik, L., Kumar, G., Keswani, T., Bhattacharyya, A., Reddy, B. P., and Rao, K. V. B. (2013b). Marine actinobacterial mediated gold nanoparticles synthesis and

their antimalarial activity. *Nanomedicine: Nanotechnology, Biology and Medicine, 9*(7), 951-960.

Khadivi Derakhshan, F., Dehnad, A., and Salouti, M. (2012). Extracellular biosynthesis of gold nanoparticles by metal resistance bacteria: Streptomyces griseus. *Synthesis and Reactivity in Inorganic, Metal-Organic, and Nano-Metal Chemistry, 42*(6), 868-871.

Khalil, H., Mahajan, D., Rafailovich, M., Gelfer, M., and Pandya, K. (2004). Synthesis of zerovalent nanophase metal particles stabilized with poly (ethylene glycol). *Langmuir, 20*(16), 6896-6903.

Khan, A. K., Rashid, R., Murtaza, G., and Zahra, A. (2014). Gold Nanoparticles: Synthesis and Applications in Drug Delivery. *Tropical Journal of Pharmaceutical Research, 13*(7).

Khan, S. T., Komaki, H., Motohashi, K., Kozone, I., Mukai, A., Takagi, M., and Shin-ya, K. (2011). Streptomyces associated with a marine sponge Haliclona sp.; biosynthetic genes for secondary metabolites and products. *Environ Microbiol, 13*(2), 391-403.

Kim, D., and Jon, S. (2012). Gold nanoparticles in image-guided cancer therapy. *Inorganica Chimica Acta, 393*, 154-164.

Kim, F., Sohn, K., Wu, J., and Huang, J. (2008). Chemical synthesis of gold nanowires in acidic solutions. *Journal of the American Chemical Society, 130*(44), 14442-14443.

Kim, H.-s., Seo, Y., Kim, K., Han, J. W., Park, Y., and Cho, S. (2016). Concentration Effect of Reducing Agents on Green Synthesis of Gold Nanoparticles: Size, Morphology, and Growth Mechanism. *Nanoscale research letters, 11*, 230.

Kim, J. H., Jang, H. H., Ryou, S. M., Kim, S., Bae, J., Lee, K., and Han, M. S. (2010). A functionalized gold nanoparticles-assisted universal carrier for antisense DNA. *Chem Commun (Camb), 46*(23), 4151-4153.

Kim, M., and Chun, J. (2014). Chapter 4 - 16S rRNA Gene-Based Identification of Bacteria and Archaea using the EzTaxon Server. In M. Goodfellow, I. Sutcliffe, & J. Chun (Eds.), *Methods in Microbiology* (Vol. 41, pp. 61-74): Academic Press.

Kojima, C., Umeda, Y., Harada, A., and Kono, K. (2010). Preparation of near-infrared light absorbing gold nanoparticles using polyethylene glycol-attached dendrimers. *Colloids and Surfaces B: Biointerfaces, 81*(2), 648-651.

Kong, F. Y., Zhang, J. W., Li, R. F., Wang, Z. X., Wang, W. J., and Wang, W. (2017). Unique Roles of Gold Nanoparticles in Drug Delivery, Targeting and Imaging Applications. *Molecules, 22*(9).

Konishi, Y., Tsukiyama, T., Saitoh, N., Nomura, T., Nagamine, S., Takahashi, Y., and Uruga, T. (2007). Direct determination of oxidation state of gold deposits in metal-reducing bacterium Shewanella algae using X-ray absorption near-edge structure spectroscopy (XANES). *Journal of Bioscience and Bioengineering, 103*(6), 568-571.

Kshirsagar, P., Sangaru, S. S., Brunetti, V., Malvindi, M. A., and Pompa, P. P. (2014). Synthesis of fluorescent metal nanoparticles in aqueous solution by photochemical reduction. *Nanotechnology, 25*(4), 045601.

Kumar, K. S., Kumar, G., Prokhorov, E., Luna-Bárcenas, G., Buitron, G., Khanna, V., and Sanchez, I. (2014). Exploitation of anaerobic enriched mixed bacteria (AEMB) for the silver and gold nanoparticles synthesis. *Colloids and Surfaces A: Physicochemical and Engineering Aspects, 462*, 264-270.

Lai, H.-Z., Chen, W.-Y., Wu, C.-Y., and Chen, Y.-C. (2015). Potent antibacterial nanoparticles for pathogenic bacteria. *ACS applied materials & interfaces, 7*(3), 2046-2054.

Lane, D. (1991). 16S/23S rRNA sequencing. Nucleic acid techniques in bacterial systematics (Stackebrandt E & Goodfellow M, eds). In: Wiley, New York.

Lee, J.-S., Green, J. J., Love, K. T., Sunshine, J., Langer, R., and Anderson, D. G. (2009). Gold, poly (β-amino ester) nanoparticles for small interfering RNA delivery. *Nano letters, 9*(6), 2402-2406.

Lee, K. X., Shameli, K., Yew, Y. P., Teow, S.-Y., Jahangirian, H., Rafiee-Moghaddam, R., and Webster, T. J. (2020). Recent Developments in the Facile Bio-Synthesis of Gold Nanoparticles (AuNPs) and Their Biomedical Applications. *International journal of nanomedicine, 15*, 275-300.

Li, L., Fan, M., Brown, R. C., Van Leeuwen, J., Wang, J., Wang, W., . . . Zhang, P. (2006). Synthesis, Properties, and Environmental Applications of Nanoscale Iron-Based Materials: A Review. *Critical Reviews in Environmental Science and Technology, 36*(5), 405-431.

Li, W. R., Xie, X. B., Shi, Q. S., Zeng, H. Y., Ou-Yang, Y. S., and Chen, Y. B. (2010). Antibacterial activity and mechanism of silver nanoparticles on Escherichia coli. *Appl Microbiol Biotechnol, 85*(4), 1115-1122.

Link, S., and El-Sayed, M. A. (1999). Size and temperature dependence of the plasmon absorption of colloidal gold nanoparticles. *The journal of physical chemistry B, 103*(21), 4212-4217.

Liu, B., Xie, J., Lee, J., Ting, Y., and Chen, J. P. (2005). Optimization of high-yield biological synthesis of single-crystalline gold nanoplates. *The journal of physical chemistry B, 109*(32), 15256-15263.

Liu, Y., Liu, Y., Mernaugh, R. L., and Zeng, X. (2009). Single chain fragment variable recombinant antibody functionalized gold nanoparticles for a highly sensitive colorimetric immunoassay. *Biosensors and Bioelectronics, 24*(9), 2853-2857.

Magnusson, M. H., Deppert, K., Malm, J.-O., Bovin, J.-O., and Samuelson, L. (1999). Gold nanoparticles: production, reshaping, and thermal charging. *Journal of Nanoparticle Research, 1*(2), 243-251.

Manivasagan, P., Venkatesan, J., Sivakumar, K., and Kim, S.-K. (2014). Pharmaceutically active secondary metabolites of marine actinobacteria. *Microbiological research, 169*(4), 262-278.

Manivasagan, P., Venkatesan, J., Sivakumar, K., and Kim, S. K. (2016). Actinobacteria mediated synthesis of nanoparticles and their biological properties: A review. *Crit Rev Microbiol, 42*(2), 209-221.

Menon, S., S, R., and S, V. K. (2017). A review on biogenic synthesis of gold nanoparticles, characterization, and its applications. *Resource-Efficient Technologies, 3*(4), 516-527.

Michael Goodfellow, Peter Kämpfer, Hans-Jürgen Busse, Martha E. Trujillo, Ken-ichiro Suzuki, Wolfgang Ludwig, and Whitman, W. B. (2012). Bergey's Manual of

Systematic Bacteriology, . *Springer New York, NY, 5: The Actinobacteria* (2nd edition).

Mie, G. (1908). A contribution to the optics of turbid media, especially colloidal metallic suspensions. *Ann. Phys, 25*(4), 377-445.

Mishra, A., Tripathy, S. K., and Yun, S.-I. (2012). Fungus mediated synthesis of gold nanoparticles and their conjugation with genomic DNA isolated from Escherichia coli and Staphylococcus aureus. *Process Biochemistry, 47*(5), 701-711.

Mittal, a. k., Kaler, A., Mulay, A., and Banerjee, U. (2013). Synthesis of Gold Nanoparticles Using Whole Cells of Geotrichum candidum. *Journal of Nanoparticles, 2013*.

Mody, V. V., Siwale, R., Singh, A., and Mody, H. R. (2010). Introduction to metallic nanoparticles. *Journal of Pharmacy and Bioallied Sciences, 2*(4), 282.

Mohanpuria, P., Rana, N. K., and Yadav, S. K. (2008). Biosynthesis of nanoparticles: technological concepts and future applications. *Journal of Nanoparticle Research, 10*(3), 507-517.

Montes, M., Mayoral, A., Deepak, F., Parsons, J., Jose-Yacamán, M., Peralta-Videa, J., and Gardea-Torresdey, J. (2011). Anisotropic gold nanoparticles and gold plates biosynthesis using alfalfa extracts. *Journal of Nanoparticle Research, 13*(8), 3113-3121.

Murawala, P., Tirmale, A., Shiras, A., and Prasad, B. (2014). In situ synthesized BSA capped gold nanoparticles: effective carrier of anticancer drug methotrexate to MCF-7 breast cancer cells. *Materials Science and Engineering: C, 34*, 158-167.

Muthuvel, A., Adavallan, K., Balamurugan, K., and Narendran, d. n. k. (2014). Biosynthesis of gold nanoparticles using Solanum nigrum leaf extract and screening their free radical scavenging and antibacterial properties. *Biomedicine & Preventive Nutrition, 4*.

Narayanan, K. B., and Sakthivel, N. (2010). Biological synthesis of metal nanoparticles by microbes. *Advances in colloid and interface science, 156*(1-2), 1-13.

Ohyama, J., Teramura, K., Shishido, T., Hitomi, Y., Kato, K., Tanida, H., . . . Tanaka, T. (2011). In Situ Au L3 and L2 edge XANES spectral analysis during growth of thiol protected gold nanoparticles for the study on particle size dependent electronic properties. *Chemical Physics Letters, 507*(1-3), 105-110.

Okitsu, K., Ashokkumar, M., and Grieser, F. (2005). Sonochemical synthesis of gold nanoparticles: effects of ultrasound frequency. *The journal of physical chemistry B, 109*(44), 20673-20675.

Papasani, M. R., Wang, G., and Hill, R. A. (2012). Gold nanoparticles: the importance of physiological principles to devise strategies for targeted drug delivery. *Nanomedicine, 8*(6), 804-814.

Park, T. J., Lee, S. Y., Lee, S. J., Park, J. P., Yang, K. S., Lee, K.-B., . . . Kim, S. K. (2006). Protein nanopatterns and biosensors using gold binding polypeptide as a fusion partner. *Analytical chemistry, 78*(20), 7197-7205.

Peng, C., Xu, J., Yu, M., Ning, X., Huang, Y., Du, B., . . . Zheng, J. (2019). Tuning the in vivo transport of anticancer drugs using renal‐clearable gold nanoparticles. *Angewandte Chemie, 131*(25), 8567-8571.

Pileni, M. (1997). Nanosized particles made in colloidal assemblies. *Langmuir, 13*(13), 3266-3276.

Pissuwan, D., Niidome, T., and Cortie, M. B. (2011). The forthcoming applications of gold nanoparticles in drug and gene delivery systems. *Journal of controlled release, 149*(1), 65-71.

Poinern, G. E. J. (2014). *A laboratory course in nanoscience and nanotechnology*: CRC Press.

Prakash, D., Mahale, V., Bankar, A., Nawani, N., Mahale, V., and Prakash, D. (2013). Biosynthesis of colloidal gold nanoparticles by Streptomyces sp. NK52 and its anti-lipid peroxidation activity. *Indian J Exp Biol, 51*(11), 969-972.

Procópio, R. E. d. L., Silva, I. R. d., Martins, M. K., Azevedo, J. L. d., and Araújo, J. M. d. (2012). Antibiotics produced by Streptomyces. *Brazilian Journal of Infectious Diseases, 16*(5), 466-471.

Ramalingam, V., Revathidevi, S., Shanmuganayagam, T., Muthulakshmi, L., and Rajaram, R. (2017). Gold nanoparticle induces mitochondria-mediated

apoptosis and cell cycle arrest in nonsmall cell lung cancer cells. *Gold Bulletin, 50*(2), 177-189.

Ranjitha, V. R., and Rai, V. R. (2017). Actinomycetes mediated synthesis of gold nanoparticles from the culture supernatant of Streptomyces griseoruber with special reference to catalytic activity. *3 Biotech, 7*(5), 299.

Rau, R. (2005). Have traditional DMARDs had their day? Effectiveness of parenteral gold compared to biologic agents. *Clin Rheumatol, 24*(3), 189-202.

Raval, N., Maheshwari, R., Kalyane, D., Youngren-Ortiz, S. R., Chougule, M. B., and Tekade, R. K. (2019). Chapter 10 - Importance of Physicochemical Characterization of Nanoparticles in Pharmaceutical Product Development. In R. K. Tekade (Ed.), *Basic Fundamentals of Drug Delivery* (pp. 369-400): Academic Press.

Reller, L. B., Weinstein, M. P., and Petti, C. A. (2007). Detection and Identification of Microorganisms by Gene Amplification and Sequencing. *Clinical Infectious Diseases, 44*(8), 1108-1114.

Ren, X., Song, Y., Liu, A., Zhang, J., Yang, P., Zhang, J., . . . Wu, G. (2015). Role of polyethyleneimine as an additive in cyanide-free electrolytes for gold electrodeposition. *Rsc Advances, 5*.

Rice, L. B. (2010). Progress and challenges in implementing the research on ESKAPE pathogens. *Infection Control & Hospital Epidemiology, 31*(S1), S7-S10.

Rinehart, and Winston. (2005). Chapter 4 Periodic Table. *Chapter 4 Periodic Table*.

Rossi, A., Donati, S., Fontana, L., Porcaro, F., Battocchio, C., Proietti, E., . . . Fratoddi, I. (2016). Negatively charged gold nanoparticles as a dexamethasone carrier: stability in biological media and bioactivity assessment in vitro. *Rsc Advances, 6*(101), 99016-99022.

Sadhasivam, S., Shanmugam, P., Veerapandian, M., Subbiah, R., and Yun, K. (2012). Biogenic synthesis of multidimensional gold nanoparticles assisted by Streptomyces hygroscopicus and its electrochemical and antibacterial properties. *Biometals, 25*(2), 351-360.

Saitou, N., and Nei, M. (1987). The neighbor-joining method: a new method for reconstructing phylogenetic trees. *Mol Biol Evol, 4*(4), 406-425.

Sapsford, K. E., Tyner, K. M., Dair, B. J., Deschamps, J. R., and Medintz, I. L. (2011). Analyzing nanomaterial bioconjugates: a review of current and emerging purification and characterization techniques. *Analytical chemistry, 83*(12), 4453-4488.

Sathish Kumar, S. R., and Bhaskara Rao, K. V. (2016). Postprandial anti-hyperglycemic activity of marine Streptomyces coelicoflavus SRBVIT13 mediated gold nanoparticles in streptozotocin induced diabetic male albino Wister rats. *IET Nanobiotechnol, 10*(5), 308-314.

Scaiano, J. C., Billone, P., Gonzalez, C. M., Marett, L., Marin, M. L., McGilvray, K. L., and Yuan, N. (2009). Photochemical routes to silver and gold nanoparticles. *Pure and Applied Chemistry, 81*(4), 635-647.

Schaffer, B., Hohenester, U., Trügler, A., and Hofer, F. (2009). High-resolution surface plasmon imaging of gold nanoparticles by energy-filtered transmission electron microscopy. *Physical Review B, 79*(4), 041401.

Shah, M., Badwaik, V., Kherde, Y., Waghwani, H. K., Modi, T., Aguilar, Z. P., . . . Webb, C. (2014). Gold nanoparticles: various methods of synthesis and antibacterial applications. *Front Biosci, 19*(8), 1320-1344.

Shah, M., Badwaik, V. D., and Dakshinamurthy, R. (2014). Biological applications of gold nanoparticles. *Journal of nanoscience and nanotechnology, 14*(1), 344-362.

Shah, M., Fawcett, D., Sharma, S., Tripathy, S. K., and Poinern, G. E. J. (2015). Green synthesis of metallic nanoparticles via biological entities. *Materials, 8*(11), 7278-7308.

Shahzadi, S., Zafar, N., and Sharif, R. (2018). Antibacterial Activity of Metallic Nanoparticles. In *Bacterial Pathogenesis and Antibacterial Control*.

Shaikh, S., Fatima, J., Shakil, S., Rizvi, S. M., and Kamal, M. A. (2015). Antibiotic resistance and extended spectrum beta-lactamases: Types, epidemiology and treatment. *Saudi J Biol Sci, 22*(1), 90-101.

Shaikh, S., Shakil, S., Abuzenadah, M. A., Danish Rizvi, M. S., Roberts, M. P., Mushtaq, G., and Kamal, A. M. (2015). Nanobiotechnological Approaches Against

Multidrug Resistant Bacterial Pathogens: An Update. *Current Drug Metabolism, 16*(5), 362-370.

Shankar, S. S., Rai, A., Ahmad, A., and Sastry, M. (2004). Rapid synthesis of Au, Ag, and bimetallic Au core–Ag shell nanoparticles using Neem (Azadirachta indica) leaf broth. *Journal of colloid and interface science, 275*(2), 496-502.

Shanmugasundaram, T., Radhakrishnan, M., Gopikrishnan, V., Pazhanimurugan, R., and Balagurunathan, R. (2013). A study of the bactericidal, anti-biofouling, cytotoxic and antioxidant properties of actinobacterially synthesised silver nanoparticles. *Colloids and Surfaces B: Biointerfaces, 111*, 680-687.

Sharma, A., Sharma, S., Sharma, K., Chetri, S. P., Vashishtha, A., Singh, P., . . . Agrawal, V. (2016). Algae as crucial organisms in advancing nanotechnology: a systematic review. *Journal of applied phycology, 28*(3), 1759-1774.

Sharma, V., Park, K., and Srinivasarao, M. (2009). Colloidal dispersion of gold nanorods: Historical background, optical properties, seed-mediated synthesis, shape separation and self-assembly. *Materials Science and Engineering: R: Reports, 65*(1-3), 1-38.

Shaw, C. F. (1999). Gold-based therapeutic agents. *Chemical reviews, 99*(9), 2589-2600.

Shnoudeh, A. J., Hamad, I., Abdo, R. W., Qadumii, L., Jaber, A. Y., Surchi, H. S., and Alkelany, S. Z. (2019). Chapter 15 - Synthesis, Characterization, and Applications of Metal Nanoparticles. In R. K. Tekade (Ed.), *Biomaterials and Bionanotechnology* (pp. 527-612): Academic Press.

Shukla, A. K., and Iravani, S. (2017). Metallic nanoparticles: green synthesis and spectroscopic characterization. *Environmental Chemistry Letters, 15*(2), 223-231.

Shukla, A. K., and Iravani, S. (2018). *Green synthesis, characterization and applications of nanoparticles*: Elsevier.

Shukla, R., Bansal, V., Chaudhary, M., Basu, A., Bhonde, R. R., and Sastry, M. (2005). Biocompatibility of gold nanoparticles and their endocytotic fate inside the cellular compartment: a microscopic overview. *Langmuir, 21*(23), 10644-10654.

Singh, R., Smitha, M. S., and Singh, S. P. (2014). The role of nanotechnology in combating multi-drug resistant bacteria. *J Nanosci Nanotechnol, 14*(7), 4745-4756.

Składanowski, M., Wypij, M., Laskowski, D., Golińska, P., Dahm, H., and Rai, M. (2017). Silver and gold nanoparticles synthesized from Streptomyces sp. isolated from acid forest soil with special reference to its antibacterial activity against pathogens. *Journal of Cluster Science, 28*(1), 59-79.

Slavin, Y. N., Asnis, J., Häfeli, U. O., and Bach, H. (2017). Metal nanoparticles: understanding the mechanisms behind antibacterial activity. *Journal of nanobiotechnology, 15*(1), 1-20.

Soltani, M., N., Khatami, M., and Shahidi Bonjar, G. H. (2016). Extracellular synthesis gold nanotriangles using biomass of Streptomyces microflavus. *IET Nanobiotechnol, 10*(1), 33-38.

Soltani, Meysam, N., Shahidi, B. G., and Khaleghi, N. (2015). Biosynthesis of gold nanoparticles using Streptomyces fulvissimus isolate. *Nanomedicine, 2*, 153-159.

Song, J., Lee, S. C., Kang, J. W., Baek, H. J., and Suh, J. W. (2004). Phylogenetic analysis of Streptomyces spp. isolated from potato scab lesions in Korea on the basis of 16S rRNA gene and 16S-23S rDNA internally transcribed spacer sequences. *Int J Syst Evol Microbiol, 54*(Pt 1), 203-209.

Sperling, R. A., Gil, P. R., Zhang, F., Zanella, M., and Parak, W. J. (2008). Biological applications of gold nanoparticles. *Chemical Society Reviews, 37*(9), 1896-1908.

Srinath, B., and Rai, R. V. (2015). Biosynthesis of gold nanoparticles using extracellular molecules produced by Enterobacter aerogenes and their catalytic study. *Journal of Cluster Science, 26*(5), 1483-1494.

Strasser, P., Koh, S., Anniyev, T., Greeley, J., More, K., Yu, C., . . . Ogasawara, H. (2010). Lattice-strain control of the activity in dealloyed core–shell fuel cell catalysts. *Nature chemistry, 2*(6), 454-460.

Sun, L., Liu, D., and Wang, Z. (2008). Functional gold nanoparticle– peptide complexes as cell-targeting agents. *Langmuir, 24*(18), 10293-10297.

Sun, S., Mendes, P., Critchley, K., Diegoli, S., Hanwell, M., Evans, S. D., . . . Richardson, T. H. (2006). Fabrication of gold micro-and nanostructures by photolithographic exposure of thiol-stabilized gold nanoparticles. *Nano letters, 6*(3), 345-350.

Sun, X., Zhang, G., Keynton, R. S., O'Toole, M. G., Patel, D., and Gobin, A. M. (2013). Enhanced drug delivery via hyperthermal membrane disruption using targeted gold nanoparticles with PEGylated Protein-G as a cofactor. *Nanomedicine: Nanotechnology, Biology and Medicine, 9*(8), 1214-1222.

Svedberg, T., and Pedersen, K. O. (1940). The ultracentrifuge. *The Ultracentrifuge.*

Tahir, K., Nazir, S., Li, B., Khan, A. U., Khan, Z. U. H., Gong, P. Y., . . . Ahmad, A. (2015). Nerium oleander leaves extract mediated synthesis of gold nanoparticles and its antioxidant activity. *Materials Letters, 156*, 198-201.

Takeuchi, T., Sawada, H., Tanaka, F., and Matsuda, I. (1996). Phylogenetic Analysis of Streptomyces spp. Causing Potato Scab Based on 16S rRNA Sequences. *International Journal of Systematic and Evolutionary Microbiology, 46*(2), 476-479.

Tang, Z., Kotov, N. A., and Giersig, M. (2002). Spontaneous organization of single CdTe nanoparticles into luminescent nanowires. *Science, 297*(5579), 237-240.

Taylor, M. W., Radax, R., Steger, D., and Wagner, M. (2007). Sponge-associated microorganisms: evolution, ecology, and biotechnological potential. *Microbiology and molecular biology reviews, 71*(2), 295-347.

Tedesco, S., Doyle, H., Blasco, J., Redmond, G., and Sheehan, D. (2010). Oxidative stress and toxicity of gold nanoparticles in Mytilus edulis. *Aquatic toxicology, 100*(2), 178-186.

Wan Mat Khalir, W. K. A., Shameli, K., Jazayeri, S. D., Othman, N. A., Che Jusoh, N. W., and Hassan, N. M. (2020). Biosynthesized Silver Nanoparticles by Aqueous Stem Extract of Entada spiralis and Screening of Their Biomedical Activity. *Frontiers in Chemistry, 8*. doi:10.3389/fchem.2020.00620

Wang, L., Hu, C., and Shao, L. (2017). The antimicrobial activity of nanoparticles: present situation and prospects for the future. *International journal of nanomedicine, 12*, 1227.

Wangoo, N., Bhasin, K., Mehta, S., and Suri, C. R. (2008). Synthesis and capping of water-dispersed gold nanoparticles by an amino acid: bioconjugation and binding studies. *Journal of colloid and interface science, 323*(2), 247-254.

Weir, E., Lawlor, A., Whelan, A., and Regan, F. (2008). The use of nanoparticles in anti-microbial materials and their characterization. *Analyst, 133*(7), 835-845.

Weisburg, W. G., Barns, S. M., Pelletier, D. A., and Lane, D. J. (1991). 16S ribosomal DNA amplification for phylogenetic study. *Journal of bacteriology, 173*(2), 697-703.

Wong, S. S., Joselevich, E., Woolley, A. T., Cheung, C. L., and Lieber, C. M. (1998). Covalently functionalized nanotubes as nanometre-sized probes in chemistry and biology. *Nature, 394*(6688), 52-55.

Wu, Y., Wang, H., Gao, F., Xu, Z., Dai, F., and Liu, W. (2018). An injectable supramolecular polymer nanocomposite hydrogel for prevention of breast cancer recurrence with theranostic and mammoplastic functions. *Advanced Functional Materials, 28*(21), 1801000.

Yang, B., Wang, Y., and Qian, P.-Y. (2016). Sensitivity and correlation of hypervariable regions in 16S rRNA genes in phylogenetic analysis. *BMC bioinformatics, 17*(1), 1-8.

Yang, J., Deng, S., Lei, J., Ju, H., and Gunasekaran, S. (2011). Electrochemical synthesis of reduced graphene sheet–AuPd alloy nanoparticle composites for enzymatic biosensing. *Biosensors and Bioelectronics, 29*(1), 159-166.

Ye, H., Shen, Z., Yu, L., Wei, M., and Li, Y. (2018). Manipulating nanoparticle transport within blood flow through external forces: an exemplar of mechanics in nanomedicine. *Proceedings. Mathematical, physical, and engineering sciences, 474*(2211), 20170845-20170845.

Yee, F. Y., Periasamy, V., and Malek, S. N. A. (2015). *Green synthesis of gold nanoparticles using aqueous ethanol extract of Curcuma mangga rhizomes as reducing agent.* Paper presented at the AIP conference proceedings.

Yeh, Y. C., Creran, B., and Rotello, V. M. (2012). Gold nanoparticles: preparation, properties, and applications in bionanotechnology. *Nanoscale, 4*(6), 1871-1880.

Yiing Yee, F., Periasamy, V., and Abd Malek, S. N. (2014). Green synthesis of gold nanoparticles using aqueous ethanol extract of Curcuma mangga rhizomes as reducing agent. *1657*.

Yuan, H., Khoury, C. G., Hwang, H., Wilson, C. M., Grant, G. A., and Vo-Dinh, T. (2012). Gold nanostars: surfactant-free synthesis, 3D modelling, and two-photon photoluminescence imaging. *Nanotechnology, 23*(7), 075102.

Zainab Mazhari, B. B. (2022). Antiviral Properties of Streptomyces tuirus DBZ39 Mediated Gold Nanoparticles Against Bluetongue virus. *Pak J Biol Sci, 25*(1), 90-99.

Zeng, S., Yu, X., Law, W.-C., Zhang, Y., Hu, R., Dinh, X.-Q., . . . Yong, K.-T. (2013). Size dependence of Au NP-enhanced surface plasmon resonance based on differential phase measurement. *Sensors and Actuators B: Chemical, 176*, 1128-1133.

Zhang, X., Sun, B., Tang, Q., Chen, R., and Han, S. (2019). Molecular Identification and Phylogenetic Analysis of Nuclear rDNA Sequences of Clonorchis sinensis Isolates From Human Fecal Samples in Heilongjiang Province, China. *Frontiers in Microbiology, 10*.

Zhang, Y., Shareena Dasari, T. P., Deng, H., and Yu, H. (2015). Antimicrobial activity of gold nanoparticles and ionic gold. *Journal of Environmental Science and Health, Part C, 33*(3), 286-327.

Zhao, N., Wei, Y., Sun, N., Chen, Q., Bai, J., Zhou, L., . . . Qi, L. (2008). Controlled synthesis of gold nanobelts and nanocombs in aqueous mixed surfactant solutions. *Langmuir, 24*(3), 991-998.

Zhou, Y., Kong, Y., Kundu, S., Cirillo, J. D., and Liang, H. (2012). Antibacterial activities of gold and silver nanoparticles against Escherichia coli and bacillus Calmette-Guérin. *Journal of nanobiotechnology, 10*(1), 1-9.

Zonooz, N. F., Salouti, M., Shapouri, R., and Nasseryan, J. (2012). Biosynthesis of gold nanoparticles by Streptomyces sp. ERI-3 supernatant and process optimization for enhanced production. *Journal of Cluster Science, 23*(2), 375-382.

Zotchev, S. B. (2012). Marine actinomycetes as an emerging resource for the drug development pipelines. *Journal of biotechnology, 158*(4), 168-175.
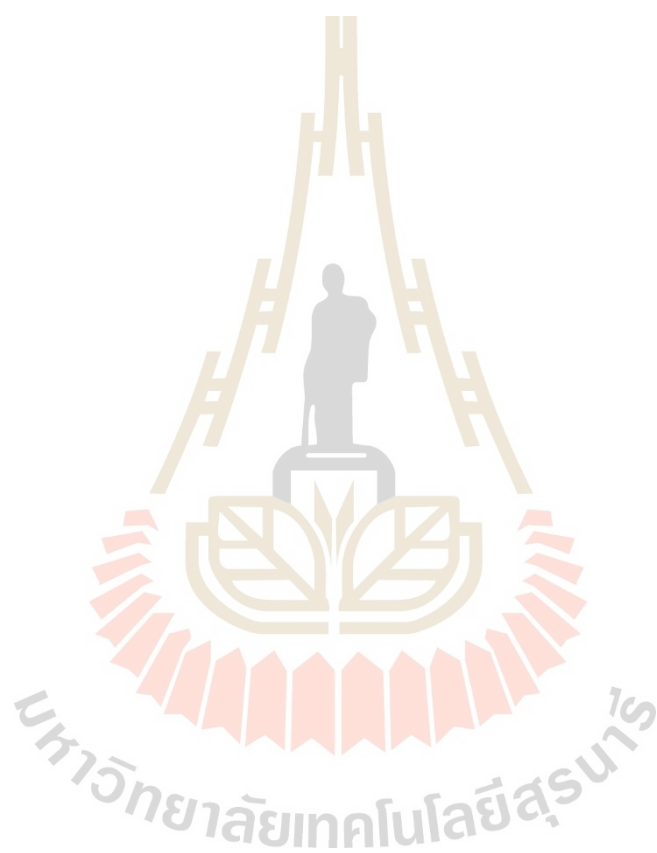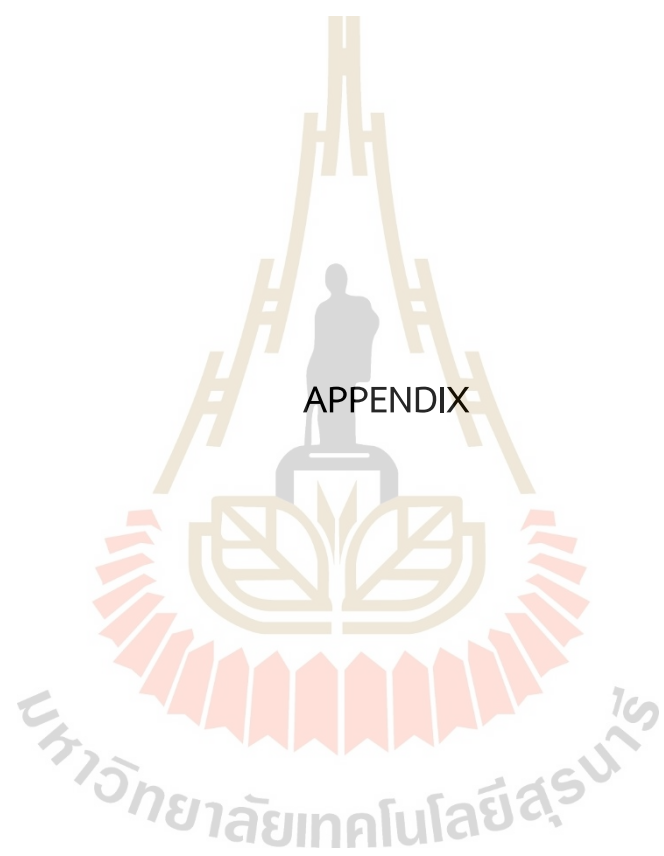
APPENDIX

APPENDIX

PREPARATION OF MEDIA AND REAGENTS

International Streptomyces Project 2 (ISP2) medium

Malt extract	10.00	g/L
Yeast extract	4.00	g/L
D-glucose	4.00	g/L
Agar	15.00	g/L
pH was adjusted to 7.2		

Starch Casein medium

Soluble starch	10.00	g/L
KNO_3	2.00	g/L
K_2HPO_4	2.00	g/L
NaCl	2.00	g/L
Casein acid hydrolysate	0.30	g/L
$MgSO_4.7H_2O$	0.05	g/L
$CaCO_3$	0.02	g/L
$FeSO_4.7H_2O$	0.01	g/L
pH was adjusted to 7.0		

Lysis buffer

1 mM Tris-HCl (pH 8)	40% (v/v)
0.5M EDTA	12% (v/v)
10% SDS	10% (v/v)
5M NaCl	3% (v/v)

10x Tris-Borate-EDTA (TBE) buffer

Tris base	108.00	g/L
Boric acid	55.00	g/L
EDTA	7.50	g/L

TE buffer

1M Tris-HCl	1.00	mL/L
0.5M EDTA	0.02	mL/L

SEQUENCES OF SOIL ISOLATED *STREPTOMYCES*

Streptomyces sp. MSK03

GTCGAACGATGAAGCCCTTCGGGGTGGATTAGTGGCGAACGGGTGAGTAACACGTGGG
CAATCTGCCCTTCACTCTGGGACAAGCCCTGGAAACGGGGTCTAATACCGGATATGACCATCTT
GGGCATCCTTGATGGTGTAAAGCTCCGGCGGTGAAGGATGAGCCCGCGGCCTATCAGCTTGTTG
GTGAGGTAATGGCTCACCAAGGCGACGACGGGTAGCCGGCCTGAGAGGGCGACCGGCCACACT
GGGACTGAGACACGGCCCAGACTCCTACGGGAGGCAGCAGTGGGGAATATTGCACAATGGGCG
AAAGCCTGATGCAGCGACGCCGCGTGAGGGATGACGGCCTTCGGGTTGTAAACCTCTTTCAGCA
GGGAAGAAGCGAGAGTGACGGTACCTGCAGAAGAAGCGCCGGCTAACTACGTGCCAGCAGCCG
CGGTAATACGTAGGGCGCAAGCGTTGTCCGGAATTATTGGGCGTAAAGAGCTCGTAGGCGGCTT
GTCACGTCGGGTGTGAAAGCCCGGGGCTTAACCCCGGGTCTGCATTCGATACGGGCTAGCTAG
AGTGTGGTAGGGGAGATCGGAATTCCTGGTGTAGCGGTGAAATGCGCAGATATCAGGAGGAAC
ACCGGTGGCGAAGGCGGATCTCTGGGCCATTACTGACGCTGAGGAGCGAAAGCGTGGGGAGCG
AACAGGATTAGATACCCTGGTAGTCCACGCCGTAAACGGTGGGAACTAGGTGTTGGCGACATTC
CACGTCGTCGGTGCCGCAGCTAACGCATTAAGTTCCCCGCCTGGGGAGTACGGCCGCAAGGCT
AAAACTCAAAGGAATTGACGGGGGCCCGCACAAGCAGCGGAGCATGTGGCTTAATTCGACGCA
ACGCGAAGAACCTTACCAAGGCTTGACATACACCGGAAAACCCTGGAGACAGGGTCCCCCTTGT
GGTCGGTGTACAGGTGGTGCATGGCTGTCGTCAGCTCGTGTCGTGAGATGTTGGGTTAAGTCCC
GCAACGAGCGCAACCCTTGTCCTGTGTTGCCAGCATGCCCTTCGGGGTGATGGGGACTCACAG
GAGACCGCCGGGGTCAACTCGGAGGAAGGTGGGGACGACGTCAAGTCATCATGCCCCTTATGT
CTTGGGCTGCACACGTGCTACAATGGCCGGTACAATGAGCTGCGATACCGTGAGGTGGAGCGA
ATCTCAAAAAGCCGGTCTCAGTTCGGATTGGGGTCTGCAACTCGACCCCATGAAGTCGGAGTTG
CTAGTAATCGCAGATCAGCATTGCTGCGGTGAATACGTTCCCGGGCCTTGTACACACCGCCCGT
CACGTCACGAAAGTTGGTAACACCCGAAGCCGGTGGCCCAACCCCTTGTGGGAGGGAGTCGTC
GAAGGTGGGACTAGCGATTGGACG

Streptomyces sp. MSK05

CGATGAAGCCCTTCGGGGTGGATTAGTGGCGAACGGGTGAGTAACACGTGGGCAATCT
GCCCTGCACTCTGGGACAAGCCCTGGAAACGGGGTCTAATACCGGATATGACACGGGATCGCAT
GATCTTGTGTGGAAAGCTCCGGCGGTGCAGGATGAGCCCGCGGCCTATCAGCTAGTTGGTGAG
GTAATGGCTCACCAAGGCGACGACGGGTAGCCGGCCTGAGAGGGCGACCGGCCACACTGGGAC
TGAGACACGGCCCAGACTCCTACGGGAGGCAGCAGTGGGGAATATTGCACAATGGGCGAAAGC
CTGATGCAGCGACGCCGCGTGAGGGATGACGGCCTTCGGGTTGTAAACCTCTTTCAGCAGGGA
AGAAGCGAAAGTGACGGTACCTGCAGAAGAAGCGCCGGCTAACTACGTGCCAGCAGCCGCGGT
AATACGTAGGGCGCGAGCGTTGTCCGGAATTATTGGGCGTAAAGAGCTCGTAGGCGGCTTGTCA
CGTCGGTTGTGAAAGCCCGGGGCTTAACCCCGGGTCTGCAGTCGATACGGGCAGGCTAGAGTT
CGGTAGGGGAGATCGGAATTCCTGGTGTAGCGGTGAAATGCGCAGATATCAGGAGGAACACCG
GTGGCGAAGGCGGATCTCTGGGCCGATACTGACGCTGAGGAGCGAAAGCGTGGGGAGCGAACA
GGATTAGATACCCTGGTAGTCCACGCCGTAAACGGTGGGCACTAGGTGTGGGCGACATTCCACG
TCGTCCGTGCCGCAGCTAACGCATTAAGTGCCCCGCCTGGGGAGTACGGCCGCAAGGCTAAAA
CTCAAAGGAATTGACGGGGGCCCGCACAAGCGGCGGAGCATGTGGCTTAATTCGACGCAACGC
GAAGAACCTTACCAAGGCTTGACATACACCGGAAACGGCCAGAGATGGTCGCCCCCTTGTGGTC
GGTGTACAGGTGGTGCATGGCTGTCGTCAGCTCGTGTCGTGAGATGTTGGGTTAAGTCCCGCAA
CGAGCGCAACCCTTGTCCCGTGTTGCCAGCAGGCCCTTGTGGTGCTGGGGACTCACGGGAGAC
CGCCGGGGTCAACTCGGAGGAAGGTGGGGACGACGTCAAGTCATCATGCCCCTTATGTCTTGG
GCTGCACACGTGCTACAATGGCCGGTACAATGAGCTGCGATACCGCGAGGTGGAGCGAATCTC
AAAAAGCCGGTCTCAGTTCGGATTGGGGTCTGCAACTCGACCCCATGAAGTCGGAGTCGCTAGT
AATCGCAGATCAGCATTGCTGCGGTGAATACGTTCCCGGGCCTTGTACACACCGCCCGTCACGT
CACGAAAGTCGGTAACACCCGAAGCCGGTGGCCCAACCCCTTGTGGGAGGGAGCTGTCGAAGG
TGGGACTGGCGA

SIZE DISTRIBUTION OF AuNPs USING ZETA SIZER

MSK03-AuNPs

Size Distribution Report by Intensity
v2.1

Malvern

Sample Details

Sample Name:	msk03-xmembrane 1		
SOP Name:	MSK_01102564.sop		
General Notes:			
File Name:	1.dts	Dispersant Name:	Water
Record Number:	24	Dispersant RI:	1.330
Material RI:	0.99	Viscosity (cP):	0.8872
Material Absorbtion:	0.000	Measurement Date and Time:	Friday, October 01, 2021 10:...

System

Temperature (°C):	25.1	Duration Used (s):	70
Count Rate (kcps):	184.8	Measurement Position (mm):	4.65
Cell Description:	Disposable sizing cuvette	Attenuator:	7

Results

			Size (r.nm):	% Intensity	Width (r.nm):
Z-Average (r.nm):	46.34	Peak 1:	66.67	100.0	34.35
PdI:	0.268	Peak 2:	0.000	0.0	0.000
Intercept:	0.841	Peak 3:	0.000	0.0	0.000
Result quality :	Good				

Size Distribution by Intensity

Record 24: msk03-xmembrane 1
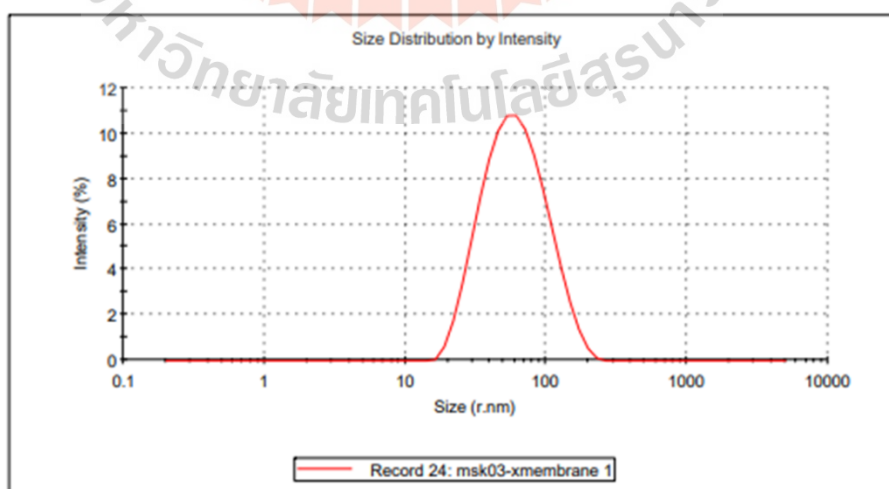
MSK05-AuNPs

Size Distribution Report by Intensity
v2.1

Malvern

Sample Details

Sample Name:	msk05-x2;8membrane2x 1
SOP Name:	MSK_01102564.sop
General Notes:	

File Name:	1.dts	**Dispersant Name:**	Water
Record Number:	41	**Dispersant RI:**	1.330
Material RI:	0.99	**Viscosity (cP):**	0.8872
Material Absorbtion:	0.000	**Measurement Date and Time:**	Friday, October 01, 2021 2:1...

System

Temperature (℃):	25.0	**Duration Used (s):**	70
Count Rate (kcps):	181.9	**Measurement Position (mm):**	4.65
Cell Description:	Disposable sizing cuvette	**Attenuator:**	7

Results

			Size (r.nm):	% Intensity	Width (r.nm)
Z-Average (r.nm):	23.33	**Peak 1:**	45.78	87.7	27.75
PdI:	0.465	**Peak 2:**	5.667	12.3	1.830
Intercept:	0.764	**Peak 3:**	0.000	0.0	0.000
Result quality :	Good				

Size Distribution by Intensity

Record 41: msk05-x2;8membrane2x 1
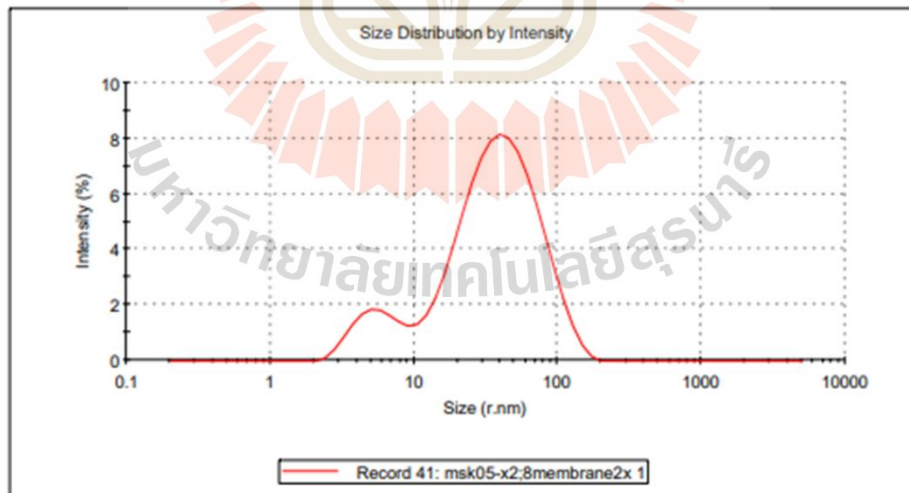
ZETA POTENCIAL OF AuNPs USING ZETA SIZER

MSK03-AuNPs

Zeta Potential Report
v2.2

Malvern Instruments Ltd – © Copyright 2008

Sample Details

Sample Name:	msk03zeta 3
SOP Name:	mansettings.nano
General Notes:	

File Name:	1.dts	Dispersant Name:	Water
Record Number:	60	Dispersant RI:	1.330
Date and Time:	Friday, October 01, 2021 4:07:11 ...	Viscosity (cP):	0.8872
		Dispersant Dielectric Constant:	78.5

System

Temperature (°C):	25.0	Zeta Runs:	50
Count Rate (kcps):	9.1	Measurement Position (mm):	4.50
Cell Description:	Zeta dip cell	Attenuator:	11

Results

			Mean (mV)	Area (%)	Width (mV)
Zeta Potential (mV):	-0.507	Peak 1:	-0.507	100.0	5.35
Zeta Deviation (mV):	5.35	Peak 2:	0.00	0.0	0.00
Conductivity (mS/cm):	0.0586	Peak 3:	0.00	0.0	0.00
Result quality :	See result quality report				

Zeta Potential Distribution

Record 60: msk03zeta 3
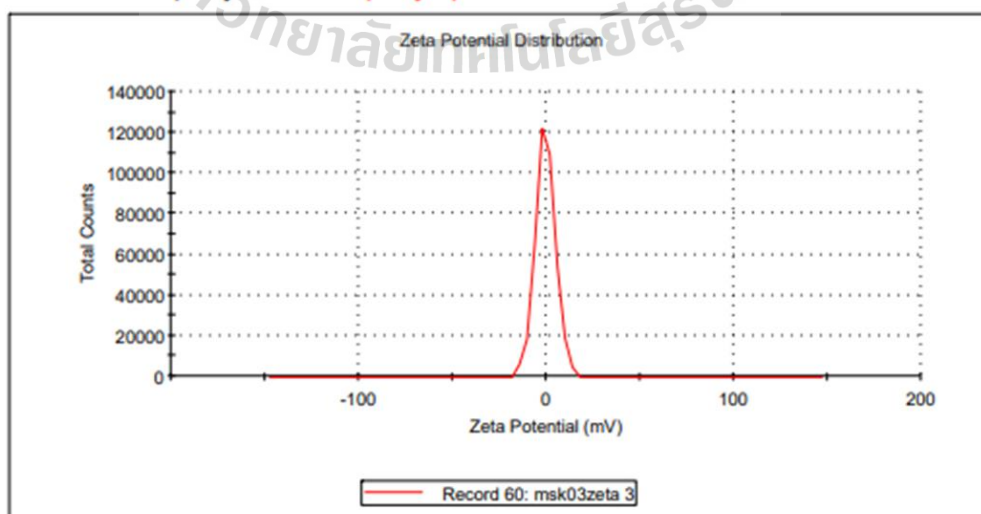
MSK05-AuNPs

Zeta Potential Report
v2.2

Malvern Instruments Ltd - © Copyright 2008

Sample Details

Sample Name:	msk05zeta 1
SOP Name:	mansettings.nano
General Notes:	

File Name:	1.dts	**Dispersant Name:**	Water
Record Number:	61	**Dispersant RI:**	1.330
Date and Time:	Friday, October 01, 2021 4:10:15 ...	**Viscosity (cP):**	0.8872
		Dispersant Dielectric Constant:	78.5

System

Temperature (℃):	25.0	**Zeta Runs:**	50
Count Rate (kcps):	2.9	**Measurement Position (mm):**	4.50
Cell Description:	Zeta dip cell	**Attenuator:**	11

Results

			Mean (mV)	Area (%)	Width (mV)
Zeta Potential (mV):	-0.129	**Peak 1:**	-0.129	100.0	2.83
Zeta Deviation (mV):	2.83	**Peak 2:**	0.00	0.0	0.00
Conductivity (mS/cm):	0.00586	**Peak 3:**	0.00	0.0	0.00
Result quality :	See result quality report				

Zeta Potential Distribution

Record 61: msk05zeta 1
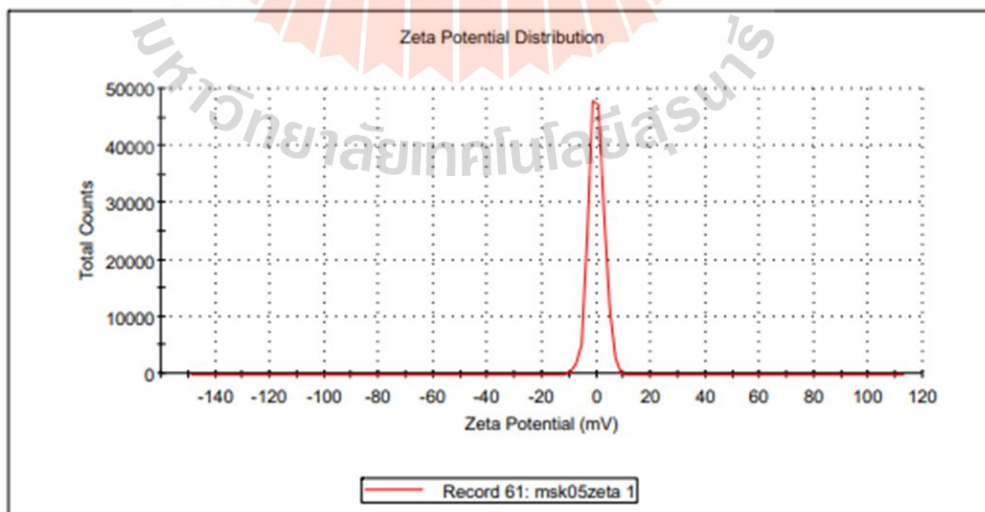
TEM IMAGE OF AuNPs

MSK03-AuNPs
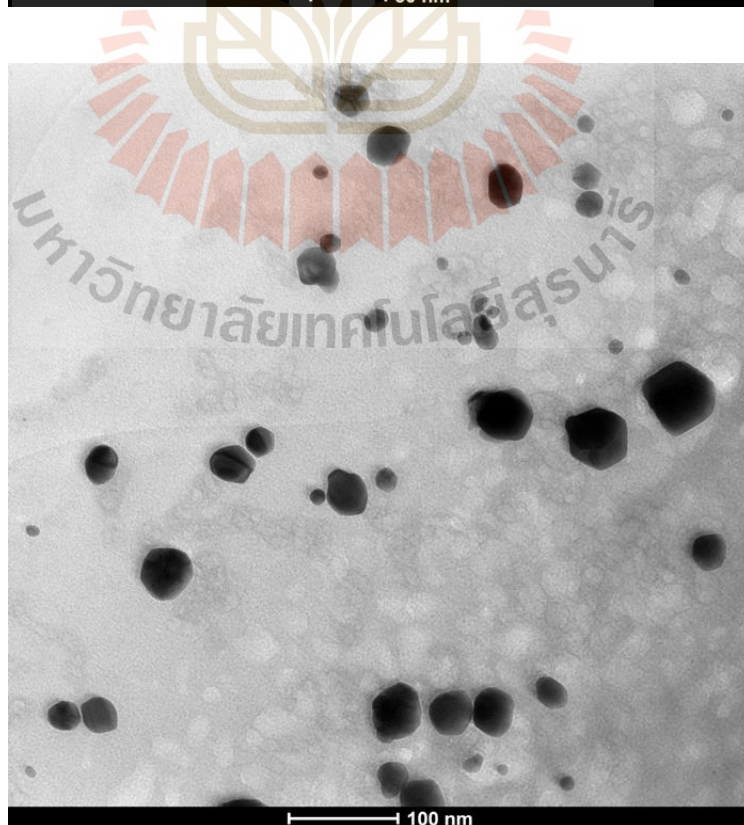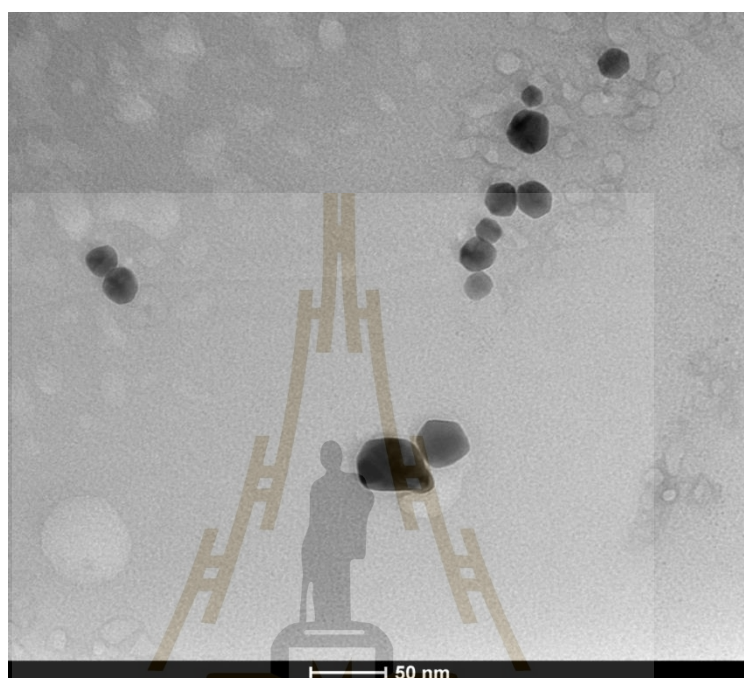
MSK05-AuNPs
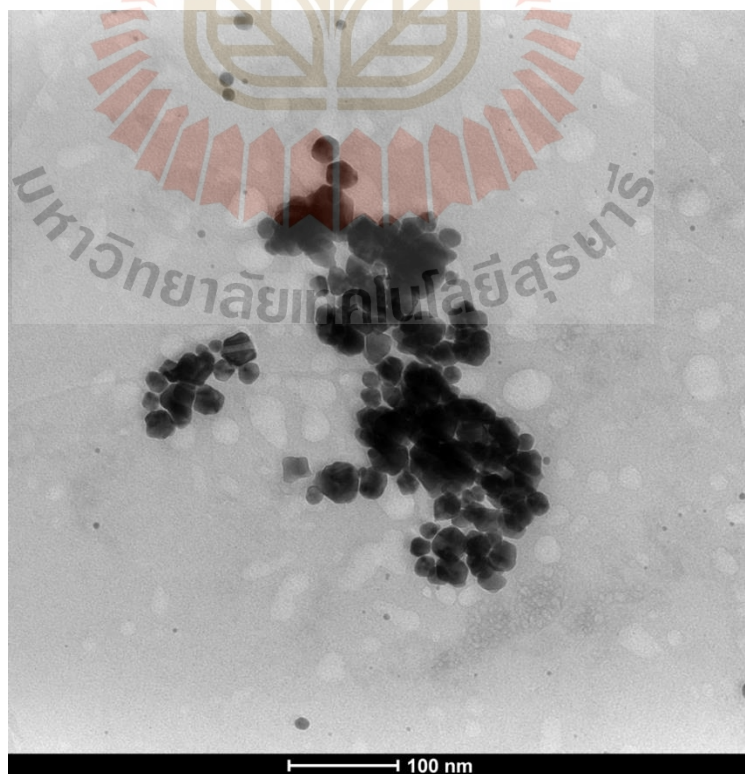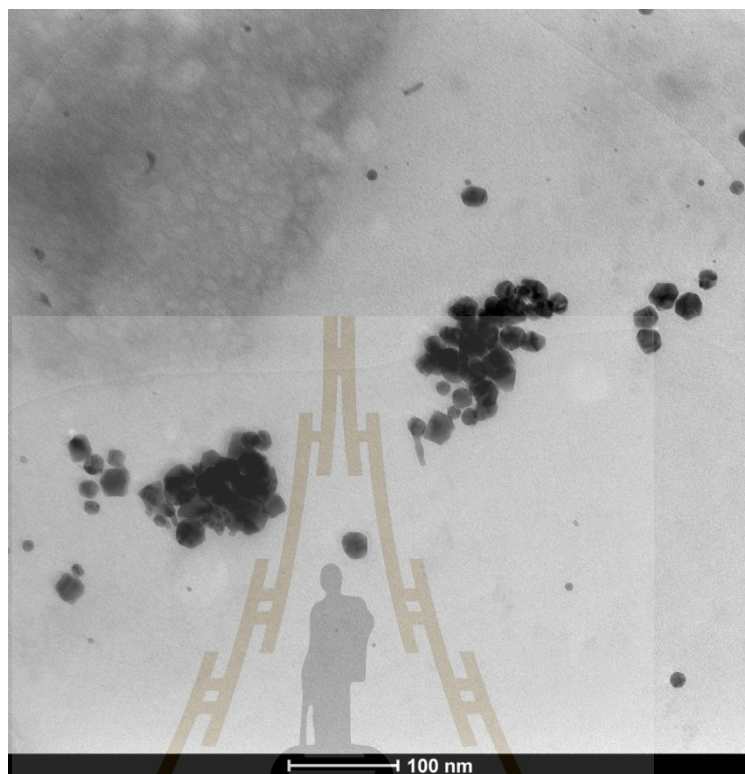
EDXRF PATTERN OF AuNPs

MSK03-AuNPs
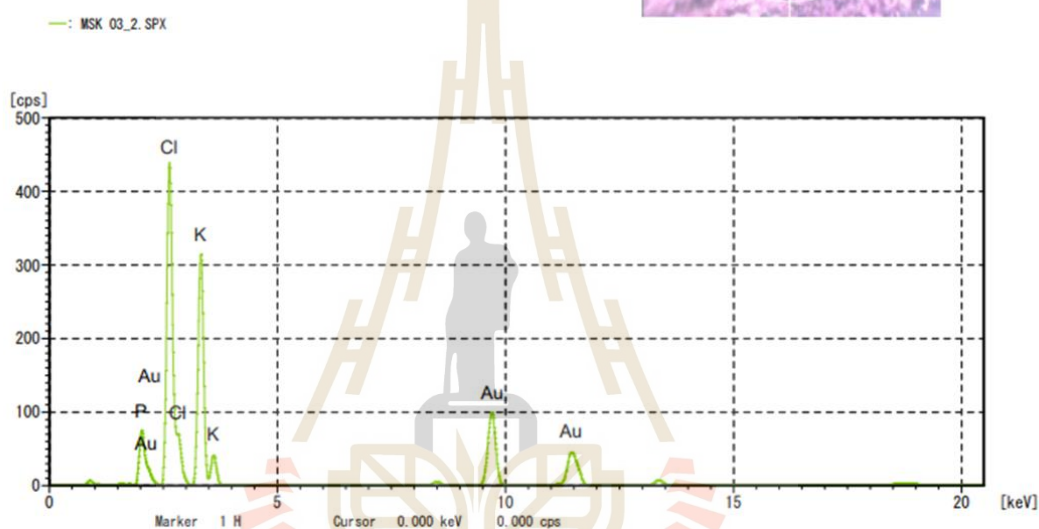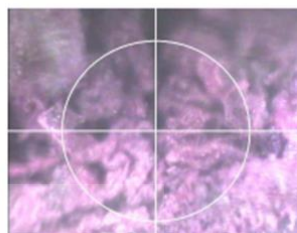
—: MSK 03_2. SPX

MSK 03_2. SPX

Live time	:	100 s	Processing Time	: P2
XGT Dia.	:	1.2 mm	X-ray tube vol.	: 30 kV
Current	:	1.000 mA		
X-ray Filter	:	Nonexistence	Cell	: Nonexistence

Quant. Corr. : Standard-less

Elem.	Line	Mass [%]	2sigma [%]	Atomic [%]	Intensity [cps/mA]	Formula	Mass [%]	Molecule [%]
15 P	K	8.098	0.048	8.109	1104.59	P2O5	18.558	9.383
17 Cl	K	26.933	0.078	23.560	5676.36	Cl	26.933	54.524
19 K	K	37.726	0.086	29.920	4617.46	K2O	45.445	34.622
79 Au	L	8.079	0.044	1.272	2021.78	Au2O3	9.063	1.472
8 O		19.163	0.065	37.140				

MSK05-AuNPs

—: MSK 05_2.SPX

Marker 1 H   Cursor 0.000 keV   0.000 cps
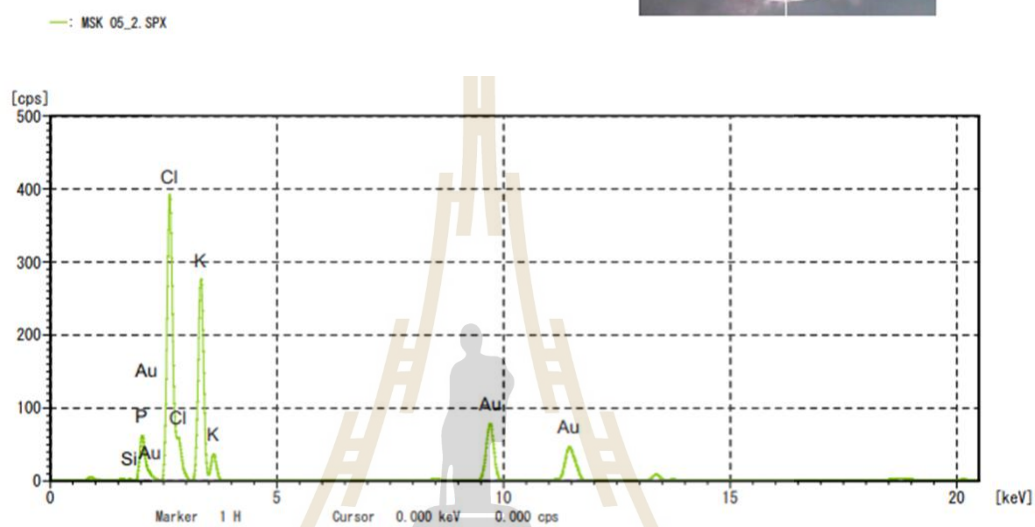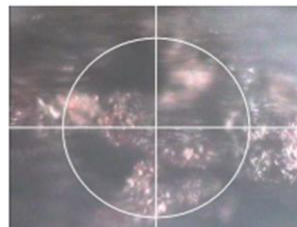
MSK 05_2.SPX

```
Live time      :    100 s      Processing Time : P2
XGT Dia.       :    1.2  mm    X-ray tube vol. : 30 kV
Current        :    1.000 mA
X-ray Filter   : Nonexistence  Cell            : Nonexistence

Quant. Corr.   : Standard-less
```

Elem. Line	Mass [%]	2sigma [%]	Atomic [%]	Intensity [cps/mA]	Formula	Mass [%]	Molecule [%]
14 Si K	0.785	0.037	0.863	42.79	SiO2	1.678	1.954
15 P K	7.283	0.048	7.266	850.61	P2O5	16.690	8.226
17 Cl K	27.639	0.085	24.087	5114.58	Cl	27.639	54.542
19 K K	37.976	0.094	30.007	4031.54	K2O	45.746	33.973
79 Au L	7.351	0.044	1.153	1605.94	Au2O3	8.246	1.305
8 O	18.967	0.077	36.624				

INFORMATION ON CLINICALLY ISOLATED PATHOGENS

Strains	Source	Susceptible	Drug resistant
K. pneumoniae (1617)	Sputum	Gentamycin	Ampicillin Amikacin Amocxicillin-Clavulanate Piperacillin-Tazabactam Cefoxitin Cefazolin Ceftriaxone Ceftazidime Cefepime Trimetroprim-Sulfamethoxazole Ciprofloxacin Levofloxacin Imipenem Ertapenem Meropenem
E. coli (8465)	Urine	Amikacin Amocxicillin-Clavulanate Piperacillin-Tazabactam Cefoxitin Ceftazidime Imipenem Ertapenem Meropenem	Ampicillin Gentamycin Cefazolin Ceftriaxone Ciprofloxacin Levofloxacin Trimetroprim-Sulfamethoxazole

Strains	Source	Susceptible	Drug resistant
A. baumannii (MDR)	Sputum	Colistin (MIC=2.0)	Ampicillin-Sulbactam
			Piperacillin-Tazabactam
			Ceftazidime
			Ceftriaxone
			Cefepime
			Imipenem
			Meropenem
			Trimetroprim-Sulfamethoxazole
			Gentamycin
			Amikacin
			Ciprofloxacin
			Levofloxacin

CURRICULUM VITAE

Name: Supavadee Kerdtoob

Date of birth: March 17, 1989

Place of birth: Phichit Province, Thailand

Education:

2017-Present   Ph.D. Candidate in Biomedical Sciences, School of Preclinical Sciences, Institute of Science, Suranaree University of Technology, Nakhon Ratchasima, Thailand

2011-2013   Master of Science in Chemistry, Naresuan University, Phitsanulok Province, Thailand

2007-2011   Bachelor of Science in Chemistry, Naresuan University, Phitsanulok Province, Thailand